ISSN 0078－6659

MEMOIRS

OF THE

FACULTY OF ENGINEERING

OSAKA CITY UNIVERSITY

VOL. 51

DECEMBER 2010

PUBLISHED BY THE
GRADUATE SCHOOL OF ENGINEERING
OSAKA CITY UNIVERSITY

This Memoirs is annually issued. Selected original works of the members of the Faculty of Engineering are compiled herein. Abstracts of paper presented elsewhere during the current year are also compiled in the latter part of the volume.

All communications with respect to Memoirs should be addressed to:

Dean of the Graduate School of Engineering
Osaka City University
3-3-138, Sugimoto, Sumiyoshi-ku
Osaka 558-8585, Japan

MEMOIRS OF THE FACULTY OF ENGINEERING
OSAKA CITY UNIVERSITY

VOL. 51 DECEMBER 2010

CONTENTS

Regular Articles ……

Applied Chemistry and Bioengineering

Applied Chemistry

Change in Mechanical Properties of Styrene-Butadiene Rubber Vulcanizates during Thermal Aging
Takeo NAKAZONOand Akikazu MATSUMOTO ……

Urban Engineering

Civil Engineering

Effects of Information Provision to Encourage Public Involved Consciousness Toward Sustainable Bus Service
Noboru ISE and Yasuo HINO ……

Information Provision via Traceability System for Civil Structures
Hirokazu MATSUMOTO and Takashi UCHIDA ……

Abstracts of Papers Published in Other Journals

Mechanical and Physical Engineering

Mechanical Engineering

Intelligent Materials Engineering

Applied Mathematics

Physical Electronics and Informatics

Electrical Engineering

Applied Physics

Information and Communication Engineering

Applied Chemistry and Bioengineering

Applied Chemistry

Bioengineering

Urban Engineering

Architecture and Building Engineering

Civil Engineering

Environmental Urban Engineering

Applied Mathematics

Change in Mechanical Properties of Styrene-Butadiene Rubber Vulcanizates during Thermal Aging

Takeo NAKAZONO[*,**] and Akikazu MATSUMOTO[**]

(Received September 30, 2010)

Synopsis

The change in mechanical properties was investigated during the thermal aging process of styrene-butadiene rubbers (SBR) with different styrene, 1,2-, and 1,4-butadiene contents and the different types of plasticizers. An increase in the hardness and modulus values during the aging was confirmed to be due to the additional cross-linking reaction between the polymer chains in the SBR vulcanizates and the slow evaporation of the used process oil. We demonstrated the validity of the use of a nonvolatile liquid polymer as the plasticizer to achieve the desired physical properties of the SBR vulcanizate during thermal aging.

KEYWORDS: Cross-Linking, Liquid Polymer, Mechanical Property, Plasticizer, Polymer Chain Scission, Polymer Degradation, Styrene-Butadiene Rubber, Thermal Aging

1. Introduction

The development of high-performance rubber materials is important because the purpose for the use of synthetic rubber materials is diverse. A long-term stability is demanded for rubber materials during actual use in addition to their excellent physical and mechanical properties. The surface rubber of tires, that is called tread, is the most important component that determines the total performance of a tire because it directly contacts the road surface under the application of any force. In order to satisfy the requirements as a tire tread for automobiles under harsh conditions, styrene-butadiene rubbers (SBR) have been developed. The physical properties of SBR are controlled by the composition of the styrene and butadiene units in the copolymers as well as their tacticity and regiochemical structures.[1-6] Any degradation limits the guarantee for the performance of the rubber materials for tires. In general, the degradation of rubbers includes an irreversible change in the chemical structure of the polymer chains, and their types are classified into heat, ozone, photo, chemical, radiation, mechanical, electrical, and microbial degradations based on the type of trigger.[7-13]

The degradation of rubbers involves two types of reactions. Softening-type reactions include a decrease in the molecular weight of the polymers due to the main chain scission, while the hardening-type one involves cross-linking reactions. The styrene repeating units in the SBRs are chemically stable, while the 1,2- and 1,4-butadiene units significantly participate in any reactions occurring during the thermal aging. During a hardening-type reaction, a radical abstracts hydrogen from the polymer chain. The resulting polymer radicals combine with each other, leading to cross-linking. As a result, the rubber is more hardened and becomes brittle. For the softening-type reactions, on the other hand, a carbon radical reacts with molecular oxygen. The β-scission of the main chain finally occurs via the following chain reactions, resulting in a decrease in the molecular weight.

The mechanical properties of the rubber materials depend on a change in the polymer chain structures, such as polymer chain scission and cross-linking. There are a large number of reports on the degradation behaviors of natural rubber and SBR using various analytical methods.[14-24] The structural change in the

[*] Sumitomo Rubber Industry, Ltd. (SRI)
[**] Department of Applied Chemistry

polymer chain and networks has been discussed for the vulcanized compounds including several additives and carbon blacks. In the present study, we investigated the mechanical properties of the SBRs during a thermal aging process. It is noted that the SBR vulcanizates were prepared without antioxidants, stabilizers, the other additives, and carbon blacks for the vulcanization process to more precisely evaluate the effect of the polymer chain structures on the mechanical properties. Furthermore, we found that the use of a nonvolatile liquid polymer as the plasticizer was valid for the maintenance of the desired mechanical properties of the SBR vulcanizate.

2. Experimental

2.1. SBR

We used the SBRs with different styrene, 1,2-, and 1,4-butadiene contents and molecular weights. The SBR samples were synthesized on a laboratory scale or commercially available. These samples included no antioxidants and stabilizers. The SBR compounds (samples A–D) consisting of a synthesized styrene-butadiene copolymer (100), a process oil (Process X-260, Japan Energy Co.) (25), stearic acid (1.25), zinc oxide (2.5), *tert*-butyl benzothiazole-2-sulfenamide as the accelerator (1.25), and sulfur (1.25) were mixed, fabricated in the shape of a sheet, and cured at 170 ºC for 20 min. The values in parentheses are phr (parts per hundred rubber), i.e., the relative weight of each component. We also used the liquid type of a styrene-butadiene copolymer as the plasticizer. The formulation of the SBR vulcanizate (sample F) using the liquid polymer was as follows: a commercial styrene- butadiene copolymer (Asaprene 303, Asahi Kasei Chemicals Co.) (100), liquid styrene-butadiene copolymer (Kuraprene LSBR-820, Kuraray Co.) as the plasticizer (25), stearic acid (1.25), zinc oxide (2.1), *tert*-butyl benzothiazole-2-sulfenamide (4), and sulfur (4). The SBR vulcanizates with and without a process oil (samples E and G, respectively) were also prepared under similar conditions. Commercially available reagents were used as received without further purification.

2.2. Measurements

The weight-average molecular weight (M_w) and polydispersity (M_w/M_n) were determined by gel permeation chromatography (GPC) using Shimadzu RID-6A equipped with a refractive index detector and standard polystyrenes for calibration. The structure of the SBR was determined by nuclear magnetic resonance (NMR) spectroscopy using a Bruker Advance II 400 spectrometer and chloroform-*d* as the solvent at room temperature. The glass transition temperature (T_g) was determined by differential scanning calorimetry (DSC) using a Seiko DSC-6200 at the heating rate of 10 °C/min. The T_g values were determined as the extrapolated onset temperature of the transition, that is, the cross point of the baseline and tangent line at the maximum slope. The IR spectra were recorded using a Perkin-Elmer Auto IMAGE FT-IR spectrometer by an attenuated total reflection method.

2.3. Mechanical Properties

The SBR vulcanizates were sliced in order to obtain sheets with a 1-mm thickness for preparing the mechanical test pieces. The test pieces were put into an oven maintained at 100 ºC for one to eight weeks, and then used for each measurement to determine the mechanical properties. The hardness was measured using an automatic hardness meter (Excel, RH-101) according to the procedure described by JIS K6253. The sample number for the hardness measurement was three, and the median value was adopted. The viscoelasticity measurement was carried out using an Iwamoto VES-F-III viscoelastic analyzer at a 12% distortion, a frequency of 10 Hz, and 25 ºC, according to JIS K6394 (ISO 4664-1, 2005), in order to determine tensile complex modulus (E*) and loss angle (tanδ) values. The measurements were carried out using six test pieces and an average value and standard deviation were determined. The tensile experiment

was also carried out using a Shimadzu AGS-500 apparatus, according to JIS K6251 (ISO 37, 1994 and ASTEM D624). A dumbbell-shaped sample (35 mm × 6 mm × 1 mm) was tensed at the rate of 500 mm/min, and the modulus was recorded at 300% and 100% elongations (M_{300} and M_{100}, respectively). The median value was recorded as the M_{300} or M_{100} data according to a method similar to the hardness measurement.

2.4. Cross-Linking Density

The cross-linking density, ν (mol/mL) was calculated by the Flory-Rehner equation (Eq. 1).[25]

$$\nu\ (\text{mol/mL}) = \frac{\nu_R + \ln(1 - \nu_R) + \chi\ \nu_R^2}{-V_0\,(\nu_R^{1/3} - \nu_R/2)} \quad (1)$$

where ν_R is the volume fraction of the polymer after swelling, which was determined by the volumes of the polymers before and after being immersed in toluene at 25 ºC for 24 h, according to JIS K6258 (ISO 1817, 1999) (Eq. 2). Typically, 0.2 g of the polymer and 15−20 mL of the solvent were used for the swelling test. V_0 and χ are the molecular volume of a solvent and the interaction parameter, respectively. In this study, we used the following values; V_0 = 106.7 mL, χ = 0.352–0.365.

$$\nu_R = \frac{\text{Volume of dry polymer}}{\text{Volume of swelled polymer}} \quad (2)$$

2.5. Solvent Extraction

In order to isolate the soluble fractions of the SBR samples, successive extractions were carried out using acetone and chloroform under reflux conditions. First, the acetone extraction (AE) value was determined as the weight fraction of an acetone-soluble part by extraction with acetone under reflux for 24 h. Subsequently, the chloroform extraction (CE) value was determined by reflux with chloroform for 24 h using the same sample after the acetone extraction. Each extraction procedure was carried out using 0.2 g of the polymer and 150–200 mL of the solvent. The extracts were isolated as the AE and CE fractions after evaporating the solvents. The CE fraction was analyzed by GPC measurement.

3. Results and Discussion

3.1. Sample Characterization

The polymer repeating structure of the SBR was determined on the basis of the relative intensity of the peaks due to the styrene, 1,4-, and 1,2-butadiene units, which were observed at 6.8–7.3, 5.0–5.6, and 4.7–5.0 ppm, respectively, in the ^{1}H NMR spectra.[26] A typical example of the ^{1}H NMR spectrum is shown in Figure 1. The M_w and M_w/M_n values and the T_g values were determined by GPC and DSC measurements, respectively. The obtained results are shown in TABLE I. The DSC traces are shown in Figure 2. Samples A–D had relatively low styrene contents as the repeating unit (30.4–41.3%) and samples E and F had a high styrene content (68.6%). Sample C involved the highest 1,4-butadiene repeating unit (48.1%).

3.2. Mechanical Properties

The SBR vulcanizates (samples A–G) were heated at 100 ºC for 0–8 weeks under atmospheric conditions, and the changes in the hardness, E*, tanδ, and M_{300} (or M_{100}) values were determined. The results are summarized in TABLE II. The all values for these mechanical properties increased after the thermal aging. For example, the hardness value increased and reached the values that correspond to 1.2–1.5 times the

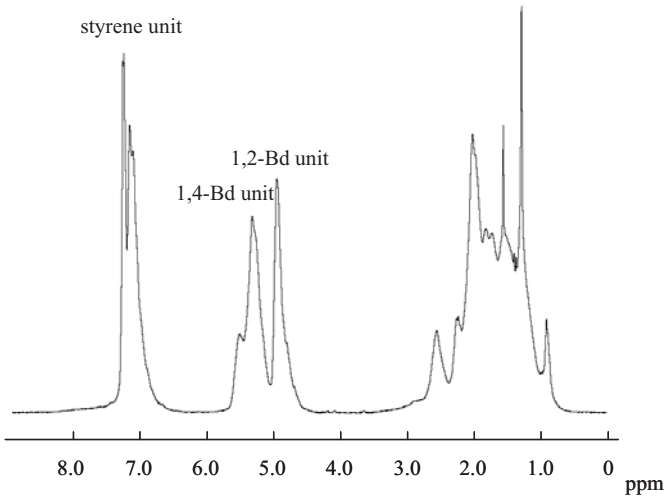

Figure 1. ^{1}H NMR spectrum of an SBR sample (Sample A before vulcanization) in chloroform-*d* at room temperature.

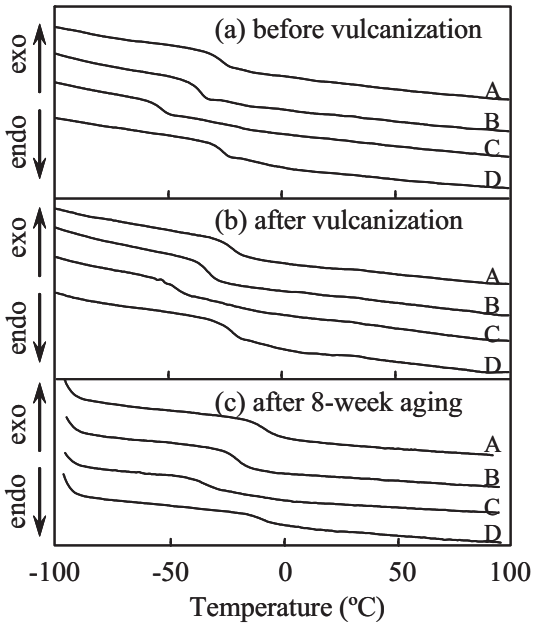

Figure 2. DSC traces of the SBR samples. (a) Before vulcanization, (b) after vulcanization (before aging), and (c) after 8-week aging.

TABLE I Characterization of Styrene-Butadiene Copolymers and the SBR Vulcanizates

Sample code	Polymer chain structure[a] (%) (NMR)			M_w × 10^{-6} (GPC)	M_w/M_n (GPC)	T_g (°C) (DSC)		
	St	1,2-Bd	1,4-Bd			Before vulcanization	After vulcanization	After 8-week aging
A	40.8	30.0	29.2	1.33	1.18	–31.3	–27.8	–16.1
B	30.4	33.0	36.6	1.57	1.24	–40.2	–37.2	–27.0
C	39.9	12.0	48.1	1.17	1.21	–58.2	–52.0	–42.2
D	41.3	28.4	30.3	0.83	1.14	–31.5	–29.1	–13.5
E	68.6	14.3	17.1	0.16	1.05	n.d.[b]	–19.8	–16.9
F[c]	68.6	14.3	17.1	0.16	1.05	n.d.[b]	–14.9	–11.5
G[d]	68.6	14.3	17.1	0.16	1.05	n.d.[b]	–13.0	–8.0

[a] St: styrene unit, 1,2-Bd: 1,2-butadiene unit, 1,4-Bd: 1,4-butadiene unit. [b] Not determined. [c] Using a liquid styrene-butadiene copolymer as the plasticizer. [d] Without plasticizers.

original one during the heating for 8 weeks. The E* values similarly increased by 1.3–2.0 times. A change in the E* and hardness values during the thermal aging is plotted in Figure 3.

The initial E* values depended on the repeating structure of the used SBRs. The E* value for sample E was the highest and changed with the largest increment during the aging, while a small change was observed

TABLE II Mechanical Properties of the SBR Vulcanizates before and after Thermal Aging

Sample Code	Before Thermal Aging				After Thermal Aging[a)]			
	Hardness	E* (MPa)	tanδ	M_{300} (MPa)	Hardness	E* (MPa)	tanδ	M_{300} (MPa)
A	32.9	2.11±0.07	0.471±0.035	1.2	47.8 (1.45)	3.54 (1.68)	0.740 (1.57)	3.2 (2.6)
B	33.1	1.11±0.03	0.145±0.015	1.1	42.2 (1.27)	1.59 (1.43)	0.256 (1.77)	1.5 (1.3)
C	35.5	1.46±0.03	0.207±0.015	1.2	44.3 (1.25)	1.91 (1.31)	0.278 (1.34)	2.0 (1.6)
D	33.6	2.43±0.30	0.745±0.056	1.0	39.9 (1.19)	3.15 (1.30)	0.855 (1.15)	2.3 (2.3)
E	44.5	3.38±0.36	0.550±0.014	1.1[b)]	68.6 (1.54)	6.64[c)] (1.96)	0.739 (1.34)	4.5[b)] (4.3)
F[d)]	48.4	4.16±0.23	0.549±0.025	1.1[b)]	62.8 (1.30)	6.59 (1.58)	0.666 (1.21)	3.2[b)] (2.9)
G[e)]	59.0	6.20±0.19	0.546±0.018	2.3[b)]	73.6 (1.25)	12.34 (1.99)	0.681 (1.25)	6.9[b)] (3.0)

[a)] After heating at 100 ºC for 8 weeks. The values in parentheses indicate the values relative to the original values before the aging. [b)] M_{100} value. [c)] After 6 weeks. [d)] Using a liquid styrene-butadiene copolymer as the plasticizer. [e)] Without plasticizers.

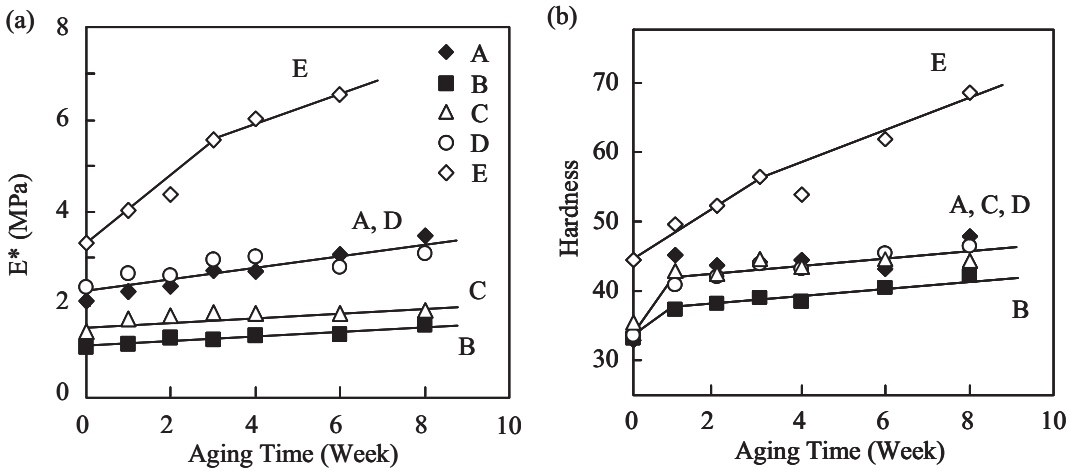

Figure 3. Change in the (a) E* and (b) hardness values of the SBR vulcanizates (samples A−E) during thermal aging.

for the other samples. The change in the hardness showed a similar tendency. Sample E had the largest hardness value as the initial value and the largest increment was observed during the aging. The samples A–D had a similar hardness values before aging. The hardness value for sample B became smaller than the others after the aging. For samples A–D, the hardness drastically changed during the initial aging process for 1 week. In TABLE II, the change in the tanδ and M_{300} values are also shown. The tanδ values increased

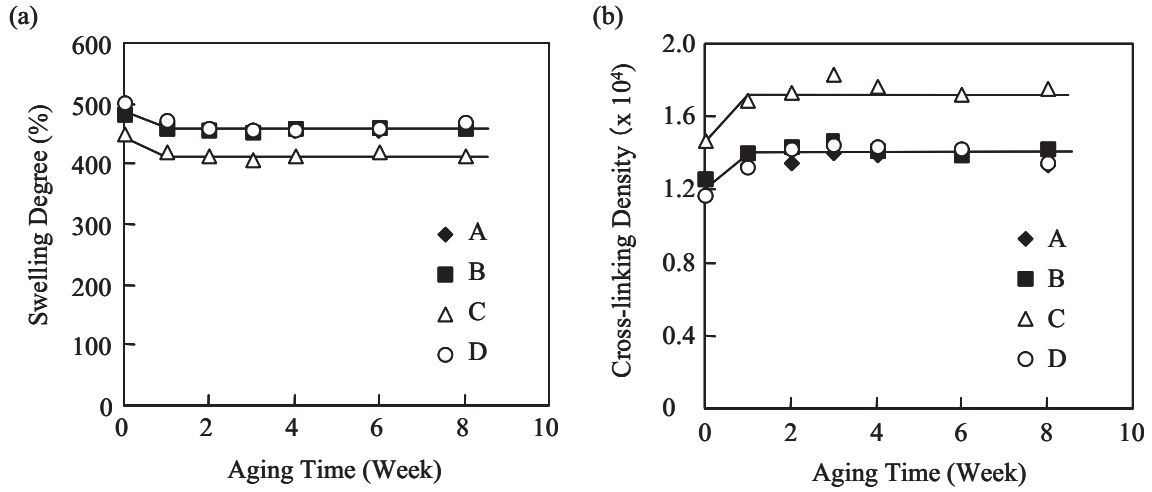

Figure 4. Change in (a) the degree of swelling and (b) the cross-linking density of the SBR vulcanizates (samples A–D) during the thermal aging.

during the aging and reached the values 1.1–1.8 times the original one. The all M_{300} values were in the small range of 1.0–1.2 MPa before heating, but the modulus increased to 1.5–4.5 MPa in the order of E > A > D > C > B after the aging. This order agrees with the order in the E* values.

Thus, some of measurement values for the mechanical properties of the SBR vulcanizates are accounted for by considering the structure of the styrene-butadiene copolymers. The E* values increased during the thermal aging, irrespective of the amount of the styrene and butadiene units in the chain, although it was expected that the contents of the unsaturated groups would influence the hardening behavior of the SBRs. Similarly, the increase in the 1,2-butadiene content also gave high E* and tanδ values. The obtained results agree with the general expectation, that is, the SBR with a high styrene or 1,2-butadiene content is harder and has higher E* value. On the other hand, no difference was observed for the hardness and M_{300} values of samples A–D as the initial values before aging. The hardness and M_{300} values reflect the mechanical properties after a large deformation (300% strain for the latter). On the other hand, the E* and tanδ values were determined by the smaller deformation (12% strain). The effects of the polymer chain structure of the SBR more sensitively appear in the smaller deformation.

3.3. Cross-linking Reactions

The results of the DSC measurements also indicate the hardening of the SBRs after the thermal aging (Figure 2 and TABLE I). The T_g values increased during the 8-week aging in the all cases. This shows a change in the polymer chain mobility by an increase in the number of cross-linking points. Therefore, we evaluated the cross-linking density (ν) for the SBRs before and after the aging. The degree of swelling was used as the index for the degree of cross-linking. Figure 4(a) shows the results of the swelling measurement for each sample after thermal aging for a different time.

Before heating, sample C showed a 451% swelling, which is the lowest among all the samples; and 483–501% for the others. Sample C involves the largest 1,4-butadiene unit (48.1%). This indicates that the 1,4-butadiene repeating unit plays an important role in the vulcanization, as expected. The ν value, which was calculated on the basis of these swelling data, according to Eq. 1, is shown in Figure 4(b). As a result, sample C has the highest ν value. The major part of the cross-linking structures of the SBR is formed during the vulcanization process, but the cross-linked SBRs still contain some other reacting points. After 1 week of aging, the ν value increased by 11–15%. This is due to the formation of additional cross-linking points by the thermal aging.

TABLE III AE and CE Fractions and GPC Data of the SBR Vulcanizate (sample C)

Aging Time (Week)	AE (%)	CE (%)	GPC for CE Fraction		Relative Peak Intensity
			$M_w \times 10^{-4}$	M_w/M_n	
0	21.3	0.1	2.39	1.47	0.18
2	20.0	0.1	2.49	1.55	0.30
4	19.9	0.2	2.44	1.64	0.49
6	19.2	0.4	2.45	1.71	0.80
8	19.1	0.6	2.19	1.75	1.00

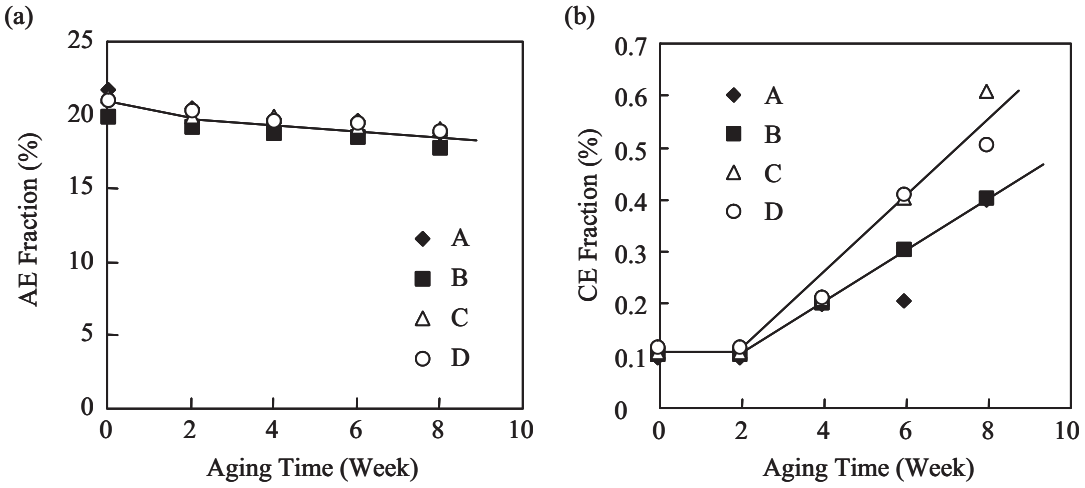

Figure 5. Change in the (a) AE and (b) CE fractions of the SBR vulcanizates (samples A−D) during the thermal aging.

3.4. Polymer Chain Scission

There is the possibility that cross-linking occurs during the thermal aging process on the one hand and the degradation of the polymer chains simultaneously occurs on the other hand. When the bond scission occurs at the branched part of the polymers, a linear free-polymer would be produced. Therefore, we carried out the two-step extraction of the soluble parts from the SBR samples using two kinds of organic solvents. First, oily and low-molecular-weight components, which were added during the vulcanization process, were extracted with acetone under reflux conditions (AE fraction). Subsequently, soluble and free polymers from the residue of the acetone extraction were then extracted with chloroform (CE fraction). The changes in the amounts of the AE and CE fractions are shown in Figure 5(a) and (b), respectively. The amount of AC fraction decreased during the thermal aging, while that of CE fraction increased.

The M_w and M_w/M_n values of the free polymers were determined by GPC analysis. As shown in TABLE III, the M_w and M_w/M_n values were (2.2−2.5) × 10^4 and 1.5−1.7, respectively, and kept constant during the thermal aging. The M_w value of the free polymers was 10^2 times lower than the M_w value (1.17 × 10^6) for the original styrene-butadiene copolymer. An increase in the relative peak intensity of the GPC elusion curves

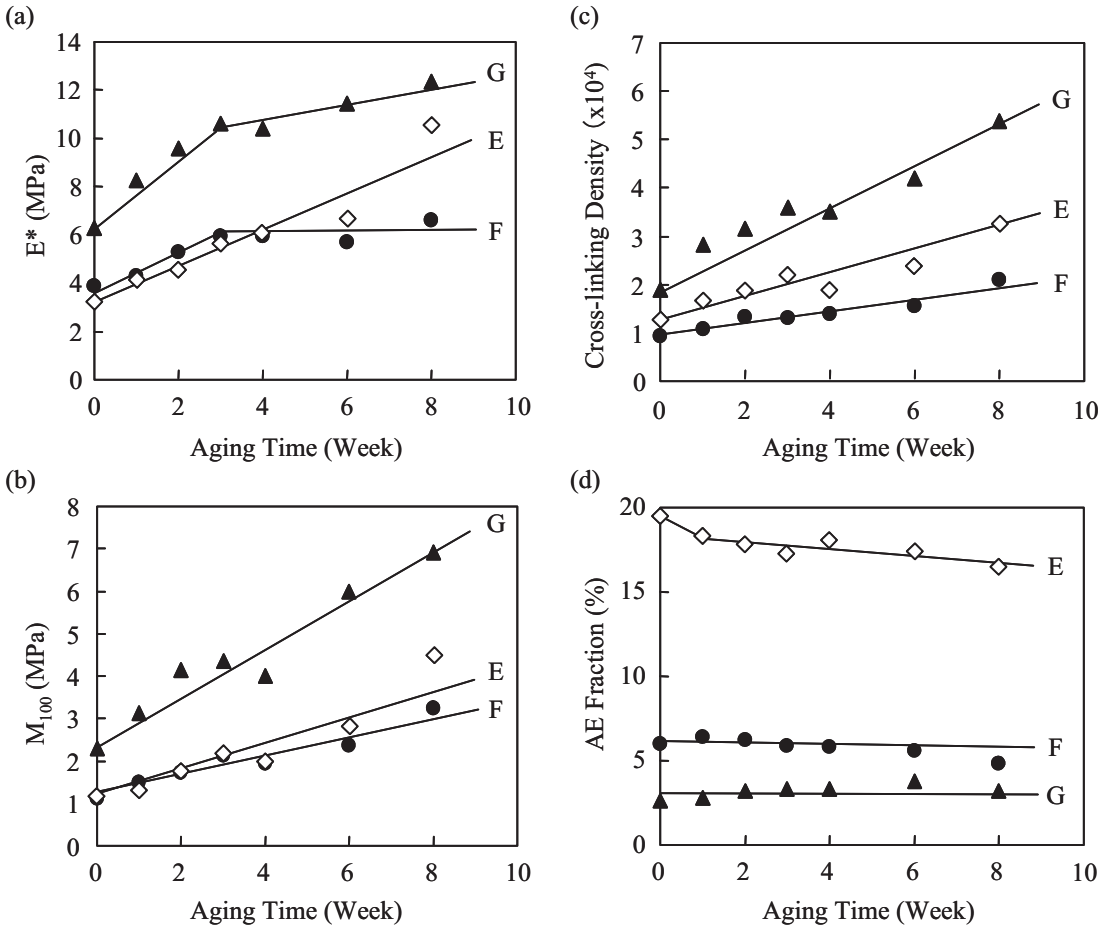

Figure 6. Change in the mechanical and the other properties of the SBR vulcanizates during thermal aging. (a) E*, (b) M_{100} values, (c) the cross-linking density, and (d) AE fraction during the thermal aging. Plasticizer: (◊) a process oil (sample E), (●) liquid styrene-butadiene copolymer (sample F), and (▲) without plasticizers (sample G).

agrees with the fact that the CE fraction increased according to the aging time. The free polymers (CE fraction) seem to be formed irrespective of the chain structure of the polymers. In order to evaluate a change in the chemical structure of the polymer chains, the IR spectrum of the SBRs was recorded. If an oxidation reaction occurs, an absorption band due to the carbonyl group is detected. As a result, the peak due to the carbonyl group at 1730 cm^{-1} was detected from the initial stage of the thermal aging, although quantitative analysis was difficult because of the small intensity of the peak.

3.5. Effect of Plasticizers

Moreover, we noticed a decrease in the amounts of the AE fractions during the thermal aging [Figure 5(a)]. The oily components that were added to the samples during the vulcanization process slowly vaporize during the thermal aging over a long time.[27] A constant decrease in the amount of the oily component influences the overall mechanical properties. In fact, when nonvolatile compounds as the plasticizers, such as liquid types of polybutadiene, a styrene-butadiene copolymer, and natural rubber, were used instead of the conventional process oil, we obtained the SBR vulcanizates that show the superior physical properties of during the thermal aging process. Here we show preliminary results for the mechanical properties of the SBR prepared using a liquid styrene-butadiene copolymer.[28] The SBR with a high styrene content was only used

for the vulcanization using liquid polymer as the plasticizer, because the other SBRs with a low styrene content gave vulcanized samples with insufficient mechanical strength.

When the liquid styrene-butadiene copolymer was used as the plasticizer (sample F), the increase in the hardness and modulus was suppressed during the aging, as shown in TABLE II and Figure 6. This is in contrast to a large increase in the hardness, E*, and M_{100} values for the cases without any plasticizer. The SBR vulcanizate was also prepared using a liquid polyisoprene as the plasticizer. The dynamic mechanical spectroscopy and DSC experiments have revealed the phase separation after vulcanization. The phase-separated structure is due to the immiscibility of the SBR and polyisoprene domains, and changed to the homogeneous structure during the aging process after 2−3 weeks. The aging behavior also changed according to the change in the phase structure. The liquid polymer chains incorporated into the SBR networks play an important role in the suppression of the polymer cross-linking, leading to the hardening of the rubber materials.

In order to examine a change in the chemical structure of the SBR vulcanizates, the observation of morphological change was attempted, but no valuable information was obtained during scanning and transmission electron microscopic observations. The rubber materials used for tires usually consist of not only polymer materials but also carbon blacks and the other inorganic materials. The dispersion and interfacial structures of carbon blacks in a polymer matrix can be observed by microscopic methods. In contrast, the SBR vulcanizates prepared in the present study imply no carbon blacks. In this case, it is difficult to detect the phase separated structure of the added polymers as the plasticizers and the SBR domains. During the thermal aging process, carbon and oxygen radicals are formed and they readily abstract hydrogens from the liquid polymer chains rather than from the SBR networks. Consequently, the cross-linking reaction between the polymer chains would be retarded. The free polymer chains are important for maintaining the stable network structure and the acceptable physical properties. The detailed results for the effects of the nonvolatile liquid polymers as the plasticizers on the properties of the SBRs are separately reported in our recent papers.[29,30]

4. Conclusions

The change in the mechanical properties of the SBRs with different styrene and butadiene contents and molecular weights during thermal aging was analyzed on the basis of the experimental results for the determination of the hardness and modulus values as well as the swelling and extractions experiments. During the thermal aging process, an increase in the cross-linking density of the SBRs resulted in increases in the hardness, E*, tanδ, and M_{300} values. Furthermore, we also noticed the contribution of the constant evaporation of the oily component, which was added to the vulcanization process, to increases in the modulus during the long-time aging process. We demonstrated the validity of the use of nonvolatile liquid polymer as the plasticizer to obtain the desired physical properties of the SBR vulcanizates during the thermal aging.

5. References

1) M. Demirors, *Encyclopedia of Polymer Science and Technology; 3rd edition*, Vol. 4, Ed., J. I. Kroschwitz,; Wiley-Intersciecne: New York, 2003, p. 229.
2) A. F. Halasa, J. Prentis, B. Hsu, and C. Jasiunas, *Polymer*, **2005**, *46*, 4166.
3) S. S. Choi, *J. Anal. Appl. Pyro.,* **2002**, *62*, 319.
4) R. E. Wetton, *Polym. Test.,* **1991**, *10*, 175.
5) J. Zhao and G. N. Ghebremeskel, *Rubber Chem. Tech.,* **2001**, *74*, 409.
6) L.Pellicioli, S. K. Mowdood, F. Negroni, D. D. Parker, and J. L. Koenig, *Rubber Chem. Tech.,* **2002**, 75, 65.
7) W. Schnabel, *Polymer Degradation: Principles and Practical Applications*; Hanser: Munchen, 1981.
8) G. -Y. Li and J. L. Koenig, *Rubber Chem. Tech.,* **2005**, *78*, 355.
9) T. Saito, *J. Soc. Rubber Ind. Japan,* **1995**, *68*, 284.

10) A. Ahagon, M. Kida, and H. Kaidou, *Rubber Chem. Tech.,* **1990**, *63*, 683.
11) H. Kaidou and A. Ahagon, *Rubber Chem. Tech.,* **1990**, *63*, 698.
12) A. Santoso, U. Giese, and R. H. Schuster, *Rubber Chem. Tech.,* **2007**, *80*, 762.
13) K. R. J. Ellwood, J. Baldwin, and D. R. Bauer, *Rubber Chem. Tech.,* **2006**, *79*, 249.
14) R. L. Clough and K. T. Gillen, *Polym. Deg. Stab.,* **1992**, *38*, 47.
15) G. Mathew, P. V. Pillai, and A. P. Kuriakose, *Rubber Chem. Tech.,* **1992**, *65*, 277.
16) C. Fulber, B. Blumich, K. Unseld, and V. Herrmann, *Kaut. Gum. Kunst.,* **1995**, *48*, 254.
17) F. M. Helaly, W. M. Darwich, and M. A. Abd El-Ghaffar, *Polym. Deg. Stab.,* **1999**, *64*, 251.
18) G. R. Hamed and J. Zhao, *Rubber Chem. Tech.,* **1999**, *72*, 721.
19) V. Nandanan, R. Joseph, and K. E. George, *J. Appl. Polym. Sci.,* **1999**, *72*, 487.
20) S. S. Choi, *J. Appl. Polym. Sci.,* **2000**, *75*, 1378.
21) H. Modrow, J. Hormes, F. Visel, and R. Zimmer, *Rubber Chem. Tech.,* **2001**, *74*, 281.
22) B. T. Poh, H. Ismail, E. H. Quah, and P. L. Chin, *J. Appl. Polym. Sci.,* **2001**, *81*, 47.
23) V. Tanrattanakul and W. Udomkichdecha, *J. Appl. Polym. Sci.,* **2001**, *82*, 650.
24) D. H. Yin, Y. Zhang, Y. X. Zhang, Z. L. Peng, Y. Z. Fan, and K. Sun, *J. Appl. Polym. Sci.,* **2002**, *85*, 2667.
25) P. J. Flory and J. Rehner, Jr., *J. Chem. Phys.,* **1943**, *11*, 521.
26) K.Matsuzaki, T. Uryu, and T. Asakura, *NMR Spectroscopy and Stereoregularity of Polymers*; Japan Scientific Societies: Tokyo, 1996.
27) T. Kataoka, P. B. Zetterlund, and B. Yamada, *Rubber Chem. Tech.,* **2003**, *76*, 507.
28) T. Nakazono and A. Matsumoto, *J. Appl. Polym. Sci.,* **2010**, *118*, 2314.
29) T. Nakazono, A. Ozaki, and A. Matsumoto, *Chem. Lett.,* **2010**, *39*, 268.
30) T. Nakazono, A. Ozaki, and A. Matsumoto, *J. Appl. Polym. Sci.,* in press (DOI 10.1002/app.33165).

Effects of Information Provision to Encourage Public Involved Consciousness Toward Sustainable Bus Service

Noboru ISE* and Yasuo HINO**

(Received September 30, 2010)

Synopsis

Recently, the public involved approach has been introduced to local public transportation planning, because the operation of bus service based on taxes was not sustainable. However, it seems that public involved approach has not yet fully generated, and much more still remains to be improved, such as information provision, components of approach and division of roles.

This study focused on the effectiveness of information provision in cooperative activities to encourage the public involved consciousness. As a result, it was revealed that it was important to provide information for understanding the future situation of individual and area through the cooperative activities, in order to realize the sustainable bus transportation services.

Keywords: Bus service, Public involved approach, Information provision, Public transportation planning

1. Introduction

Recently, bus companies have been reducing bus services because of decrease of passengers due to the motorization. Therefore, many local governments have introduced "community bus", as the substitute of a route served bus, or the welfare service for the inconvenient areas for public transport. However, in some cases, the number of bus users has grown slowly and public financial conditions have been deteriorated, because these services did not match the travel needs of residents.

Meanwhile in the planning of local public transportation, it has been clarified that it is necessary to involve not only supply-side such as bus company and local government but also local residents[1), 2)]. In addition, Okamura pointed out that both needs and critical consciousness for mobility were essential to keep the sustainable local public transportation[3)]. These findings mean that, it is essential to set up meetings to own jointly some information of current condition of public transportation and consider the necessity for local public transportation. However, it is still unclear what kind of information is effective to consider the necessity for local public transportation.

In this study, we aimed to clarify the effective kinds of information to realize the sustainable bus services by analyzing the relation between understanding of information and recognition of necessity of bus services, public involved consciousness or needs of bus use.

2. Outline of Case Study

2.1 Outline of Surveyed City and Background

A case study was carried out in Kawachi-nagano city as suburban city of Osaka prefecture, Japan. Recently, this city faces some problems such as declining and aging population and increasing nuclear family. Therefore, the basic plan to build up "the network of public transportation" for residents' mobility has been developed by the research group, which was organized by multiple sections of Kawachi-nagano city, with the support of academic staffs of Osaka City University in 2005. As a result, the report of "proposal for public transportation in Kawachi-nagano city" was published in October 2008, based on activities for two years.

In addition, the plan of comprehensive cooperation for local public transportation was also published in November 2009. In this plan, the process of public involved approach was concretely proposed.

* Research Associate, Urban Research Plaza
** Professor, Department of Civil Engineering

2.2 Outline of Case Study Area

Shimosato-Monzen-Nakao area was selected as a case study area to introduce the public involved approach, because in this plan, this area was pointed out as one of areas which require the bus service because of the strong needs for bus services.

This area is a mountain area located around 4km to south-west from the Kawachi-nagano station in central of Kawachi-nagano city. The local population is about 900 and the ratio of aged population is around 26%, and the longest distant from bus stop is around 1.1km away, as shown in Figure 1.

If the available area for bus transportation service is defined within 400m from bus stop, the ratio of population who can use bus transportation service is 29.7%. In the case of 200m, the ratio is just 10.6%. In addition to low level of bus service, the decreasing trend of the number of bus users in this area is stronger than that in the whole city as shown in Figure 2.

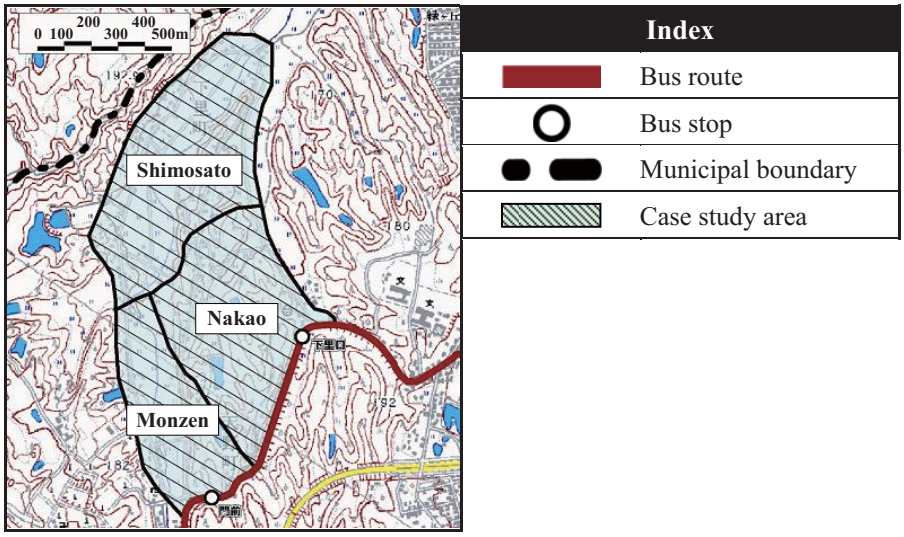

Figure 1 Location of Shimosato-Monzen-Nakao area as a case study

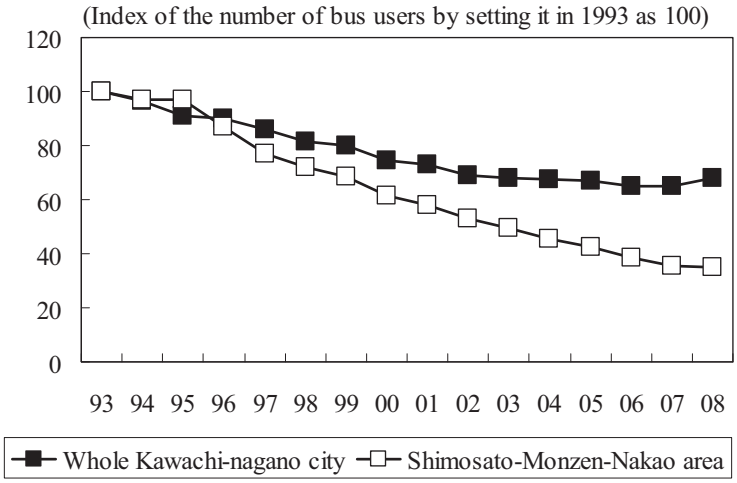

Figure 2 Change of bus passengers in Shimosato-Monzen-Nakao area and whole Kawachi-nagano city

3. Activities of Public Involved Approach in Case Study Area

The public involved process in this case study is shown in Table 1. The cooperative organization consists of residents (including members of community association), local government, staff of bus company and academic experts of Osaka City University.

Table 1 Process of public involved activities in case study area

Activity content	Details
Meeting of cooperative organization (1)	・Discussion of activity policy for bus services
Meetings of cooperative organization (2)-(4)	・Consideration of first questionnaire survey
First questionnaire survey	・Investigation of bus demands and problems
Meetings of cooperative organization (5)	・Explanation of results of first questionnaire survey and the plan of a trial bus service
Meeting to explain to local residents	・Discussion for the improvement of a plan of trial bus service
Event (1)	・Inspection of a trial bus route and bus stops
Event (2)	・Test-riding event of a trial bus service
Second questionnaire survey	・Investigation of 1) intention to use trial bus 2) public involved consciousness 3) recognition of the necessity of bus transportation service 4) understanding of provided information
Start of trial operation	—

3.1 Meetings of Cooperative Organization

At the first meeting on October 31st, 2008, it reached an agreement that it is necessary to investigate bus needs of local residents, in order to consider the direction of bus service. Then, in order to consider survey items and method, three times of meetings were held from November to December 2008. As a result, the questionnaire survey for investigating bus needs was conducted from February to March 2009.

3.2 First Questionnaire Survey for Determining Bus Needs

The questionnaire survey was conducted for all residents aged 7 or over in this area from February to March 2009, 675 respondents were obtained for 1000 questionnaire sheets distributed.

Figure 3 shows that more than 50% of the respondents of all age groups intend to use new bus service. Especially, it is clarified that there are a number of bus needs for commuting to school by residents who are 19years old or under and for going to hospital by residents who is 70 years old or over.

Figure 4 shows that there are a number of residents who intend to go around Kawachi-nagano station in the city center, Osaka city and Sakai city. That is, Kawachi-nagano station is main destination for bus users in this area.

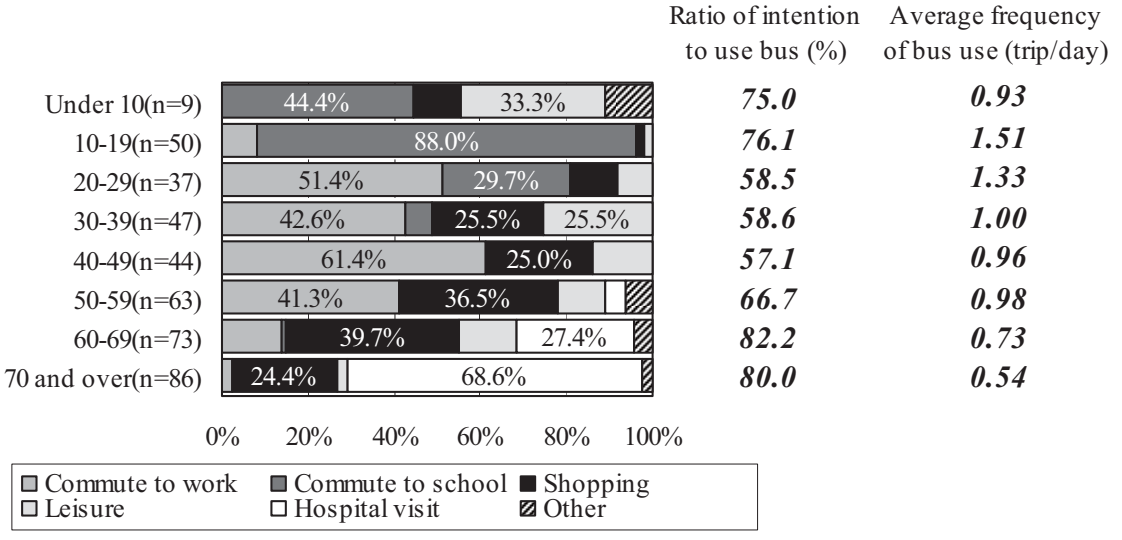

Figure 3 Bus needs by age-group

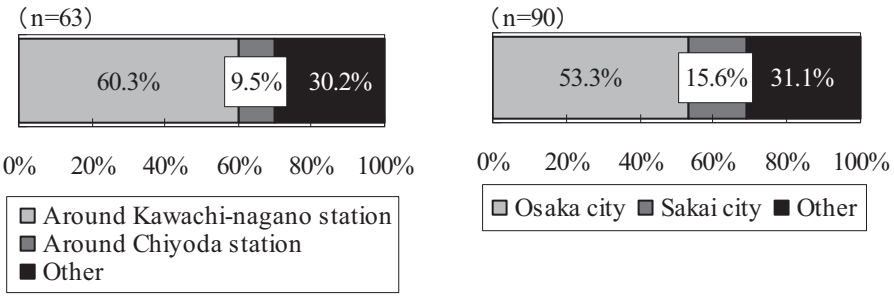

Figure 4 Passengers' destination by using bus

3.3 Introduction of Trial Bus Service

Based on the results of questionnaire survey, it should be evaluated that the introduction of new bus service connected to existing bus route is helpful to improve convenience of bus transportation service and mobility of residents. Therefore, local government proposed the route and bus stops for new bus service based on the results of questionnaire survey at the meeting. Finally, the cooperative organization modified the first proposal of trial bus service as shown in Figure 5, according to major opinions of the meeting.

After the new bus service was decided, some events such as test-riding and inspecting bus route and bus stops were taken place, in order to make the new bus service known to all local residents.

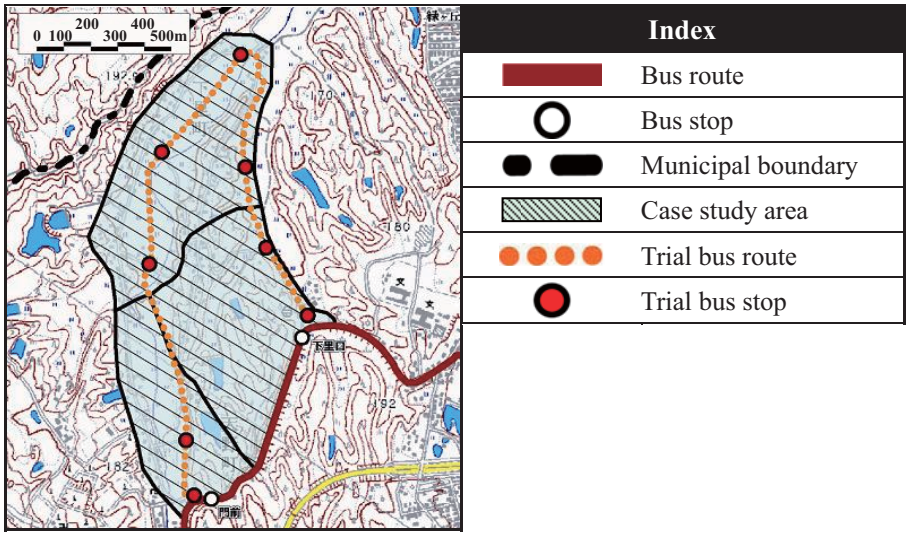

Figure 5 Trial bus route map

4. Evaluation of Information Provision in Public Involved Activities

4.1 Provided Information in Public Involved Activities

Some information was provided in public involved activities in order to consider the necessity of bus service for not only present situation but also future prospects. Also for the non-participated residents, participants of meetings were recommended to inform the contents of information to them. Furthermore, all information, as shown below, was provided to all residents by using notice for circulation.

1) The number of bus users in this area and the whole of city have been decreasing, year by year.
2) Almost of all people become to need the bus service with aging.
3) It may difficult to sustain the current bus services in the future due to the recent trend of decrease of bus users.
4) The timetable, route and location of bus stops of the trial bus service were decided.
5) 514 JPY in taxes was provided to some bus operations every year.

6) It is important to cooperate with residents, local government and bus company, as the public involved activities.
7) It may be investigated whether or not the bus service will be sustained, based on the results of trial service.

4.2 Outline of Second Questionnaire Survey

After explanation of trial bus service at the meetings, the second questionnaire survey was conducted for all residents in this area in December 2009, in order to evaluate effect of information provision. Especially, the relation between the contents and method of information provision and the common consciousness about necessity of bus service, and the public involved consciousness, and the intention to use trial bus service, was investigated. The items of questionnaire survey are shown in Table 2. 289 respondents were obtained for 880 questionnaire sheets distributed.

Table 2 Second questionnaire items

Kind of attribute	Items
Individual attribute	address, sex, age, occupation
Intention to use bus	need of bus use, destination, trip frequency, trip purpose
Understanding of information	understanding of each information
Recognition of the necessity of bus transportation services	recognition of the necessity of bus services and some reasons
Public Involved consciousness	workable activities to contribute to sustain bus service

* 18 years old or under answered only “Individual attribute” and “Intention to use bus”.

4.3 Recognition of the Necessity of Bus Transportation Services

Some interesting finds for recognition of the necessity of bus transportation services and some reasons came out of this survey as follows (See Figure 6).

1) Around 90% of the respondents answered what bus services were necessary.
2) 35% of the respondents answered ”It is necessary for me at present”. On the other hand, more than 50% answered “It is necessary for other residents at present”.
3) 55% of the respondents answered “It is necessary for me in the future”.

As a result, it is clarified that the future situation is important factor to consider the necessity of bus services.

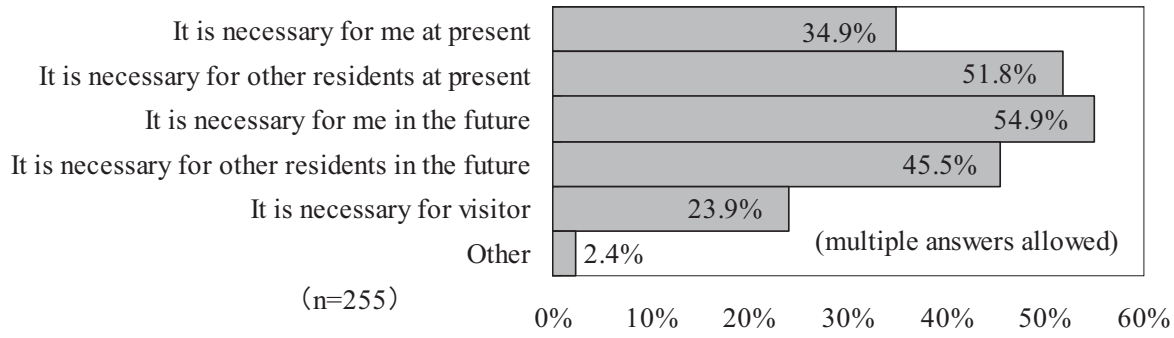

* 90.6% (n=231) of 255 respondents answered “bus transportation services is necessary”.

Figure 6 Reasons for necessity of bus services

4.4 Intention to Use Trial Bus Transportation Service

The ratio of intention to use the bus services did not changed before and after explanation of trial bus transportation services at the meetings. This result means that the real possibility of bus service was increased by introducing the public involved approach; nevertheless the available area of the trial bus service was limited for the planned route.

4.5 Relation between Recognition of Information and Necessity of Bus Service

Here, the result of factor analysis, which is evaluated the effect of provision information to promote the common consciousness about necessity of bus service, is shown as follows (See Table 3).

1) Relation between individual characteristics and recognition of the necessity of bus service

Although the residential areas influenced with the statistically-significant difference in recognition of necessity of bus service, as for other factors, there were no statistically-significant difference.

2) Relation between understanding of information and recognition of the necessity of bus service

Some kinds of information which had the statistically-significant difference in recognition of the necessity of bus service are shown as follows.

a) [Information No.1] The number of bus users in this area and the whole of city has been decreasing ($\chi^2(1)=4.23$, $p=0.05$)

b) [Information No.2] Almost of all people become to need the bus service with aging ($\chi^2(1)=9.25$, $p=0.01$)

c) [Information No.3] It may become difficult to sustain current bus transportation services in the future based on recent trend of the decreasing bus users ($\chi^2(1)=3.37$, $p=0.10$)

d) [Information No.6] It is important to cooperate with residents, local government and bus company ($\chi^2(1)=4.86$, $p=0.05$)

Table 3 Analysis of factors which contribute to recognize the necessity of bus services

Factor			Answered necessity		Answered non-necessity		Result of chi-square test
			Frequency	Relative frequency	Frequency	Relative frequency	
Sex	Male		102	0.879	14	0.121	
	Female		126	0.926	10	0.074	
Age	Under 20		11	0.786	3	0.214	
	20-39		44	0.880	6	0.120	
	40-59		62	0.912	6	0.088	
	60-79		83	0.922	7	0.078	
	80 and over		15	0.882	2	0.118	
Occupation	Agriculture, forestry and fishery		13	0.929	1	0.071	
	Self-owned business		20	0.952	1	0.048	
	Company employee, civil servant		65	0.890	8	0.110	
	Student		12	0.750	4	0.250	
	Part-time jobber		18	0.900	2	0.100	
	Housekeeper		49	0.925	4	0.075	
	Disemployment		41	0.911	4	0.089	
Residential area	Shimosato area		126	0.947	7	0.053	***
	Monzen area		64	0.800	16	0.200	
	Nakao area		36	0.973	1	0.027	
Provided information	Decreasing of the number of bus users in this area and the whole of Kawachi-nagano city	Comprehend	76	0.962	3	0.038	**
		Un-comprehend	155	0.881	21	0.119	
	Increase in the ratio of bus use with aging	Comprehend	66	1.000	0	0.000	***
		Un-comprehend	165	0.873	24	0.127	
	It is difficult to sustain bus transportation services	Comprehend	70	0.959	3	0.041	*
		Un-comprehend	161	0.885	21	0.115	
	Trial bus transportation service such as route and time table etc	Comprehend	71	0.934	5	0.066	
		Un-comprehend	160	0.894	19	0.106	
	Amount of tax used for bus transportation services (JPY/person)	Comprehend	34	0.971	1	0.029	
		Un-comprehend	197	0.895	23	0.105	
	Importance of cooperation	Comprehend	48	1.000	0	0.000	**
		Un-comprehend	183	0.884	24	0.116	
	Information for making a decision about continuing bus transportation service	Comprehend	56	0.949	3	0.051	
		Un-comprehend	175	0.893	21	0.107	

* Chi-square test for independence *** : $p \leq 0.01$ ** : $p \leq 0.05$ * : $p \leq 0.10$

3) Relative analysis among factors related to recognition of the necessity of bus services

The relation between understanding of information and residential area was analyzed, because residential area has statistically-significant difference in recognition of the necessity of bus transportation service. As a result, there is just statistically-significant difference between residential area and the information No.6 as shown in Table 4.

Therefore, it was revealed that the information No. 1, 2 and 3 are effective to promote the recognition of the necessity of bus service, and effectiveness of the information No.6 depends on the area characteristics such as service level of public transportation.

These results mean that provision of information related to the changes of utilization ratio of bus service with aging and the trend of the number of bus users is essential for promoting the common consciousness of necessity of bus transportation services.

Table 4 Relative analysis between factors which contribute to recognize of the necessity of bus services

Factor			Shimosato area		Monzen area		Nakao area		Result of chi-square test
			Frequency	Relative frequency	Frequency	Relative frequency	Frequency	Relative frequency	
Provided information	Decreasing of the number of bus users in this area and the whole of Kawachi-nagano city	Comprehend	43	0.323	21	0.263	13	0.351	
		Un-comprehend	90	0.677	59	0.738	24	0.649	
	Increase in the ratio of bus use with aging	Comprehend	38	0.286	16	0.200	12	0.324	
		Un-comprehend	95	0.714	64	0.800	25	0.676	
	It is difficult to sustain bus transportation services	Comprehend	39	0.293	22	0.275	11	0.297	
		Un-comprehend	94	0.707	58	0.725	26	0.703	
	Importance of cooperation	Comprehend	37	0.278	7	0.088	3	0.081	***
		Un-comprehend	96	0.722	73	0.913	34	0.919	

* Chi-square test for independence *** : p≤0.01 ** : p≤0.05 * : p≤0.10

4.6 Relation between Common Consciousness for Necessity of Bus Service and Other Consciousness

As a hypothesis, in the case at least selected one of all activities to contribute to sustain bus service in this area (Table 5), it was defined “high cooperative consciousness”, on the other hand it was defined “low cooperative consciousness” in the case selected No.7 in Table 5. Then the relation between this grouping and the common consciousness for bus necessity was analyzed. As a result, some significant findings came out of analysis, as follows (See Figure 7).

1) As the ration of the necessity of bus services was higher, the understanding ratio of the public involved consciousness was higher ($\chi^2(1)=34.4$, p=0.01).
2) There is also same tendency about the intention to use trial bus service ($\chi^2(1)=33.0$, p=0.01).

From these findings, it must be clear that, if residents build consensus which bus transportation services are necessary for this area, not only the public involved consciousness is promoted but also bus users increase.

Table 5 Kind of activities to contribute to sustain bus service in this area

Kind of works to contribute to sustain bus transportation service in this area
1) Ride bus vehicle and help elderly people to board and exit bus vehicle, as volunteer
2) Call for residents to use bus
3) Increase the number of individual bus use
4) Participate the meetings to discuss bus transportation services
5) Make bus stop more comfortable
6) Pay part of the cost for operating bus transportation
7) Nothing special

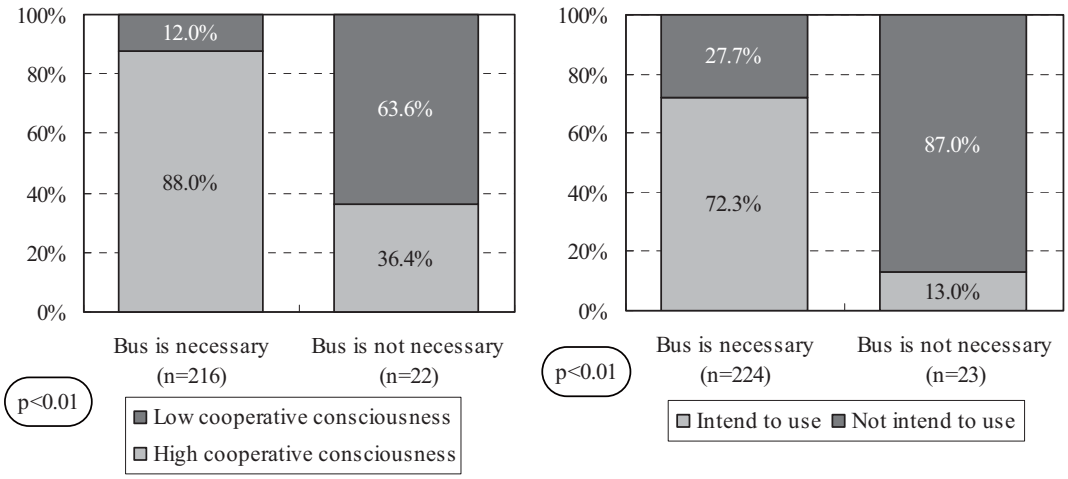

Figure 7 Relations between common consciousness for necessity of bus service and other consciousness

5. Conclusion

This study mainly aimed to evaluate the effect of information provision to promote the public involved consciousness for realizing the sustainable bus service. Some major results came out of these analyses are summarized as follows.

1) It is essential to provide appropriate information, in order to build the common recognition of the necessity of bus transportation service.
2) Especially, it is effective to provide three information, such as “The number of bus users in this area and the whole of city has been decreasing”, ”Almost of all people become to need the bus service with aging” and ”It may become difficult to sustain current bus transportation services in the future based on recent trend of the decreasing bus users”.
3) If residents build the consensus that bus services are necessary for this area, not only the public involved consciousness is promoted but also bus users increase.

As a result, it must be concluded that it is important to provide information for understanding the future situation of individual and area through the public involved activities, in order to realize the sustainable bus services.

6. Acknowledgements

This study was implemented as a part of a joint research with Kawachi-nagano city. We would like to thank members of research group, cooperators in the questionnaire surveys.

7. References

1) Nakamura, F., Morita, T., Akimoto, N. and Takahashi, K. (1998) A Fundamental Study on Role of A Process of Public Involvement Approach, **Infrastructure Planning Review**, **No.15**, 133-144.
2) Kato, H. and Takasuga, D. (2003) An Upward Process Management Scheme in order to Create Self-controlled Local Transit System under Deregulated Situation, **Proceedings of Infrastructure Planning**, **Vol.27**, 4pages (CD-ROM).
3) Okamura, T., Nakamura, F. and Yokoyama, T. (2009) A Study on Support from local residents for the Realization of the Sustainable local public transportation, **Journal of Traffic Engineering**, **Vol.29**, 361-364.

Information Provision via Traceability System for Civil Structures

Hirokazu MATSUMOTO* and Takashi UCHIDA**

(Received September 30,2010)

Synopsis

Recently, public administration is increasingly required to disclose information. Now, therefore, the law related to information disclosure is enhanced and local governments are increasingly releasing their information. However, citizens rarely access that information, partly because of the procedural time and effort necessary. It is important that people be able to know information about civil structures easily, especially that which is closely associated with daily life.

We propose a “Traceability System for Civil Structures” as one information service system. This paper shows a process to produce the system and experimentation using a prototype system. The results show citizens’ high interest in administrative information and the feasibility of the system.

KEY WORDS: Information provision, Accountability, Civil consciousness change, Joint effort of public and private sectors

1. Introduction

1.1 Purpose

The Act on Access to Information Held by Administrative Organs went into operation in 2001. This law was intended to require agencies to produce explanations of governmental activities for the public and promote fair and democratic administration through correct public understanding and criticism. However, only a few people have accessed administrative information, partly because such large amounts of time and effort are necessary under the present system.

However, public administrative organs have stored much information about civil structures. Such information is sometimes provided when public works projects are conducted with residents' views considered through public involvement. In such cases, however, information that forms a gap separating administrative officers and citizens becomes a problem. The necessary information is too much to understand at one time and is usually specialized.

Against this background, we propose a “Traceability System for Civil Structures” (TSCS) as a means to provide public information. For this study, we built a prototype system with actual information and a screen.

---

*Student, Doctor Course of Department of Civil Engineering

**Associate Professor, Department of Civil Engineering

Furthermore, by experimentation using the system, we investigate citizens' concerns with administrative information and we evaluate the system.

1.2 Outline of TSCS

For using the system, a mobile phone with a QR code scanning function is needed. First, a person finds a QR code sign on civil structures. After accessing it anyone can obtain basic information about the structure from the sign. If more information is demanded, the person can access a database of civil structures on-site with the mobile phone.

2. Process of the study

The process of the study is presented in Fig. 2. It comprises two distinct parts: the Preparation part (chapters 3–5) and the Impact part (chapters 6–7).

Two perspectives in the Preparation part are presented below.

1) How should public administration present the information? In other words, we want to know how to translate internal administrative information into public information.
2) What kind of information should public administration reveal? We produce guidelines incorporating three methods, a similar system in other areas, necessity as public information, and existing data in public administration.

Based on these results, we develop a web system and a QR code sign as a prototype TSCS.

In the Impact part, we investigate citizens' concern with public information and evaluate the prototype. The way is hearing of opinions. After test subjects run through web pages with the prototype, we ask them several prepared questions.

In the last chapter, we present the results achieved to date. In addition, future possibilities that can come from TSCS are explained.

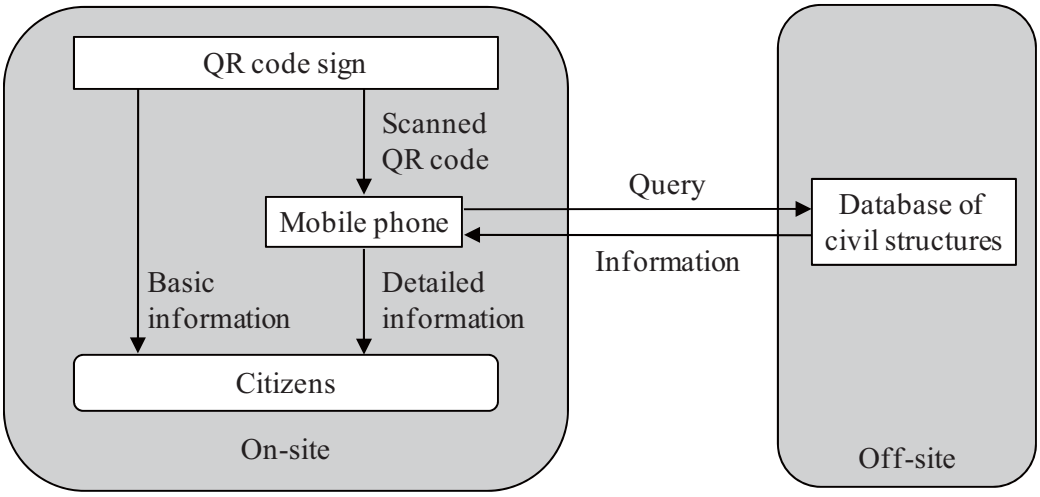

Fig. 1 Outline of TSCS.

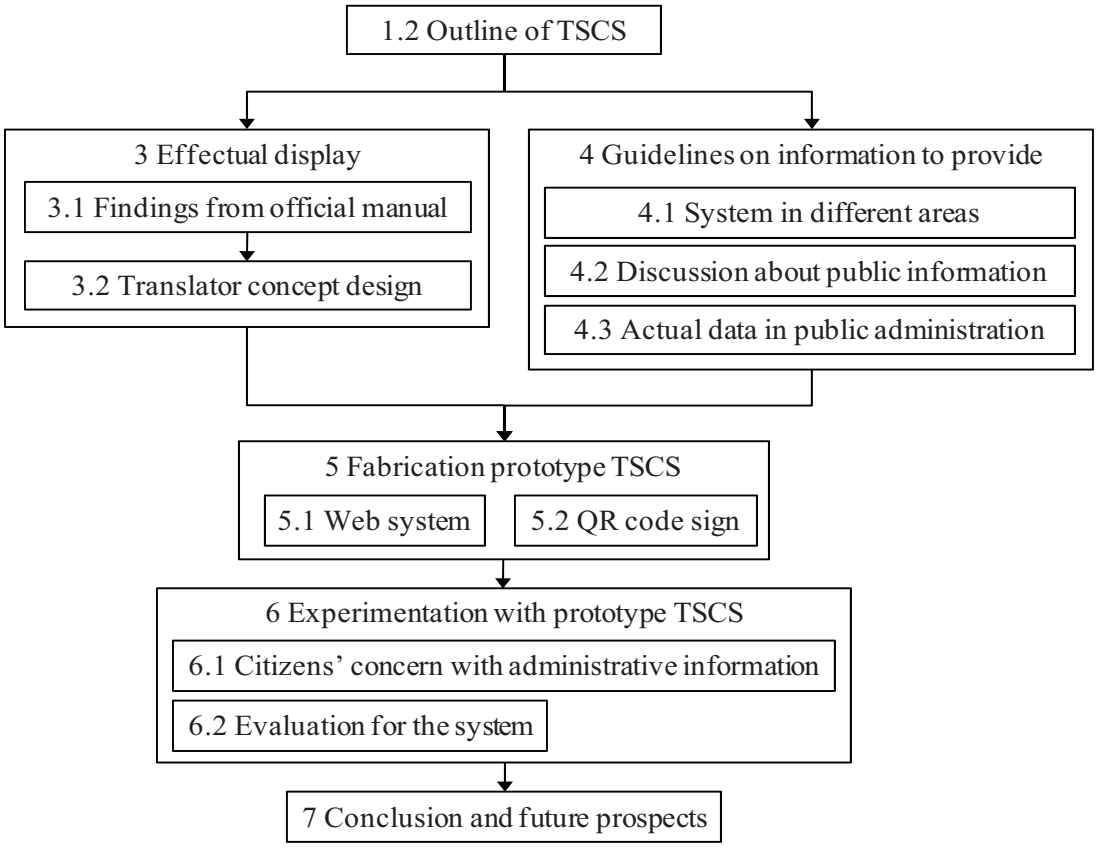

Fig. 2 Process of the study.

3. Effectual display

3.1 Finding from official manual

We treat costs and benefits for road-related projects using the official manual[1)-4)] because such projects have been conducted for a very long time, and because the system is quite complicated. The information can provide an excellent example of the view that specialist information should be provided simply to citizens.

Some findings are those listed below.

1) Indicators used for project evaluation differ from those in the past. Therefore, past and current projects are incommensurable with those indicators alone.
2) Values for benefit analysis are various: conceptualistic value, representative value, average, temporary value, constant etc. For citizens to understand them, a composite indicator should be broken down to base data.

3.2 Translator concept design

Based on the results described above, we design the Translator concept to show the information appropriately. Three concepts are shown below.

1) Time Translator … It enables comparison between past and present data. Sometimes, it involves the use of a new indicator.

2) Breakdown Translator … It breaks down the composite indicator to base data and helps users judge independently.
3) Interdepartmental Translator … It represents unification of words treated differently in each department, which can discover the potential in the information. Additionally, it bridges the language gap separating administrative officers and citizens.

4. Guidelines on information to provide

4.1 System in different areas

The investigation objects for this study are three traceability systems in operation. The industrial segments are: 1) food manufacturing industry, 2) agriculture, forestry and fisheries industry, and the 3) food-service industry.

We first create a list of every item shown by the systems. The items are broadly divisible into two categories by purpose. One category consists of information that is safeguarded to protect the public trust. Another category consists information that can be used to build value of a company or commercial products.

The former category can be divided further into three categories according to contents of information. We label them as “Producer”, “How to”, “Content”. The latter category is labeled as “Appeal”. Each category and the explanation is presented in Table 1.

We think that public information must be provided exhaustively. Therefore, TSCS should have information assigned to these categories.

4.2 Discussion about public information

A big difference between TSCS and other traceability system is a system-managed object. The objects in TSCS are civil structures, into which are injected public funds. Therefore, information related to costs must be provided.

Furthermore, when citizens determine the need for a civil structure, information of benefits is necessary. It is impossible to provide all such information simultaneously.

In addition to the categories listed in Table 1, two categories are necessary for TSCS. Each category and its explanation is shown in Table 2.

Table 1 Categories of information required for a traceability system

Producer	・information about person, company, organization related to the development
How to	・information about a production method or construction rule
Content	・information about material contained in a structural object
Appeal	・associated information and ingenuity to increase value

Table 2 Categories of information required in case public funding is used

Cost	・financial information to achieve accountability
Benefit	・profit from the structural object or beneficiaries

4.3 Actual data in public administration

We obtained a database and five administrative record files about civil structures from a certain city's construction bureau. This study is based on those data.

Next, a correspondence relation between actual data and the categories Tables 1 and 2 is confirmed. It is necessary for public administration to provide information responding to the categories. Management of information in public administration can accomplish that.

5. Fabricated prototype of TSCS

5.1 Web system

Display items on each page are determined using the information presented in chapters 3 and 4. We classified information to show to citizens into six web pages. Titles of the respective web pages are shown in Table 3.

Table 3 List of display items on each page

Title of Web page	Itemized description
Basic Information	＜name of facility＞ ＜serial number＞ ＜location＞ ＜facilities purpose＞ ＜construction organization＞ ＜management organization＞※ ≪appearance of facility≫ ≪map of the area≫
Construction Information	＜date of building＞ ＜floor number＞ ＜structure＞※ ＜site area＞ ＜architectural area＞ ＜total floor area＞ ＜building company＞ ＜design company＞ ≪special design≫ ＜design drawing＞ ＜history of reconstruction work＞
Cost Information	○running cost : ＜total amount＞ ＜electricity＞ ＜gas＞ ＜water＞ ＜telephone＞ ○initial cost : ＜construction＞ ＜land acquisition＞ ＜cost burden division＞ ＜others＞
Benefit Information	＜number of users＞ ＜utilization time＞ ＜beneficiary＞ ＜number of beneficiaries＞ ＜how and why to build＞ ＜user's opinion＞
Safety Information	＜date of seismic retrofitting＞ ＜type of evacuation center＞ ＜type of seismic diagnosis＞※ ＜seismic index of structure＞※ ＜q-factor＞※ ＜check pursuant to Section 12 of the Building Standards Act＞※ ＜accident record＞
Other Informaiton	○barrier-free : ＜physically challenged toilet＞ ＜physically challenged parking＞ ＜elevator＞ ＜textured paving blocks＞ ＜guide sign in Braille＞ ○attached information : ＜attached facility＞ ＜rental facility＞

※:with link page for interpretation ≪≫:with link to go to other Web page

We selected public halls for prototypes because they contain widely various information related to money, safety, and users. If no item of a category of data existed in the provided database and administrative record, then we created virtual data and adopted its use for this study.

5.2 QR code sign

First, requirements of the QR code signs for information are presented below.

1) To show a willingness to provide administrative information.
2) To show that it is possible to know detailed information.
3) To ensure easy access to desired information.
4) To stimulate public interest in civil structures.

Secondly, the physical requirements are shown below.

1) To have resistance to abrasion.
2) To be installed easily and saving installation space.
3) To keep production costs down.

We created a signboard that meets those requirements. We also created a QR code linking to each Web page; a brief description about them is displayed. The signboard material is acrylic with a printed seal, which is inexpensive and replaceable.

6. Experimentation with prototype TSCS

Experimentation was conducted for 5 days during 9–14 March, 2010. The test subjects were 20 in all. At first in the experimentation, we let test subjects read the information freely. Subsequently, a hearing was started. The experimentation time per person was about 50 min.

6.1 Citizens' concern with administrative information

The first question asked of participants was "Which information are you interested in? or uninterested in?" At this time, we took care to inform the participant to speak as freely as possible.

Items that examinees mentioned are classified in to groups as depicted in Fig. 3. During the experiment, the level of interest was rated in five levels. In Fig. 3, the number of "interested" was the sum of responses "strongly interested" and "interested". The number of "uninterested" was calculated similarly.

Figure 3 shows that citizens have interest in information of various kinds. Especially, some people are interested in the construction of a building or the seismic diagnosis. We confirmed the citizens' interest with specialized and technical information.

In addition, there is considerable interest in costs and benefits. In reference to the information, many people point out that both pages should be shown. Furthermore, one examinee stated that every page is needed to evaluate the facility. We confirmed the effectiveness of encompassing information provision.

6.2 Evaluation for the system

We asked examinees about problems related to the system. The hearing was done with free-response questions. The answers were organized by problems of type on each page. The results are shown in Table 4.

Common problems are the information quantity and the many requirements to increase the amount of information. It is said that the staff cost should be stated on the Cost page, the usage fee on the Benefit page, and the relation between an indicator and a past earthquake on the Safety page. This shows that citizens want to know more administrative information.

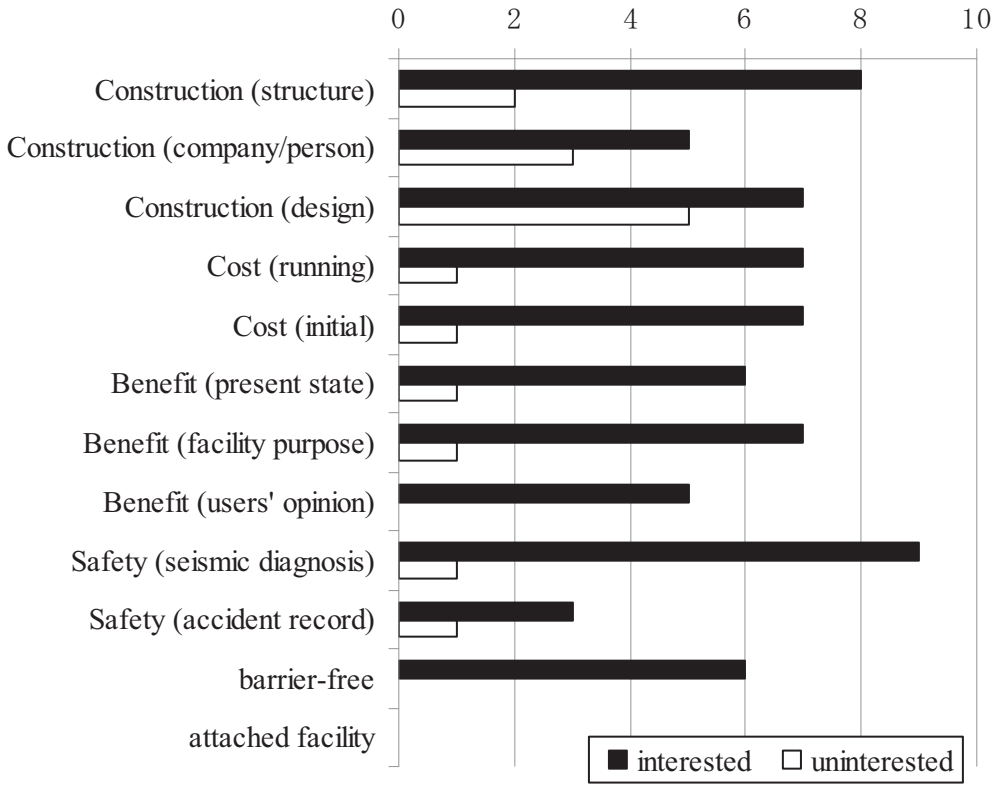

Fig. 3 Level of citizens' concern about information of each type.

Table 4 Number of problems reported by test subjects

		quantity		expression	composition	total
		less	more			
Title of Web page	Construction	8	5	20	14	47
	Cost	15		2	7	24
	Benefit	21		5	3	29
	Safety	22		19	4	45
	Other	14	1	8	1	24
total		80	6	54	29	169

Another problem is the poor quality of expressions. In the Construction and Safety page, many were pointed out. The Construction page includes information about design, which uses specialized terms without explanation. Although the Safety page includes an explanation, technical terms such as “brace” and “shear force” are used. We must strive for a readily interpreted page for every term that is not used by a typical person on a daily basis. Furthermore, we must use illustrations more actively.

7. Conclusions and future prospects

The study proposes a Traceability System for Civil Structures to enable citizens to access administrative information easily. This paper presents requirements to convey information about civil structures to citizens and the process to produce such a system. Furthermore, we conduct an experiment using the prototype TSCS.

The result of experimentation shows high public interest with information related to civil structures. However, the subjects of their interest are various. Therefore, information of every kind should be released. Furthermore, we confirmed that existing data in public administration should be translated to information that is delivered in a form that citizens can understand easily.

In the future, the system is expected to offer enhanced accountability in public administration and increased awareness about administrative activities. Additionally, it can encourage administrative officers to take more pride in their work. It is important that public administration regard information provision as an opportunity to increase citizens’ attention in matters of civil society.

References

1) *ed*. Japan Society of Civil Engineers, *Traffic Maintenance Institution – mechanism and problem –,* pp.154-255, 1991. (in Japanese)
2) Ministry of Land, Infrastructure, Transport and Tourism City and Regional Development Bureau, *Cost and Benefit Analysis Manual*, pp.7-14, 2003. (in Japanese)
3) Japan Society of Traffic Engineers, *Cost and Benefit Analysis of Road Investment – theory and application –*, pp.115-152, 2008. (in Japanese)
4) *ed*. Study Group on Road Investment Evaluation, *Guidelines for the Evaluation of Road Investment Projects (Title 2 Companies) – comprehensive evaluation –*, pp.3-8, pp.99-104, 1998. (in Japanese)

Mechanical and Physical Engineering

Mechanical Engineering

Comprehensive Assessment of Influence of Enhanced Component in Vapor Compression Air Conditioning System on Performance －Influence of Grooved Tube－
Naruaki SHINOMIYA,Nobuya NISHIMURA and Hiroyuki IYOTA
Trans. of the Japan Society of Refrigerating and Air Conditioning Engineers, Vol.27, No.1, pp.11-20 (2010) (in Japanese)
System performance prediction model for air-cooled air conditioner has been developed, and influences of Grooved tubes on performance of air conditioners with R410A were quantitatively investigated. Calculated results with simulation model correspond approximately to measured results by the authors and other researchers. After that, performances of air conditioners with grooved tubes were predicted. Results show that condensation heat transfer coefficients decrease with the rise of air conditioning load rate, and boiling heat transfer coefficients increase with the rise of air conditioning load rate. On the other hand, pressure drops increase 1.2-1.4 times in evaporator. Then, COPs of air conditioners with the grooved tube are 1.16 times higher than COP of air-conditioners with the smooth tube.

Development of a Compact Absorption Refrigerator Assisted by Low Temperature Level Heat Sources
Nobuya NISHIMURA, Tatsuya FUKUDA and IYOTA
Proc. of 5th Asian Conference on Refrigeration and Air-conditioning, Paper ID: 137 (CD-ROM) (2010)
A micro-scale distributed power generation system, which means a micro-cogeneration system in most cases, has received great attention from the standpoint of saving fossil fuel consumption and preventing global warming. Especially, a polymer electrolyte fuel cell (PEFC) is considered the most promising power generation system for small- scale commercial and residential use. In the PEFC cogeneration system, a small amount of waste heat at low temperature from a cell stack is used to produce hot water. We propose a new heat utilization method of this waste heat for air conditioning. In this paper, theoretical investigations of a high-performance absorption refrigerating machine were carried out by computer simulation. The influences of the cooling water temperature, surfactant, and highly efficient heating surface on the refrigeration ability were clarified quantitatively.

Development of a Biomass Gasifier which uses the Superheated Steam and its Application to Micro Co-Generation System
Nobuya NISHIMURA, Shunse RYO, Tomohiro NOMURA, Hiroyuki IYOTA, Takashi FUJII and Kenji KANAZAWA
Proc. of the Int.Conference on Power Engineering-09, Vol.1, pp.207-212 (2009)
Micro scale gasifier of biomass, which are refuse derived fuel and wood pellets, using the superheated steam has been developed and the feasibility of the generation pyrolysis gas as a fuel for micro co-generation was verified. The thermal cracking experiments were conducted at the superheated steam temperature from 500 to 700 degree C. The quantitative analysis of pyrolysis gases were carried out and residue amounts of char and tar were determined. Moisture and tar in the pyrolysis gas were removed by a cooling device which was kept at 0 degree C. The calorific values of the pyrolysis gases were about 14 to 19 MJ/Nm^3 , and were 1/3 to 1/2 than that of town gas(13A). Then, the refined gas was supplied to a micro gas engine of 1 kW output as a fuel. The experiments were conducted repeatedly by changing the mixture ratio of pyrolysis gas and town gas. As a result, it turned out that the mixture of 13% of pyrolysis gas to the town gas is possible under keeping constant power output.

Sterlization of Paddy Seed Using Mixture of Superheated Steam and Hot Air
Hiroyuki IYOTA, Tamotsu INOUE, Takahiro NODA, Yasuyuki HIDAKA and Shogo ISSHIKI
Proc. of the 6th Asia-Pacific Drying Conference, pp.454-460(CD-ROM) (2009)
A method for rapidly sterilizing paddy seeds using a mixture of superheated steam and hot air as a heating medium without any antiseptic substance was proposed. Paddy seeds were heated mainly by steam condensation using a fluidized bed experimental system. Then, the seeds were cooled and dried in room air just after the heating and sterilization processes. Effects of heating and drying times on the sterilization and germination rates were investigated experimentally using several kinds of Japanese paddy seeds. As a result, under suitable conditions of the heating medium, the heating time required for sterilization was a few seconds; the wet-bulb and dry-bulb temperatures of the heating medium were around 80ºC and 200ºC, respectively. Under this condition, the sterilization was found to be 80%, and there was no adverse effect on germination rates using the proposed method. Further, changes in the temperature and moisture content of the seeds during this process were

investigated numerically.

Method for Measuring Solar Reflectance of Retroreflective Materials Using Emitting-Receiving Optical Fiber

Hiroyuki IYOTA, Hideki SAKAI, Kazuo EMURA, Norio IGAWA, Hideya SHIMADA and Nobuya NISHIMURA

Proc. of the Second International Conference on Countermeasure to Urban Heat Islands, 6 pages (online publishing) (2009)

The heat generated by reflected sunlight from buildings to surrounding structures or pedestrians can be reduced by using retroreflective materials as building exteriors. However, it is very difficult to evaluate the solar reflective performance of retroreflective materials because retroreflective light cannot be determined directly using the integrating sphere measurement. To solve this difficulty, we proposed a simple method for retroreflectance measurement that can be used practically. A prototype of a special apparatus was manufactured; this apparatus contains an emitting-receiving optical fiber and spectrometers for both the visible and the infrared bands. The retroreflectances of several types of retroreflective materials are measured using this apparatus. The measured values correlate well with the retroreflectances obtained by an accurate (but tedious) measurement. The characteristics of several types of retroreflective sheets are investigated.

Reduction of Reflected Heat of the Sun by Retroreflective Materials

Hideki SAKAI, Kazuo EMURA, Norio IGAWA and Hiroyuki IYOTA

Proc. of the Second International Conference on Countermeasure to Urban Heat Islands, 6 pages (online publishing) (2009)

It is demonstrated that the walls made of retroreflective materials can reduce the reflected heat of the sun in the directions of neighboring roads and buildings. For mitigating the urban heat island effects, the applicable area of retroreflective materials is larger than that of high-reflective paints, because retroreflective materials can be used not only as "cool roofs" but also as "cool walls." Then, the solar retroreflectances of several retroreflective materials, which cannot be measured directly by a spectrophotometer, were measured for the first time. The procedures were as follows: First, the reflectance without retroreflection was measured by using a spectrophotometer with the integrating sphere. Then, the total reflectance was deduced from the amount of temperature rise by solar irradiation. Finally, the retroreflective component was calculated by subtracting the former from the latter. The measured retroreflectances are 20 to 30 percent for the prism-array type, about 20 percent for the capsule-lens type, and about 10 percent for the bead-embedded type.

Bubble Formation from an Air Jet Injected into a Turbulent Boundary Layer (Bubble Separation from the Continuous Jet)

Kenji KATOH, Yusuke ARII and Tatsuro WAKIMOTO

Trans. of Jpn Soc. Mech. Engrs., Ser. B, Vol. 75, pp. 1590-1597 (2009) (in Japanese)

A theoretical and experimental consideration is conducted to investigate the bubble separation from an air injected into a liquid turbulent boundary layer. There exist three patterns of bubble separation dependent on the jet velocity, i.e., (a) single bubble, (b) coalescent bubble, and (c) continuous jet. First, the critical jet velocity from (a) to (b) is theoretically estimated from the condition that the jet from the nozzle overtakes the rear end of the separated bubble which shrinks due to the action of surface tension. The calculated results roughly reproduce the experimental results observed by the high-speed video camera. The process of bubble separation from the continuous jet (c) can be classified into two patterns, i.e., (i) the bubble separates from the swell at the front end of jet, (ii) the jet breaks due to the instability on the liquid-gas interface. The separated bubble diameter of pattern (i) is theoretically determined by considering the force balance at the front end of jet between surface tension, drag from the free stream and virtual mass force. Also the bubble diameter of pattern (ii) is calculated from the most unstable wavelength of Rayleigh instability. Both theoretical results agree well with those obtained experimentally.

Volume of Liquid Droplet Detaching from a Sphere

Kenji KATOH, Hiroyuki IYOTA, Tamotsu INOUE and Tomoya TSUJINO

Trans. of Jpn Soc. Mech. Engrs., Ser. B, Vol. 75, pp. 1503-1509 (2009) (in Japanese)

A theoretical and experimental study is conducted to investigate the detached volume from the pendant drop on sphere surface. From the observation of droplet detachment by use of a high speed video camera, the movement of upper part from the neck of droplet is quite slow compared with that of detaching lower part. The surface profile of upper part was calculated approximately as a static problem by using the axi-symmetric Laplace equation. Using the droplet profile, the system energy was calculated including the work done by the solid-liquid wetting behavior. Based on the condition of

energy minimum, the volume of upper part was determined among the solutions satisfying the boundary conditions and the volume of detached part V was calculated. The volume V increases with the sphere diameter and approaches to that for the plate. V is strongly dependent on the wettability between sphere and liquid, and decreases with the receding contact angle. The detached volume of water droplet was measured for spheres of porous brick with various diameters. The results agreed well with theoretical ones obtained in this study

Critical Volume of Liquid Droplets Attached to A Vertical Cylinder
Tatsushi NISHIDA, Kenji KATOH and Tatsuro WAKIMOTO
Trans. of Jpn Soc. Mech. Engrs., Ser. B, Vol. 75, pp. 2273-2279 (2009) (in Japanese)
The critical volume of liquid droplet (CV) was investigated when the droplet starts to slide on the wall of a vertical cylinder. The critical condition was theoretically considered from the force balance between the gravitational force and the resultant of surface tension acting on the three-dimensionally curved contact line. The results show that the critical condition can be simplified to the similar one for the droplets on the inclined plates treated in the previous reports, and CV can be estimated from the maximum width of the contact area on the cylinder. The maximum width was calculated based on the energy minimum condition for the droplets in a similar manner to the inclined plate. CV was experimentally measured for each combination between two kinds of test liquids and polypropylene with different roughness. The results fairly agree with those of theory within 10% deviation. CV increases with the cylinder diameter and approaches the value for the plate asymptotically. This is due to the fact that the volume of droplets increases with the curvature under the same width of contact area.

Heat Transfer Enhancement and Drag Increase in a Channel with a Wing-type Vortex Generator (Effect of Prandtl number)
Kenji KATOH, Takashi. NISHIMURA, Tatsuro. WAKIMOTO and Toshinobu TANIGAWA
Proc. of the Int. Conf. on Power Engineering (ICOPE-09), Vol. 3, pp.7-12 (2009)
The efficiency of heat transfer η, i.e., the ratio between heat transfer enhancement and drag increase from the smooth channel, is discussed for the turbulent and laminar flows in a channel with a wing-type vortex generator (VG) installed on the wall. In this report, the effect of Prandtl number Pr on η is mainly discussed. Various effects on the heat transfer enhancement are investigated by using the results of direct numerical simulation and the energy equations integrally averaged over the whole flow field. η decreases slightly in the turbulent flow with Pr while it increases noticeably in the laminar flow. In the turbulent flow, the temperature fluctuation in the smooth channel is suppressed by the strong thermal diffusion effect at low Pr. The fluctuation promoted by VG becomes effective relatively in such region. In the laminar flow, on the other hand, since there is no background turbulence in the smooth channel, the fluctuation generated by VG directly enhances the heat transfer, which is greater in high Pr region where the thermal diffusion effect is weakened. In addition, the increase of convective heat transfer near the wall has an important effect on the good efficiency for the laminar flow.

Characteristics of Liquid Film Flowing around a Horizontal Circular Cylinder (Film Thickness and Wave Length of Standing Wave)
Kenji KATOH and Tatsuro WAKIMOTO
Journal of JSEM, Vol. 10(Special Issue), pp.67-72 (2010)
An experimental and theoretical study was conducted to investigate the characteristics of liquid film flowing around a horizontal circular cylinder. The standing wave with a peak line pointing to the flow direction appears on the film surface. The wave length was obtained theoretically from the force balance on the film surface including the effect of centrifugal force. The calculated wave lengths agree with those measured experimentally for three kinds of test liquids. When the film Reynolds number increases larger than 500, the viscous effect on the wave motion can be neglected.

On the Sliding and Profile of a Liquid Droplet on a Rotating Disk
Kenji KATOH, Mituyoshi HIGASHINE, Tatsuro WAKIMOTO and Ryohei MASUDA
Heat Transfer-Asian Research, Vol. 39, pp. 59-75 (2010).
The theoretical and experimental study was conducted to investigate the critical condition at which a liquid droplet starts to move on a rotating disk. The critical rotational speed ω was theoretically calculated based on the force balance between the surface tension and the centrifugal force. ω was experimentally measured for each combination between three kinds of test plates and liquids. The calculated rotational speeds agreed well with the measured ones for arbitrary contact angle. The three-dimensional surface profiles of droplets were calculated from the approximate Laplace equation. The measured profiles on the rotating disk were approximated well by the method proposed in this study.

A Study on Capillary Flow under the Effect of Dynamic Wetting

Kenji KATOH, Tatsuro WAKIMOTO and Sinnchiro NITTA
Journal of JSEM, Vol. 10(Special Issue), pp. 62-66 (2010)
A theoretical model was proposed to consider the dynamic contact angle from a macroscopic viewpoint. A slight convex profile of liquid surface is assumed to avoid the divergence of viscous stress near the three-phase contact line on the wall. The theoretical results of the dynamic contact angle are dependent on the parameter ε, i.e., the ratio of surface area occupied by the defects on the solid surface. The movement of liquid column in a capillary is investigated experimentally. The modified Lucas-Washburn equation including the effect of dynamic wetting represents well the measured results. The theoretical model can approximate the measured dynamic contact angles within the experimental uncertainty.

A Study on Disintegration Process of a liquid sheet formed with Surfactant Aqueous Solution
Tatsuro WAKIMOTO, Kenji KATOH and Takashi ARIMA
Trans. of Jpn Soc. Mech. Engrs., Ser. B, Vol. 75, pp. 2440-2447 (2009) (in Japanese)
Atomization characteristics of surfactant aqueous solutions injected from a fan spray nozzle have been clarified. Surfactant solutions generally have unusual properties, that is, surface tension depending on time (dynamic surface tension) and strong stability of a thin liquid sheet such as a soap film. These special effects result from the adsorption of surfactant molecules to newly formed liquid surface. In this study, the influence of the dynamic surface tension and surface stabilizing effect by the surfactant molecules on the liquid sheet atomization was discussed. The dynamic surface tension and surface-stabilizing effect were measured by oscillating jet method and Ross-Miles method, respectively; Ross-Miles method is generally used to estimate the abilities to form and maintain foams. The break-up length of the liquid sheet and wave amplitude inducing break-up were also measured by photography. Test liquids with several surfactant concentrations indicated that increase of surfactant concentration reduced the relaxation time of the dynamic surface tension, expanded the break-up length and amplify the wave amplitude. This means that adsorption of surfactant molecules increases the break-up length regardless of large wave amplitude. To investigate this inconsistency, two test liquids, which were basically ethanol and surfactant solutions, were specially produced so that they have different surface-stabilizing effect with same density, viscosity and surface tension. The break-up length of the surfactant solution became longer than that of the ethanol solution. This indicates that the surface-stabilizing effect by the surfactant molecules suppresses the liquid sheet atomization.

A Novel Method of Measuring Dynamic Surface Tension From the Profile of Capillary Jet (2nd report: Measurement of Dynamic Surface Tension)
Tatsuro WAKIMOTO, Kenji KATOH and Toshiya TANI
Trans. of Jpn Soc. Mech. Engrs., Ser. B, Vol. 76, pp. 291-297 (2010) (in Japanese)
A novel measuring method for dynamic surface tension of surfactant aqueous solutions is proposed. In this method, the dynamic surface tension is measured by comparing the trajectory of a free laminar liquid jet ejected horizontally from a circular orifice to a theoretical trajectory. The theoretical trajectory is obtained by solving ordinary differential equations, which is conducted from momentum balances between inertial force, surface tension, gravitational force and pressure. Circular cross section and simplified pressure distribution in the liquid jet are assumed in the theoretical analysis. Surface tension affects the trajectory of the horizontal jet with inertial force and gravitational force under the condition of Weber number We≈1 and Bond number Bo≈1, whereas viscous force is negligible because the order of capillary number is 10-3 under the experimental condition of this study. The experimental trajectory is obtained by photography. The experimental trajectory is compared with a theoretical trajectory calculated at an assumed surface tension, and the theoretical trajectory in agreement with the experimental trajectory gives the time varying surface tension (dynamic surface tension) of liquid. The obtained dynamic surface tensions of several kinds of surfactant aqueous solutions by this method agree well with ones measured by conventional oscillating jet method and maximum bubble pressure method. This agreement proves the validity of this method.

A Study on Nonlinear Growth of Disturbance Waves in a Radial Liquid Sheet
Tatsuro WAKIMOTO and Kenji KATOH
Journa of JSEM, Vol. 9, pp. 330-337 (2009) (in Japanese)
Nonlinear growth of disturbance waves in a radial liquid sheet has been clarified. The radial liquid sheet was formed by releasing of a radial water film flowing along the disk into still air. In this liquid sheet, a velocity profile with an inflection point is formed during the relaxation of the velocity profile. This velocity profile causes inflection point instability, and the instability amplifies disturbances in the liquid sheet. The deformed liquid surface by the amplified disturbance produces disturbance waves. In this study, the growth of the disturbance waves depending on the amplitude of the wave was analyzed by numerical simulation and experiment. The thickness and surface velocity at the disk edge were selected to be 80μm and 14.2m/s, respectively. The disturbance waves with different amplitudes were numerically

simulated, and the simulated disturbance waves demonstrated that the growth rate decreases when the amplitude exceeds 15μm, which is 19% of the sheet thickness. In addition, the comparison of measured amplitude by the laser reflection method with that of the simulated disturbance waves revealed that the amplitude of experimentally observed disturbance waves are strongly decayed by nonlinear effect.

A Study on Three-dimensional Deformation and Merging of Disturbance Waves formed by Inflectional Instability of a Liquid Sheet

Tatsuro WAKIMOTO and Kenji KATOH

Journa of JSEM, Vol. 9, pp. 318-323 (2009) (in Japanese)

Three-dimensional deformation and merging of disturbance waves in a radial liquid sheet has been clarified. The radial liquid sheet is generated when flowing liquid film on a disk emerges radially from the disk edge. The radial liquid sheet is unstable because of a velocity profile with an inflection point (inflectional instability). The growth and deformation of the two-dimensional disturbance waves (D waves), which is formed by the instability, lead to laminar-turbulent transition just outside of the disk edge. In this study, the deformation process of the D waves was observed in detail with a CCD camera providing high temporal and spatial resolution images. Comparing the observed deformation of the D waves with the reported typical deformation of vortices formed by inflectional instability in a single-phase free shear flow, three-dimensional deformations of the D waves and vortices were very similar. This suggests that three-dimensional deformation of the D waves is caused by enhancement of perturbed vortex filament in a braid region. However, merging of the D waves hardly occurred even though vortices in the free shear flow merge frequently. This implies that existence of liquid surface prevents the merging of the D waves.

New Optical Method to Measure Slight Difference of Contact Angle

Tatsuro WAKIMOTO, Kenji KATOH and Mituyoshi HIGASHINE

Journa of JSEM, Vol. 9, pp. 324-329 (2009) (in Japanese)

A new optical measurement method for detection of slight difference of contact angle has been developed. This new method is applied to detect the micro blemish of self assembled monolayers (SAMs) because the blemished SAMs causes slight difference of contact angle from that of normal SAMs. In this method, a test plate is preliminarily set up at a tilt angle, which is same as the contact angle of normal SAMs. This setting forms a very small two-dimensional meniscus near the plate depending on the contact angle difference between blemished SAMs and normal SAMs. When a laser beam is emitted to the meniscus from above, the incident laser beam is reflected at a certain angle depending on the inclined angle of the liquid surface formed by the meniscus. In consequence, the contact angle difference is measured based on the reflection angle of the laser beam. This method is capable of detecting slight angle difference under 1 degree between blemished SAMs and normal SAMs.

Investigation of Optimal Seismic Design Methodology for Piping Systems Supported by Elasto-Plastic Dampers (Part 1: Evaluation Functions)

Tomohiro, ITO, Masaki, MICHIUE, Katsuhisa, FUJITA

Journal of System Design and Dynamics JSME, Vol.3, No.1, pp.59-69 (2008)

In this paper, the optimal seismic design methodology that can consider the structural integrity of not only the piping systems but also elasto-plastic supporting devices is developed. This methodology employs a genetic algorithm and can search the optimal conditions such as the supporting location, capacity and stiffness of the supporting devices. Here, a lead extrusion damper is treated as a typical elastic-plastic damper. Four types of evaluation functions are considered. It is found that the proposed optimal seismic design methodology is very effective and can be applied to the actual seismic design for piping systems supported by elasto-plastic dampers. The effectiveness of the evaluation functions is also clarified.

Dynamic Buckling Analysis of Cylindrical Water Storage Tanks: a New Simulation Method Considering Coupled Vibration between Fluid and Structure

Akira, MAEKAWA, Katsuhisa, FUJITA

Proceedings of ASME Pressure Vessels and Piping Division Conference, Prague, Czech-Republic,
PVP2009-70083 in CD-ROM (2009)

This paper proposes a dynamic buckling analysis method which can accurately simulate the buckling behavior of cylindrical water storage tanks during an earthquake. The proposed method takes into account the behavior of oval-type vibration as well as beam-type vibration, which are coupled vibrations between the shell structure of the tank and the water stored in the tank. In the proposed method, both the tank and the stored water are three-dimensionally modeled by finite elements and time history analysis is conducted. Moreover, coupled analysis between the fluid and structure and large deformation analysis to the shell structure of the tank are also

considered. The analytical results by the proposed method agreed well with those of experiments regarding occurrence of oval-type vibration, mode of buckling and buckling load.

Simulation Analysis Using CFD on Vibration Behaviors of Circular Cylinders Subjected to Free Jets through Narrow Gaps in the Vicinity of Walls
Katsuhisa FUJITA
Proceedings of Fluid Structure Interaction V, WIT Transactions on The Built Environment, Vol.105, pp.85-95 (2009)
A vibration of circular cylinders subjected to a cross-flow jetted from a narrow gap that exists in a same fluid is investigated. The numerical simulation analysis using a commercial computational fluid dynamics on the vibration of a single circular cylinder supported by a spring and damper system is performed. Next, the similar simulation analysis on a circular cylinders array composed of 6 cylinders is performed. In CFD simulation analysis, the equation of continuity, Navier-Stokes equations are transformed in discrete system using finite element methods. The upstream differential model is applied as a laminar flow model, and model as a turbulence flow model, respectively. These results are also compared with experiments.

Numerical Simulation of Nonlinear Oval-Type Vibration in Cylindrical Water Storage Tanks
Akira, MAEKAWA, Katsuhisa, FUJITA
Proceedings of Fluid Structure Interaction V, WIT Transactions on The Built Environment, Vol.105, pp.237-246 (2009)
This paper describes a nonlinear behavior of oval-type vibration in a cylindrical water storage tank which is higher order vibration mode in the circumferential direction of the wall (axial wave number $m \geq 1$ and circumferential wave number $n \geq 2$). The vibration experiment of a cylindrical water storage tank with exciting its base was conducted to cause oval-type vibration. At large excitation, oval-type vibration with sub-harmonics of order one-half occurred in spite of that with the fundamental harmonics at large excitation. The nonlinear behavior of oval-type vibration was simulated by the numerical analysis method proposed in this paper.

Effect of Structural Dimensions on Dynamic Stability of Elastic Beam Subjected to Axial Flow in Confined Narrow Passage
Katsuhisa FUJITA, Ayumi OHKUMA
Transactions of the Japan Society of Mechanical Engineers, 76-765, C, pp.1209-1216 (2010) (in Japanese)
The evaluation methodologies for the flow-induced vibration of an elastic beam due to the axial flow in confined narrow passage are reported. One of authors has already proposed the analytical method using Navier-Stokes equation for the dynamic stability of elastic beam subjected to axial flow in confined narrow passage. In this paper, by using proposed analytical methods, we perform the numerical studies taking three kinds of support conditions as parameters, those are a cantilever fixed at the upstream side, a cantilever fixed at the downstream side, and a simple supported beam at the both sides, respectively. Moreover, we perform also parameter-studies concerning with a width of annular gap, viscosity of a fluid, and structural damping. And we clarify the effects of these parameters for proposing the safety dynamic design guideline concerning axial flow-induced vibration in industries.

Optimal Seismic Design of L-Shape Piping System Supported by Elasto-Plastic Supports Subjected to Three-Dimensional Seismic Inputs (Optimization of the Mounting Angle of Dampers)
Yoshiyuki MIYOSHI, Tomohiro ITO, Atsuhiko SHINTANI, Katsuhisa FUJITA
Transactions of the Japan Society of Mechanical Engineers, 76-765, C, pp.1226-1231 (2010) (in Japanese)
In this paper, we propose the optimal seismic design methodology which can consider the soundness of elasto-plastic dampers in addition to that of the piping systems. This methodology employs genetic algorithm and can search the optimal conditions such as the number of supports, supporting location, mounting angle and capacity of dampers. Five types of evaluation functions are considered. As a result, it is found that it is very important to optimize the mounting angle of dampers for the piping systems subjected to the actual seismic waves with particular frequency components.

Investigation of Optimal Seismic Design Methodology for Piping Systems Supported by Elasto-plastic Dampers (Part2: Applicability for Seismic Waves with Various Frequency Characteristics)
Tomohiro ITO, Masashi MICHIUE, Katsuhisa FUJITA
Journal of System Design and Dynamics JSME, Vol.4, No.2, pp.348-359 (2010)
In this study, the applicability of a previously developed optimal seismic design methodology, which can consider

the structural integrity of not only piping systems but also elasto-plastic supporting devices, is studied for seismic waves with various frequency characteristics. This methodology employs a genetic algorithm and the capacity and stiffness of the supporting devices. Here a lead extrusion damper is treated as a typical elasto-plastic damper. Numerical simulations are performed using a simple piping system model. As a result, it is shown that the proposed optimal seismic design methodology is applicable to the seismic design of piping systems subjected to seismic waves with various frequency characteristics. The mechanism of optimization is also clarified.

Dynamic Buckling Simulation of Cylindrical Liquid Storage Tanks Subjected to Seismic Motions
Akira MAEKAWA, Katsuhisa FUJITA
Proceedings of ASME Pressure Vessels and Piping Division Conference, Bellevue, Washington, USA, PVP2010-25412 in CD-ROM (2010)
A three-dimensional and elastic-plastic dynamic buckling analysis method that takes into consideration fluid-structure coupling and large deformation is proposed in order to accurately simulate the seismic response of cylindrical liquid storage tanks. The results of a dynamic buckling experiment of a tank using seismic motions closely match those of numerical simulation by the proposed method. The mesh size of the analytical model greatly influences the buckling analysis results. Optimization of the size is also discussed.

Motion and Vibration of a Roller Coaster on the 3D Trajectory Considering Running Resistance
Katsuhisa FUJITA, Yoshitaka UEMURA, Yuji FUNAKOSHI
Transactions of the Japan Society of Mechanical Engineers, 76-768, C, pp.2049-2058 (2010) (in Japanese)
The motion and vibration of a moving body running on a complicated 3 dimensional (3D) trajectory considering running resistances are investigated. A roller coaster is treated with here as a concrete example of moving body. The equations of motion of a roller coaster in which a trajectory and a vehicle are coupled are derived by using differential-algebraic equation (DAE). The effect of an air resistance and a rolling resistance are taken into consideration in this analysis. Also, the motion and vibration experiments have been performed using an actual roller coaster in site. The acceleration responses in simulation are compared to those in experiment. Both show a good coincidence qualitatively. Moreover, influences of running resistances on the required time from the starting point to the arriving one are made clear.

Effect of Structural and Fluid Characteristics on Dynamic Stability of an Elastic Beam Subjected to Axial Flow in A Narrow Passage
Katsuhisa FUJITA, Ayumi OHKUMA
Proceedings of ASME 2010 3rd Joint US-European Fluids Engneering Summer Meeting and 8th International Conference on Nanochannels, Microchannels, and Minichannels, FEDSM- ICNMM 2010-30205
The evaluation methodologies for the flow-induced vibration of an elastic beam subjected to an axial flow in a narrow passage are reported. One of authors has already proposed an analytical method using the Navier-Stokes equation for the dynamic stability of an elastic beam subjected to an axial flow confined in a narrow passage. By using the proposed analytical methods, we perform numerical studies taking three kinds of support conditions as parameters, that is, a cantilever fixed at the upstream side, a cantilever fixed at the downstream side, and a simple support beam at the both sides, respectively. Moreover, the parameter-studies are also performed concerning with a width of annular gap, viscosity of a fluid, and structural damping. And those effects are clarified for proposing a safety dynamic design guideline concerning axial flow-induced vibrations in industries.

Vibration Experiments and Numerical Simulations of Pulsation Behavior in Actual Size Mock-up Piping
Proc. of ASME 2010 3rd Joint US-European Fluids Engneering Summer Meeting and 8th International Conference on Nanochannels, Microchannels, and Minichannels, FEDSM-ICNMM 2010-30280 in CD-ROM
Akira MAEKAWA, Tuneo TTAKAHASHI, Takashi TSUJI, Michiyasu NODA, Minoru KATO, Katsuhisa FUJITA
Vibration experiments for pressure pulsation behavior were made using actual size mock-up piping of nuclear power facilities. The mock-up was a closed loop consisting of a three-stand plunger pump, tanks, piping and valves. It was 40 m long to allow interaction of the acoustic resonance frequency of fluid inside with the mechanical natural frequency of the piping. The influence of valve closing and opening operations to change inner pressure during pump operations on the pulsation boundary condition was investigated in this study. A drastic change in boundary condition of the acoustic resonance behavior by using a slightly different valve opening ratio to set a different inner pressure was shown in the experimental results. The phenomenon was numerically simulated by using the methods of characteristics.

Dynamics of Two-Wheels Modeling Roller Coaster Running on A Complicated 3 Dimensional (3D)

Trajectory Considering Air Resistance
Katsuhisa FUJITA, Koichi KATSUOKA
Proc. of 5th Asian Conference on Multibody Dynamics 2010, Kyoto, Japan
The motion and vibration of a moving body running on a complicated 3 dimensional (3D) trajectory considering an air resistance are investigated. The equations of motion of a roller coaster are derived by using differential algebraic equation. In the previous paper, a roller coaster has been modeled as a one-wheel vehicle. Here, it is modeled as a two-wheel vehicle. The Baumgarte method is adopted for numerical stabilization. The influence of an air resistance and a rolling resistance, and the interaction between a vehicle and passengers as for a riding comfort of roller coaster are investigated. And also, the transmissibility of vibration through suspensions of roller coaster is studied to keep the safe security in the strength of rotating wheels and shafts. Besides, a part of simulations are compared with the experiments reported by previous paper.

Bacterial Attachment and Initiation of Biofilms on the Surface of Copper Containing Stainless Steel
Hiroshi KAWAKAMI, Kenji KITTAKA, Yoshihiro SATO and Yasushi KIKUCHI
ISIJ International, Vol. 50, No. 1, pp. 133–138 (2010)
Type 304 stainless steel, copper containing stainless steel, and oxygen free copper were subjected to antibacterial tests and short term exposure experiments in a laboratory. Antibacterial tests showed that the copper containing stainless steel, as well as oxygen free copper, was antibacterial, yet the antibacterial activity of the copper containing stainless steel was lower than that of the oxygen free copper. In short term exposure experiments, the copper containing stainless steel, as well as type 304 stainless steel, didn't sterilize planktonic bacterial cells, while the oxygen free copper reduced the number of alive planktonic bacterial cells. The copper containing stainless steel did not protect itself from bacterial adhesion, but sterilized about 75% of sessile bacterial cells and reduced formation of biofilms on its surface. Such experimental results indicate that the copper containing stainless steel is effective against biofilm related impacts.

Investigation of Propulsive Force and Water Flow around a Small Fish Robot by Means of PIV Measurement and Three-dimensional Numerical Analysis
Yogo TAKADA, Yukinobu NAKANISHI, Ryosuke ARAKI, Motohiro NONOGAKI and Tomoyuki WAKISAKA
Proc. of Int. Symp. On Aero Aqua Bio-Mechanisms, Shanghai, China, ISABMEC2009, 18.pdf
A fish robot with image sensors can be used to search for disaster victims in flood areas because it can go into narrow spaces. However, the swimming velocity and propulsive efficiency of fish robots are extremely low in comparison with actual live fish. Therefore, it is necessary to investigate the superior propulsive efficiency of actual fish and find measures to improve the propulsive performance of fish robots. Using the sea bream as a model, a flexible fish robot was developed to study its propulsion performance. The individual effects of the shape, thickness, flexibility and moving pattern of the tail fin on the propulsive force were investigated experimentally by using the fish robot. As a result, it was confirmed that flexibility of the tail fin is very important for the fish robot to swim efficiently. Particle image velocimetry (PIV) measurements and three-dimensional computational fluid dynamics (CFD) of the water flow around the fish robot were conducted to compare the efficiencies of flexible and rigid tail fins. In the case of the flexible tail fin, two horizontal vortices exist near the top and bottom edges of the tail fin. The horizontal vortices, along with the vertical vortices, form a vortex ring. However, in the case of the rigid tail fin, similar vortices are not seen. Consequently, it was confirmed that the propulsive performance of the fish robot can be improved when vortex rings are successively formed downstream of the tail fin to form a reverse Karman vortex street.

Effect of Combustion Chamber Shape on Performance of Spark Ignition Engines Fueled by Mixture of LPG and DME – Experimental Investigation on Knocking Limits
Hiroshi OMOTE, Tohru NAKAZONO, Yogo TAKADA and Tomoyuki WAKISAKA
Journal of the Japan Institution of Marine Engineering, Vol.44, No.6, pp.90-95 (2009) (in Japanese)
Dimethyl ether (DME) is one of the most promising alternative fuels for the near future. To rapidly promote its widespread use, it is desirable to use the mixture of DME with LPG (mainly propane), because a mature supply infrastructure already in existence can be employed. However, using a mixture of LPG and DME as a fuel for spark ignition engines causes a problem, knocking during combustion. In a previous study, the authors analyzed this knocking phenomenon in a small gas engine for a co-generation system by means of a three-dimensional combustion simulation based on a chemical kinetic model, and investigated the effect of combustion chamber shape on the knocking phenomenon. However, due to long computational times, it was difficult to evaluate various piston cavity shapes under a wide range of operating conditions. Therefore, in this study, the authors

investigated the effects of these piston cavity shapes on engine performance, especially on knocking limits with experiments performed under a wide range of operating conditions in the same engine, and explored a suitable piston cavity shape for an LPG-DME mixture fuel with a high ratio of DME.

Construction of Elementary Reaction Scheme for Three-Dimensional Combustion Analysis Based on Chemical Kinetics in Bio Gas and City Gas Mixture Fueled Engines Ignited with DME Spray
Hideki TAKASE, Daisuke YOSHIHARA, Yogo TAKADA and Tomoyuki WAKISAKA
Journal of the Japan Institution of Marine Engineering, Vol.44, No.6, pp.83-89 (2009) (in Japanese)
Bio gas fueled engines have proved effective in helping the environment; such as reducing methane gas which has a large greenhouse effect, alongside an ozone layer destructing effect, because the main composition of bio gas is methane, and it is not emitted into the atmosphere, but burned up within the engine. In this study, by combining the GRI-Kojima reduced elementary reaction scheme and the DME reduced elementary reaction scheme, which had been constructed by the authors' group, the authors constructed a reduced elementary reaction scheme originally for the mixture of bio gas, city gas, DME and air for investigating the combustion characteristics of a bio gas and city gas mixture fueled engine which was ignited with DME (dimethyl ether) spray. On the basis of chemical kinetics with the proposed elementary reaction scheme, the authors conducted three-dimensional numerical analysis of the combustion process within a practical computation time in a bio gas and city gas mixture fueled engine which was ignited with a small amount of DME spray, using different mixture ratios of bio gas and city gas.

Effects of LPG and DME Spatial Distributions on Combustion in LPG-DME Spark Ignition Engine – Three-dimensional Numerical Analysis Based on Chemical Kinetic Model
Hiroshi OMOTE, Yamanaka YUICHI, Tohru NAKAZONO, Yogo TAKADA and Tomoyuki WAKISAKA
Journal of the Japan Institution of Marine Engineering, Vol.45, No.1, pp.103-108 (2010) (in Japanese)
In order to understand the combustion phenomenon in a spark ignition engine fueled with the homogeneous mixture of LPG (main component : Propane) and DME (Dimethyl Ether), the authors previously developed a chemical kinetic model (Propane-DME reduced elementary reaction model and turbulent combustion model) for three-dimensional numerical analysis of the combustion process in the engine. The authors' GTT-CHEM code with that chemical kinetic model was able to reproduce an auto-ignition phenomenon at the last period of combustion in the engine. In this study, the authors have investigated the effects of Propane and DME heterogeneous spatial distributions on combustion in the LPG-DME spark ignition engine by three-dimensional numerical analysis using the GTT-CHEM code with the previously developed chemical kinetic model, for better understanding about the contributions of Propane and DME to the auto-ignition phenomenon. The unburned zone DME fraction and its homogeneity were employed to discuss and explain the results. It is found that a well mixed and highly DME contented propane gas locating at end gas region is in the most danger of strong auto-ignition.

Development of Small Fish Robots Powered by Small and Ultra-light Passive-type Polymer Electrolyte Fuel Cells
Yogo TAKADA, Ryosuke ARAKI, Yukinobu NAKANISHI, Motohiro NONOGAKI, Kazuaki EBITA and Tomoyuki WAKISAKA
Journal of Robotics and Mechatronics, Vol.22, No.2, pp.150-157 (2010)
Small fish robots, the size of a killifish - 5 cm long - are potentially in finding disaster victims in flooded areas, because of their ability to navigate narrow confines. Powering such robots, however, becomes a question, since the easiest answer - rechargeable batteries - has low energy density. The "Power Tube" we developed is a small and ultra-light passive-type polymer electrolyte fuel cell. Based on this fuel cell technology, we fabricated a 110 mm fish robot combining a drive, consisting of a DC motor and link, with a power tube having a hydrogen generator. We also fabricated an energy-efficient submersible fish robot with neodymium magnets and coil actuators, that methanol-fueled Power Tubes powered with a voltage booster.

Investigation of Propulsive Force and Water Flow around a Small Fish Robot by PIV Measurement and Three-dimensional Numerical Analysis
Yogo TAKADA, Yukinobu NAKANISHI, Ryosuke ARAKI and Tomoyuki WAKISAKA
Transactions of the Japan Society of Mechanical Engineers (*Ser.C*), Vol.76, No.763, pp.665-672 (2010) (in Japanese)
Swimming velocity and propulsive efficiency of fish robots are extremely low in comparison with actual living fish. Therefore, using the sea bream as a model, a flexible fish robot was developed to study its propulsion performance. The individual effects of the shape, thickness, flexibility and moving pattern of the tail fin on the

propulsive force were investigated experimentally by using Particle image velocimetry (PIV) measurements and three-dimensional computational fluid dynamics (CFD). Consequently, it was confirmed that the propulsive performance of the fish robot can be improved when vortex rings are successively formed downstream of the tail fin to form a reverse Karman vortex street.

Development of Small and Ultra-light Passive-type Polymer Electrolyte Fuel Cell and Application to Small Fish Robots

Yogo TAKADA, Ryosuke ARAKI, Motohiro NONOGAKI, Kazuaki EBITA, Toshinaga ISHI and Tomoyuki WAKISAKA

Transactions of the Japan Society of Mechanical Engineers (*Ser.B*), Vol.76, No.764, pp.650-659 (2010) (in Japanese)

Polymer electrolyte fuel cell (PEFC) is expected to applications for various usages such as a power source for small robots and personal computers because PEFC has high energy density and can generate electric power under low temperature environment. As the application, swimming fish robots with PEFC are useful for various usages such as ecological investigation in water etc. In the case that rechargeable batteries are used for supplying electricity to robots, they are not able to continue swimming for a long time because of low energy density of the batteries. Therefore, a small and ultra-light passive-type polymer electrolyte fuel cell called "Power Tube" has been developed. On the basis of this fuel cell technology, the authors have created low energy consumption small fish robots powered by Power Tubes on a float or a buoy. The fish robot with a float swims for approximately 50 minutes by only Power Tubes with a voltage booster and the other fish robot with a submersible system can also swim for about 50 minutes by a hybrid system of a lithium polymer battery and Power Tubes.

Intelligent Materials Engineering

Damage Behaviour of Ti/GFRP Laminates under Low-Velocity Impact Loading
Hayato NAKATANI, Tatsuro KOSAKA, Katsuhiko OSAKA and Yoshihiro SAWADA
J. of the Soc. of Materials Science, Japan, Vol.59 No.5, pp.383-390 (2009) (in Japanese)
In the present paper, the impact responses and overall damages of Fibre-Metal Laminates based on titanium alloys and glass fibre-reinforced polymers (Ti/GFRP) as Ti/FRP laminate system were evaluated. Low-velocity impact tests using a drop-weight tower were conducted for the cross-plied GFRP laminates and the Ti/GFRP laminates, and the impact responses during impact loading were obtained. Impact damages such as cracks in titanium layer and delamination of titanium-GFRP interface or matrix cracks and interlaminar delamination in GFRP layer were observed from the impact direction. From the experimental evidence, it was found that the Ti/GFRP laminates showed same impact damage modes as of other types of Fibre-Metal Laminates. Internal damages in the Ti/GFRP laminates were restrained by the reinforcing effect of titanium and adhesive layer compared to the cross-plied GFRP laminates. The Ti/GFRP laminates showed two patterns of the impact responses and damages with the threshold impact energy of about 4.8J. With higher impact energy than this threshold, single crack was presented in titanium layer at non-impacted side. The interlaminar delamination area in GFRP layer increased sharply due to the occurrence of this crack. Numerical analysis model that represent the impact behaviour of the Ti/GFRP laminates using finite element method was suggested based on the damage observations. The impact responses obtained by the dynamic analyses agreed well with the experimental results. The calculated area of interlaminar delamination in GFRP layer as a function of impact energy showed same behaviour as seen in the experiments. As a consequence, it was shown by the analysis as well that the drastic increase in the internal damage area of the Ti/GFRP laminates was induced by the fracture in outer titanium layer under the out-of-plane impact loading.

Cure Monitoring of Resin by Real-Time Measurement of Refractive Index Using Single-Mode Optical Fibers
Tatsuro KOSKA, Katsuhiko OSAKA and Yoshihiro SAWADA
J. of the Soc. of Materials Science, Japan, Vol.59 No.5, pp.391-397 (2009) (in Japanese)
This study proposes a real-time monitoring method for degree of cure (DOC) of curing resin by refractive index measurement using a single-mode optical fiber based on the Fresnel reflection at the fiber end. First, we particularly present an approach for measuring refractive index of resin in real time without the effects of unexpected backward reflection. We applied this approach to measurement of refractive index of an epoxy resin during cure process, and experimentally confirmed that the change of the refractive index was stably measured in real time. Next, we proposes a new approach to calculate DOC from change of refractive index by eliminating effect of temperature change on refractive index of curing resin. This approach can quantitatively evaluate the DOC in real time, which is not obtained by conventional methods, and provide information in the small region at the fiber end. The experimental results of monitoring cure process of the epoxy resin showed that the DOC could be stably measured by this approach without effect of the temperature change. Furthermore, the DOC obtained by this approach was compared with the DOC curve by the thermal analysis using differential scanning calorimeter. These experiments revealed that the DOC by the present approach represented the curing condition of the resin regardless of the cure pattern and was easily translated into the DOC by the thermal analysis. The present approach of real-time quantitative evaluation of the DOC can be applied to fast cure reaction as well as slow reaction demonstrated in this paper.

Measurement of Cure Index of Nano Carbon Composites by an Optical Fiber Sensor with Dual Light Sources
Tatsuro KOSAKA, Katsuhiko OSAKA and Yoshihiro SAWADA,
Proc. 8th Joint Canada-Japan Workshop on Composites, Jul.26-29, Montreal, Canada, 13h40- Kosaka-Mon.pdf, (2009)
Recently, nano-particle dispersed composites are expected as new high-functional materials. However, it is difficult to investigate dispersion of fillers and curing state during molding process. In the present paper, a refractive index measurement method by embedded optical fibers was applied to monitor cure procedure of carbon blacks-dispersed epoxy with dual light sources of narrowband and broadband lights. From the experimental results by a narrowband light, it appeared that scattered lights from carbon blacks produced large fluctuation when cure index was small. After constraint point which is defined amplitude of the fluctuation became suddenly slow, slow change in refractive index caused by curing and thermal shrink of resin was observed. From these experimental results, it appeared that the fluctuation behavior of refractive index indicated changes in mobility of carbon blacks and was strongly affected by changes in viscosity of resin during cure process. We

could also calculate a cure index curve successfully from the experimental results obtained by a broadband light. From both results by narrowband and broadband lights, it was found that the constraint of carbon blacks by resin was strongly governed by cure index of resin.

Development of Fiber Optic AE Sensor for Measuring Low-frequency Signals
Tatsuro KOSAKA, Nobuyuki. KOYANAGI, Katsuhiko OSAKA and Yoshihiro SAWADA, "
JISSE-11, Nov.25-27, Tokyo, Japan, SMS_3_1, (2009)
A new type of AE sensors using Fizeau interferometric optical fiber sensors has been developed for health monitoring in a electromagnetically noisy environment. The sensor was constructed from an optical fiber, two vibrating plates and a sensor case. Silicon oil was enclosed with the two plates and the sensor case. The lower plate picks up an AE signal, the silicon oil transmit the signal to the upper plate, and then the displacement of upper plate is measured by an optical fiber displacement-meter.. Several experiments were conducted to investigate performance of the sensor. From the experimental results, it appeared that the sensor had good performance to measure a pseudo-AE signal and continuous longitudinal and plate waves at a low-frequency range.

Damage Characterization of Ti/GFRP Laminates Subjected to Low-velocity Impact
Hayato NAKATANI, Tatsuro KOSAKA, Katsuhiko OSAKA AND Yoshihiro SAWADA,
Proc. 14th US-Japan Conference on Composite Materials, Sep.20-22, Dayton, USA, pp.1020-1028, (2010)
The low-velocity impact damages in Ti/GFRP laminates as titanium alloy based Fibre-Metal Laminates are investigated. The impact responses of the Ti/GFRP laminates obtained by drop-weight tests are related to impact-induced damages, and the extent of damages in in-plane direction is characterized. In particular, interactions between external and internal damages in the laminates are focused. In addition, effects of the reinforcement achieved by stiffness of titanium facesheets upon impact damages are evaluated on the basis of the damage states in GFRP layers as core material and four-point bending tests. Furthermore, finite element analyses with detailed modeling of damages in the laminates are executed to confirm the experimental results. The numerical and experimental results indicate that impact responses and behavior of internal damages are dominated by the fracture in the titanium layer at opposite side of impact and that this titanium layer plays a major role in preventing impact damages in GFRP core under the low-velocity impact loading.

Cure Monitoring of Nano-Carbon Dispersed Polymers by Fiber Optic Sensors
Tatsuro KOSAKA, Katsuhiko OSAKA, Yoshihiro SAWADA,
Proc. 14th US-Japan Conference on Composite Materials, Sep.20-22, Dayton, USA, pp.1050-1059, (2010)
Although Nano-carbon filler dispersed composites are expected as new high functional materials, it is difficult to investigate dispersion of fillers and curing state during molding process at real-time. In the present paper, a refractive index measurement method by embedded optical fibers was applied in order to develop a new method of monitoring cure procedure of nano-carbon filler dispersed polymers. In this method, dual light sources of narrowband and broadband lights were employed to monitor motion of nano-carbon filler and degree of cure (DOC) of polymers. Different temperature patterns were used to cure the resins. From the experimental results by a narrowband light, it appeared that scattered lights from carbon blacks produced large fluctuation when cure index was small. After constraint point which is defined amplitude of the fluctuation became suddenly slow, slow change in refractive index caused by curing and thermal shrink of resin was observed. From these experimental results, it appeared that the fluctuation behavior of refractive index indicated changes in mobility of carbon blacks and was strongly affected by changes in viscosity of resin during cure process. We could also calculate a cure index curve successfully from the experimental results obtained by a broadband light. From both results by narrowband and broadband lights, it was found that the constraint of carbon blacks by resin was strongly governed by cure index of resin.

Damage Characterization of Ti/GFRP Laminates under Low Velocity Impact Loading
Hayato NAKATANI, Tatsuro KOSAKA, Katsuhiko OSAKA and Yoshihiro SAWADA,
JISSE-11, Nov.25-27, Tokyo, Japan, PMC_4_2.pdf, (2009)
In the present study, impact responses and overall damages of Fibre-Metal Laminates based on titanium alloy and GFRP as Ti/FRP laminate system under low-velocity impact loading were evaluated. Impact damages such as cracks and delamination in/of titanium layer or matrix cracks and interlaminar delamination in GFRP layer were observed from the impact direction. From the experimental evidence, it was found that Ti/GFRP laminates showed two patterns of impact responses and damages with threshold impact energy of about 4.8J. With more impact energy than this threshold, single crack occurred in titanium layer at non-impacted side, and interlaminar

delaminated area in GFRP layer increased sharply. Finite element analysis models that represent the impact behaviour of Ti/GFRP laminates were suggested based on the damage observations. The impact responses and interlaminar delaminated area in GFRP as a function of impact energy obtained by the dynamic analyses agreed well with the experimental results.

Detection of Resin Flow Front in RTM Process by Electromagnetic Acoustic Transducers
Tomohiro YAMASAKI and Hiromitsu NISHINO
Proc. 13th Asia-Pacific Conf. on Non-Destructive Testing, p.119 (2009)
Electromagnetic acoustic transducers (EMATs) are applied to detection of resin flow front in manufacturing process of fiber reinforced plastics by resin transfer molding (RTM) method. Concept of smart manufacturing of FRP, accompanied by real-time monitoring of resin condition, has been suggested in order to assure the quality of the products. In the RTM, resin is injected into the mold, in which reinforcement cloths are stacked in advance. Thus monitoring of resin flow is necessary for optimization of injection setup so as to prevent the generation of voids. Dielectric sensors have been used for such a purpose. However, the sensors may lower the strength of the products, because they should be embedded in the products to obtain the sufficient sensitivity. In this study, we propose to detect the resin flow front by measuring the amplitude decay of multiple echoes in the mold. Since reflection coefficient of ultrasonic wave depends on the boundary condition, echo amplitude keeps on decreasing during the passage of flow front across the measuring area. The EMAT, set on the outer surface of the mold, generates and detects the standing wave in the mold. The strength of the product is not affected by the EMAT, and the measuring point can easily be scanned. Multi-point EMAT, which dispenses with the sensor scan, is also developed. It is ensured that the resin flow front passage can be detected as step-down of echo amplitude, independently of the presence of reinforcement in the mold. For improvement of spatial resolution, sensing area of the EMAT is investigated.

Cure Monitoring in Resin Transfer Molding by Electromagnetic Acoustic Transducer
Tomohiro YAMASAKI, Hiromitsu NISHINO and Taiki KATAYAMA
Trans. Jpn. Soc. Mech. Eng., Ser. A, Vol.76, No.762, pp.145-150 (2010)(in Japanese)
Electromagnetic acoustic transducer (EMAT) is applied to resin cure monitoring in manufacturing process of fiber reinforced plastic (FRP) by resin transfer molding (RTM) method. The RTM is suitable for fabrication of FRP products of three-dimensional complex shape. In order to reduce the cost by minimizing the cycle time, cure monitoring is required. Authors have already ensured that the EMAT can detect the resin flow front in RTM process by monitoring the change in reflection coefficient at mold surface due to resin impregnation. The reflection factor is also affected by the resin viscosity. In this study, during the curing process, we measure the attenuation coefficient of standing wave introduced in the mold. Results are compared with impedance of dielectric sensor located inside the mold, showing that the degree of cure can be evaluated by EMAT at outer surface of the mold.

On the Role of Strengthening Mechanisms in Monotonic and Cyclic Strength of Severely Plastically Deformed Metals: Single Crystals Case Study
A. VINOGRADOV, T.MARUYAMA and S. HASHIMOTO
Scripta Mater. 61, 8, pp.817-820 (2009)
The microstructure effect on the mechanical behaviour of copper single crystals subjected to equal channel angular pressing is discussed with the aim of clarifying the strengthening mechanisms affecting both monotonic strength and fatigue life. The essential role of lattice dislocation storage in cell structures is highlighted.

High-strength and Ductile Glassy-crystal Ni-Cu-Zr-Ti Composite Exhibiting Stress-induced Martensitic Transformation
D.V.LOUZGUINE, G. XIE, S. LI, A.VINOGRADOV, A.LAZAREV and A. INOUE
Philosophical Magazine, 89, 32, pp.2887–2901 (2009)
The deformation behaviour of Zr60Cu16Ni14Al10 glassy alloy was found to exhibit cleavage-like fracture relief paired with typical vein patterns. The mirror-like cleavage area fraction is found to be comparable with that of vein areas. These two types of patterns alternate on the fracture surface in a direction normal to shear deformation. The structure of the studied alloy was characterised by X-ray diffractometry and scanning and transmission electron microscopy. A small volume fraction of crystals in the form of eutectic colonies were found here and there in the specimen. No distinct difference in the glassy structure of the cleavage-like fracture areas and the areas corresponding to vein patterns was found within the resolution of experimental techniques employed.

Nanostructure Formation in the Surface Layer of Metals under Influence of High-power Electric Current Pulse

A.VINOGRADOV, A. MOZGOVOI (Institute of Experimental Physics, Sarov) , S. LAZAREV SHVEDOV (Microsensors AE, Ltd.), S. GORNOSTAI-POLSKII (Institute of Experimental Physics, Sarov), R.OKUMURA and S.HASHIMOTO,

Journal of Materials Science, 44, 17, pp.4546-4552 (2009)

The possibility to tailor the microstructure of metals is explored utilising a skin-effect for surface treatment. The theoretical simulation of the electric and magnetic fields in a metallic cylinder shows that melting followed by rapid quenching can occur in a skin layer of 5– 10-lm thickness if the amplitude of a single electric pulse of several nanoseconds duration is of the order of hundreds kiloamperes. The experiments using the SUS304 stainless steel show that besides a thin amorphous layer, a specific nano-twin structure can form at the near-surface region. The appearance of nano-twins is explained considering the stress components arising at the surface layer and in the bulk of the specimen during shock wave propagation caused by temperature gradients and the Lorentz force. It is shown that the high stress amplitudes can arise locally, furnishing the required conditions for twin nucleation and resulting in intensive plastic deformation of the sub-surface layer.

About Plastic Instabilities in Iron and Power Spectrum of Acoustic Emission

A. LAZAREV and A. VINOGRADOV,

J. of Acoustic Emission, 27, pp. 144-156 (2009).

Plastic instabilities are investigated in iron with different purity by means of acoustic emission (AE) power spectral analysis. Special attention is paid to AE accompanying the yield drop followed by Lüders-band propagation and macroscopic strain localization associated with necking followed by crack nucleation and propagation. Both the Lüders instability and necking belong to the same generic type strain-softening instability although the former refers to the so-called propagative instability while the latter is static. In both cases, significant shift of the power spectral density towards low frequencies is observed and discussed.

Electromagnetic Method of Elastic Wave Excitation for Calibration of Acoustic Emission Sensors and Apparatus

S.LAZAREV (Microsensors AE, Ltd.), A MOZGOVOI (Institute of Experimental Physics, Sarov), A.VINOGRADOV, A.LAZAREV and A. SHVEDOV (Microsensors AE, Ltd.)

J. of Acoustic Emission, 27, pp. 215-223 (2009).

We propose a new sensor testing technique, which may be a good candidate for the absolute sensor calibration, for the routine laboratory and in-field sensor response checking and for selecting the sensors with similar responses for AE source location problems. We suggest utilizing the energy of the high power electromagnetic field in a coaxial transfer line with a specific geometry to excite a mechanical wave at the surface of a conducting media. Theoretical modeling approach is discussed and the experimental validation of the proposed method is presented. Advantages of this method are as follows: i) the extremely high stability of the elastic wave at the epicentral point where the AE sensor is attached; ii) the field of mechanical displacements produced by the magnetic field pressure is computable as a function of time with an aid of finite element method; iii) dimensions are small, installation is easy and convenient both for the academic laboratory experiments and for the everyday NDT practice; iv) low cost and simple maintenance.

Fatigue of Ultrafine Grained Light Alloys

Y. ESTRIN and A. VINOGRADOV

Int. J. of Fatigue, 32, 6, pp.898-907 (2010).

The fatigue behaviour of light alloys with grain sizes reduced to the micron or submicron scale by severe plastic deformation (SPD) is reviewed. While the enhancement of tensile strength by this extreme grain refinement can be quite appreciable, the fatigue strength is usually not improved to the same extent. This observation is common to Al, Mg and Ti based alloys and does not appear to be attributable to a particular crystallographic structure. Various effects that may influence this behaviour are reviewed, and emphasis is put on the role of the alloying effects as the main contributors to fatigue strength. The direct contribution of solutes to fatigue strength is usually stronger than their indirect effect through the influence of solutes on the grain refinement. Recent examples from literature and our own work are presented to corroborate the views expressed in the article

On the Shear Bands Velocity and Detectability of Acoustic Emission in Metallic Glasses

A. VINOGRADOV

Scripta Materialia, 63, 1, pp.89–92 (2010).
The acoustic emission (AE) method is proposed for the assessment of shear band velocity in metallic glasses. The shear band velocity is discussed in light of analysis of real-time AE transient events which occur during inhomogeneous plastic flow. It is estimated that the velocity of shear events triggering shear bands should be at least as high as 1–10 m /s to be detected by AE transducers.

Formation of Deformation Twins and Related Shear Bands in Copper Single Crystals Pressed by ECAP
T.IKEDA (Doshisha Univ.), H.MIYAMOTO (Doshisha Univ.), T.UENOYA (Doshisha Univ.), S.HASHIMOTO and A.VINOGRADOV,
Mater. Sci. Forum, 654-656 pp.1231-2134 (2010).
The pure copper single crystals with specific crystallographic orientated were subjected to ECAP for one pass at room temperature. Two types of shear bands were observed. Type 1 shear bands were constructed with clusters of distorting micro shear bands and matrix. Micro shear band and matrix were delineated by large-angle grain boundaries, and these two orientations are in a twinning relationship. Parallel sets of deformation twins were observed in the matrix. Type 2 shear bands had no crystallographic feature, and shear band and matrix were considered as low-angle grain boundaries. Deformation twin was not observed both in matrix and the shear bands.

Evolution of High-Angle Grain Boundaries in a (001) Copper Single Crystal Subjected to Sliding Wear
Y.OHNO, J. INOTANI, Y.KANEKO and S.HASHIMOTO
J. Japan Inst. Metals, Vol. 73, pp. 924-929 (2009) (in Japanese)
A sliding wear test was conducted on a copper single crystal having (001) surface. In the vicinity of worn surface, equiaxed fine grains that were separated by high-angle boundaries were generated. On the other hand, formations of low-angle boundaries were predominant at the area distant from the worn surface. In the present study, the formation of low-angle boundaries that were perpendicular to the worn surface and evolution of the high-angle boundaries were investigated by the electron backscatter diffraction (EBSD) method. In the region where the low-angle boundaries were formed predominantly, lattice rotation occurred almost around the axis which is normal to the wear direction. However, from a detailed orientation analysis, local rotation axes were slightly different even in the same grain. The perpendicular low-angle boundaries could be introduced by a misorientation between adjoining areas that had such different rotation axes. Amount of the high-angle boundaries increased with decreasing depth from the worn surface. At the vicinity of the worn surface, many coincidence-site lattice (CSL) boundaries with various Σ-values were recognized. On the other hand, near the low-angle boundary region, the CSL boundaries were limited to Σ13a and Σ25a. This characteristic distribution of Σ-value could be understood from a model that the high-angle boundaries were generated by accumulated lattice rotation induced by the sliding wear.

Preferential Fatigue Crack Nucleation at Deformation Twins in a Ferritic Stainless Steel
T.TANIGUCHI, Y.KANEKO and S.HASHIMOTO
J. Japan Inst. Metals, Vol. 73, pp. 930-937 (2009) (in Japanese)
Crack nucleation along deformation twin boundary has been investigated in an Fe-20%Cr alloy. The deformation twins were introduced by compression test in liquid nitrogen. Push-pull fatigue tests on the twinned specimens were carried out at room temperature. Two kinds of cracks were detected in the vicinity of the twin boundaries: one was a serrated intragranular crack and the other was an intergranular crack formed along the twin boundary. From a monotonic tensile test on a twinned specimen, it is confirmed that the serrated crack was generated as a result of twin boundary migration during detwinning process, regardless of fatigue cycling. After the fatigue loading was sufficiently repeated, the twin boundary migration and the related serrated crack nucleation were no longer observed. Instead, extrusions were generated on the twin boundaries. The fatigue cracks were finally nucleated along the extrusions. When the twinned specimen was annealed, fatigue property was improved. This is because the nucleated twin-boundary cracks were arrested at the edge of twin bands which were highly fragmented by the annealing.

A Dislocation-Based Approach to Identify Fracture Process
Y. KANEKO, Y. HONDA and S. HASHIMOTO
IOP Conf. Series: Mater.Sci.Eng. Vol. 3, pp.012019 (2009)
Microstructures near fracture surfaces of copper specimens were investigated using electron channelling contrast imaging (ECCI) method. The purpose of the present study is to find a new criterion for analyzing fracture process instead of a conventional fractographic technique. In the present study, the ECCI observations were conducted on strip and center-cracked tensile specimens of a polycrystalline copper, which were fractured under monotonic

tensile straining or fatigue loading. The ECCI observation revealed that the cell, the vein, and the ladder-like dislocation structures were formed near the fracture surface of the strip specimen fractured under fatigue, although no vein and ladder-like structures were found in the monotonically strained specimen. It is suggested that the distinction between the fatigue fracture and the monotonic tensile fracture can be achieved from the ECCI observation near the fracture surfaces. We also measured the sizes of the region which contained the cell structures at the fatigue crack propagating in the center-cracked tensile specimen. It is confirmed that the size of the cell-structured region increased with increasing stress intensity factor range ΔK_I. By measuring the sizes of the cell-structured regions of the strip specimen, we could obtain the distribution of the ΔK_I value along the fracture surface from the preliminarily-measured relationship between the cell-structured region size and the ΔK_I value. This kind of the ΔK_I distribution will give important information such as crack nucleation site and crack growth direction, which is required for a better understanding of fatigue fracture process.

ECCI Observations of Dislocation Structures around Fatigue Cracks in Ferritic Stainless Steel Single Crystals

T.TANIGUCHI, Y.KANEKO and S.HASHIMOTO

IOP Conf. Series: Mater.Sci.Eng. Vol. 3, pp.012020 (2009)

Dislocation structures around the crack tips of ferritic stainless steel single crystals were observed with electron channelling contrast imaging (ECCI) method. The ECCI method enables us to observe dislocations lying near surface using a scanning electron microscope. Fatigue crack growth tests were conducted on compact tension (CT) specimens having loading axes of $[\bar{2}21]$ and $[\bar{1}10]$ directions. In the specimen having the $[\bar{1}10]$ loading axis at which the fatigue crack having Mode I and II component propagated, a thin band-like structure consisting of dislocation wall array was observed ahead of the crack tip. On the other hand, the dislocation structures around the crack having Mode I and III components could be divided into three regions in the specimen with the $[\bar{2}21]$ loading axis: the cell structure, the dislocation wall structure and the vein structure were observed in order of ascending distance from crack tip. Difference between the dislocation structures near the fatigue cracks could be understood from the crack mode by which edge and screw dislocation emissions from the crack tips are strongly affected.

Orientation Dependence of High-Angle Grain Boundary Formation during Sliding Wear in Copper Single Crystals

Y.OHNO, J. INOTANI, Y.KANEKO and S.HASHIMOTO

J. Japan Inst. Metals, Vol. 74, pp. 384-391 (2010) (in Japanese)

Sliding wear tests were conducted on copper single crystals having (110) and (111) surface, and polycrystalline copper. Evolution of high-angle grain boundaries during the sliding wear was investigated by the electron backscatter diffraction (EBSD) technique. The high-angle grain boundaries, which were formed in the vicinity of the worn surface, could be classified into two kinds from their morphology: one is parallel to the worn surface (Type A high-angle boundary) and the other is a grain boundary surrounding an equiaxed fine grain (Type B high-angle boundary). At Type A high-angle boundaries, a rotational axis between adjoining grains was almost parallel to *z*-axis which is defined as the direction perpendicular to both wear direction and worn surface normal. Grain boundary character distribution of Type A boundaries was sensitive to crystallographic orientation of the z-axis. When the z-axis was <110>, orientation relationship of Σ33a had high frequency. On the other hand, high Σ31a frequency was obtained at the sliding wear occurring under <111> z-axis condition. It is concluded that the evolution of Type A boundaries was caused by lattice rotation induced by sliding wear. For Type B high-angle boundaries, fractions of low-Σ coincident site lattice (CSL) boundaries were high, and the frequency distribution of CSL boundaries was almost independent of wear direction and worn surface orientation. Unlike Type A boundaries, rotational axes at Type B boundaries showed no preferred orientation. These crystallographic features suggest that recrystallization is the most plausible origin for Type B boundary evolution. Consequently, the high-angle boundaries were produced probably by two different processes during sliding wear.

A New Methodology of Fractography using ECCI and EBSD/SEM Analyses

S.HASHIMOTO and Y.KANEKO

Function & Materials, Vol. 30, pp. 69-74 (2010) (in Japanese)

Fatigue and fracture of materials have been known as significantly complicated phenomena. Through wide-area observation of lattice defects, particularly of self-organized dislocation structures, the essentials of the phenomena have been attempted to be clarified. In the present paper, we reported recent development of dislocation structure observation by the electron channelling contrast imaging technique.

Preparation and Properties of Bimodal Porous Apatite Ceramics Through Slip Casting Using Different Hydroxyapatite Powders

Yin ZHANG, Yoshiyuki YOKOGAWA, Xia Feng, Yaquiq TAO, Yuanqiang Li Yin ZHANG

Ceramics International Vol.36, pp.107–113 (2010).

A bimodal porous hydroxyapatite (HAp) body with high flexural strength was prepared through slip casting. The effect of different particle sizes on the flexural strength and microstructure of three different types of hydroxyapatite (HAp) powders was studied. The powder characteristic of laboratory-synthesized HAp powder (L-HAp) was obtained through a wet-milling method, drying and heating of a mixture of calcium hydrogen phosphate di-hydrate and calcium carbonate. The median particle size of L-HAp was 0.34 μm, and the specific surface area was 38.01 m2/g. The commercial HAp had median particle sizes for the K-HAp (Kishida chemical Co.,Ltd, K-HAp) and T-HAp (Taihei chemical Co.,Ltd, T-HAp) of 1.13 and 3.65 μm, and specific surface areas of 11.62 and 6.23 m2/g, respectively. The different powder characteristics affected the slip characteristics, and the flexural strength and microstructure of the sintered porous HAp bodies were also different. The flexural strengths of the porous HAp ceramics prepared by heating at 1200 ºC for 3 hours in air were 17.59 MPa for L-HAp with a porosity of 60.48％, 3.92 MPa for commercial K-HAp with a porosity of 79.37％, and 4.55 MPa for commercial T-HAp with a porosity of 76.46 ％.

Preparation of Thermally Stable Nanocrystalline Hydroxyapatite by Hydrothermal Method

S.Prakash PARTHIBAN, K.ELAYARAJA, E.K.GIRIJAirija, Y.YOKOGAWA, R.KESAVAMOORTHY, M.PALANICHAMY, K.ASOKAN and S.Narayana KALKURA,

Journal of Materials Science: Materials in Medicine, Vol. 20, pp.77-83(2009).

Thermally stable hydroxyapatite (HAp) was synthesized by hydrothermal method in the presence of malic acid. X-ray diffraction (XRD), Fourier transform infra-red spectroscopy (FT-IR), Raman spectroscopy, scanning electron microscopy (SEM), differential thermal analysis (DTA), thermogravimetric analysis (TGA) was done on the synthesized powders. These analyses confirmed the sample to be free from impurities and other phases of calcium phosphates, and were of rhombus morphology along with nanosized particles. IR and Raman analyses indicated the adsorption of malic acid on HAp. Thermal stability of the synthesized HAp was confirmed by DTA and TGA. The synthesized powders were thermally stable upto 1,400°C and showed no phase change. The proposed method might be useful for producing thermally stable HAp which is a necessity for high temperature coating applications.

First-Principles Calculations on Proton Migration Mechanism in Hydroxyapatite,

Ippei KISHIDA, Kengo ORITA, Atutomo NAKAMURA, and Yoshiyuki YOKOGAWA,

Bioceramics, Vol.22, pp.109-112 (2009).

In the present study, we have made a theoretical approach based upon the first principles calculations to investigate the behavior of H vacancies and H interstitials in a hydroxyapatite crystal. Stable sites and relative energies of H defects were computed. H vacancies were found to be only on OH columns and not to migrate between the columns. The obtained migration energy of the H vacancy in c direction is 1.20 eV. A unit cell has ten sites for H interstitial. Two sites of them locate near an OH column and participate in H conduction. The migration energy of the H interstitial is lower than that of a H vacancy. These results indicate H interstitials can play an important role in electric properties in hydroxyapatite.

Biomolecules Loading and Mesoporous SBA-15 Pore Sizes,

Y.YOKOGAWA, T.TOMA, A.SAITO, A.NAKAMURA, I.KISHIDA,

Bioceramics, Vol.22, pp.275-278 (2009)

The encapsulation and immobilization of biomolecules on solid materials, mesoporous SBA-15, have been studied. Highly ordered hexagonal mesoporous silicates (MPS) with different mean pore sizes have been synthesized using two kinds of triblock copolymers (P123 or L123) as a template. The mixture of tetraethyl orthosilicate (TEOS) and the triblock copolymer (poly(ethylene glycol)-poly(propylene glycol)-poly(ethylene glycol)) was stirred and hydrothermally treated at various temperatures to form the MPS structure. Higher temperatures during stirring and hydtrothermal treatment led to the enlargement of pore size. UV-spectrometry was performed to determine the amount of bovine serum albumin (BSA) encapsulated in MPS. It was found that the adsorption processes of BSA on/in MPS could be well described by intraparticle diffusion model.

Synthesis of Microporous Materials and their Adsorptive Properties of h2S for DentalApplication,

I.KISHIDA, H.UTAKA, H.MORIKAWA, A.NAKAMURA, and Y.YOKOGAWA,

Bioceramics, Vol.22, pp.291-294 (2009).

The microporous materials, Zeolite A and ZSM-5 were hydrothermally synthesized and their H_2S adsorption was studied. The obtained samples were put into separable glass flask filled with H_2S gas, and the change in concentrations of H_2S was measured for 1 – 48 hrs at rt. Then the samples were taken out and put into a pyrolysis plant attached to gas chromatography-mass spectroscopy to determine the amount of H_2S desorbed from samples. The amount of H_2S adsorbed on Zeolite A was found to be larger than that on ZSM-5. 46 % of H_2S was desorbed from Zeolite A when heated at 400ºC, while 24% of H_2S was desorbed from ZSM-5. The adsorption / desorption behavior of H_2S from zeolite materials could be interpreted by the electrostatic interaction between H_2S and adsorbent.

Synthesis of Microporous Materials and Their Sulfide Adsorption Properties
I.KISHIDA, H.MORIKAWA, H.UTAKA, A.NAKAMURA, and Y.YOKOGAA,
Arch.BioCeram Res., Vol.9, pp.75-78 (2009).
The microporous materials, zeolite and hydrotalcite, were synthesized and their H2S adsorption was studied. The obtained specimens were identified by powder X-ray diffraction method. The specimens were put into separable glass flask filled with H2S gas, and the change in concentrations of H2S was measured for 1 - 48 hrs at rt. Then the samples were taken out and put into a pyrolysis plant attached to gas chromatography-mass spectroscopy to determine the amount of H2S desorbed from samples. The amount of H2S adsorbed on Zeolite A was found to be larger than that on ZSM-5. 46 % of H2S was desorbed from Zeolite A when heated at 400 ºC, while 24% of H2S was desorbed from ZSM-5. In case of hydrotalcite, 2 % of H2S was desorbed
when heated at 400 ºC.

Influence of the Titanium Doping on 2^o Tilt Grain Boundaries in $LiNbO_3$
A. NAKAMURA, I. OKAWA, J. NAKAMURA, E. TOCHIGI, I. KISHIDA and Y. YOKOGAWA
AMTC Letters, 2, pp. 246-247 (2010).
Lithium niobate ($LiNbO^3$) is one of the most widely used electro-optic materials since it has superior ferroelectric properties with large pyroelectric, piezoelectric, electro-optic and photoelastic coefficients. So far, a lot of studies about the properties have been conducted for electro-optic applications. However, the structure and function of lattice defects in $LiNbO_3$ had not been investigated enough. In this study, therefore, the tilt grain boundary with the low misorientation of 2^o fabricated by bicrystal experiment, in order to analyze the boundary structure and the influence of Ti doping on the structure.

Conducting Nanowires Fabricated by Dislocations Engineering in Insulating Crystals
A. NAKAMURA, K. MATSUNAGA, T. YAMAMOTO and Y. IKUHARA
Materia, 7, pp. 310-311 (2010). (in Japanese)
The lattice defects on/in crystals such as surfaces, interfaces, grain boundaries, dislocations, vacancies and so on can bring about novel physical or chemical properties in materials, as a result of special structures around the defects or due to the segregation of dopants, impurities and point defects to the defects. “Using line defects” has a potential to develop new and novel properties into existent materials. Here, we introduce our study on Nature Materials vol.2 (2003), where the formation of conducting Ti-nanowires in insulating sapphire crystals “using line defects” was reported.

Structures of Dissociated <1-100> Dislocations and {1-100} Stacking Faults of Alumina (α-Al_2O_3)
E. TOCHIGI, N. SHIBATA, A. NAKAMURA, T. MIZOGUCHI, T. YAMAMOTO and Y. IKUHARA
Acta Materialia, 58, pp. 208-215 (2010).
An alumina (α-Al_2O_3) bicrystal with a {1-100}/<11-20> 2^o low-angle grain boundary was fabricated by diffusion bonding, and the grain boundary was observed by high-resolution transmission electron microscopy (HRTEM). It was found that 1/3<1-100> partial-dislocation triplets were periodically arrayed along the boundary. The atomic structure within the {1-100} stacking faults in between the partial-dislocation triplets was determined by HRTEM combined with first-principles calculations. We discuss the stacking fault structures and their excess energies in detail.

Applied Mathematics

Lateral Estimates for Iterated Elliptic Operators and Analyticity,
Shigeo TARAMA
Electron. J. Diff. Equ., Vol. 2009, No. 156, pp. 1-3 (2009).
In this short paper, we show the analyticity of a non-negative function that is still non-negative after an elliptic operator with real and analytic coefficients is applied iteratively. The idea of proof is simple. By integration by parts, we get, using the non-negativity, the estimates on functions obtained by applying iteratively the elliptic operator. The conclusion follows from these estimates and from the theorem due to Bolley, Camus and Metivier.

Physical Electronics and Informatics

Electrical Engineering

Evaluation of Electrical Characteristics in Fully Depleted SOI-MOSFETs for Variable Threshold Voltage Scheme
A. OHATA and S. CRISTOLOVEANU
Proc. EUROSOI, Grenoble 27-28 January, pp.117-118 (2010)
We investigated the impact of threshold voltage (V_{TH}) control by a back-gate bias (V_{g2}) on the electrical characteristics of high-k/metal-gate fully depleted (FD) SOI-MOSFETs. The carrier mobility (μ) and coupling effect were investigated. The results confirm that, even for small positive Vg_2, back channel activates first by sweeping front-gate bias (V_{g1}). It is found that μ decreases considerably at lower electron density for negative V_{g2}. A trade-off exists for the mobility enhancement at positive V_{g2} due to the decrease in the electric field and in the Coulomb scattering rate.

Flatbed-Type Bidirectional Three-Dimensional Display System
H. TAKAHASHI, N. KUREYAMA, K. YAMADA and T. AIDA
International Journal of Innovative and Control, Vol.5, 11 (B), pp.4115-4124 (2009)
We propose a flatbed-type bidirectional three-dimensional (3D) display system for multiple users as an improved version of our previous thin natural 3D display based on the ray reconstruction method. This system is a tool for communication among a small number of people around a 3D image. It is a flatbed-type autostereoscopic bidirectional 3D display system consisting of a flat panel display and a bidirectional holographic lens array sheet. Its notable feature is the ability to display natural 3D images which are visible to multiple viewers at the same time. Because 3D real images float in the display area of the proposed display, it allows two or more people surrounding it to simultaneously observe 3D images from their own viewpoints. This paper describes the system and also gives experimental results.

Three-Dimensional Circular Camera System for the Thin Three-Dimensional Display Based on the Reconstruction of Parallax Rays
S. MIYATAKE, H. TAKAHASHI and K. YAMADA
Proc. of the 5th International Conference on Intelligent Information Hiding and Multimedia Signal Processing (IIHMSP2009), pp.174-167 (2009)
We have previously proposed the three-dimensional (3D) display system based on the reconstruction of parallax rays. In order to display real 3D object, applying image-based rendering technique, we have also proposed a camera system that captures light ray data needed for reconstructing natural 3D images by using parallax rays reconstruction method from multiple images captured from multiple viewpoints. However, because the previous camera system was straight arrangement, the ray information of the object could be acquired only from one side. In order to reconstruct a 3D image of a real object which can be observed from surrounding multiple viewing points, multiple images which captured from multiple viewing points around a real object are required. Thus, we propose a circular camera system that captures light ray data of a real object from circular multiple viewpoints. To reduce the number of component cameras of the circular camera system, we also propose an interpolation algorithm. This paper describes an interpolation algorithm of the circular camera system.

Evaluation of Multiwavelength Band-Pass Filter Endoscope Using Compound Eye Optical System
K. TABATA, K. YAMADA, and H. TAKAHASHI
Proc. of the 4th International Conference on Innovative Computing Information and Control (ICICIC2009), IS14-01 (CD-ROM) (2009)
We propose the novel endoscope system with compound eye and wavelength band pass filter. The system is composed of micro-lens array, wavelength band pass filter, separation layer and image sensor. Several wave

length band pass filters are covered with each microlens. The proposed system makes it possible to take any images from the membrane surface to deep blood vessel simultaneously. With several test targets, the characteristics of the prototype system are evaluated.

Circular Camera Array System for 3-D Displays Based on the Reconstruction of Parallax Rays
H. TAKAHASHI, S. MIYATAKE, K. YAMADA and T. AIDA
Journal of the Society for Information Display, Vol.18, 7, pp.501-506 (2010)
In this paper, we propose a circular camera system employing an image-based rendering technique that captures light ray data needed for reconstructing three-dimensional (3D) images by using reconstruction of parallax rays from multiple images captured from multiple viewpoints around a real object in order to display a 3D image of a real object that can be observed from multiple surrounding viewing points on a 3D display. We also propose an interpolation algorithm that is effective in reducing the number of component cameras in the system. This paper describes the interpolation and experimental results which were performed on our previously proposed 3D display system based on the reconstruction of parallax rays. When the radius of the proposed circular camera array was 1100 mm, the central angle of the camera array was 40 degrees, and the radius of a real 3D object was between 60 mm and 100 mm, the proposed camera system, consisting of 14 cameras, could obtain sufficient 3D light ray data to reconstruct 3D images on the 3D display.

Implementation of a Circular Light field Camera Array for 3D Display Based on the Reconstruction of Parallax Rays
H. TAKAHASHI, K. HIROOKA, K. YAMADA and T. AIDA
Proc. of the 3rd International Symposium on Intelligent Informatics (ISII2010), ISII2010-291 (CD-ROM) (2010)
We have previously proposed the three-dimensional (3D) camera array system for 3D display based on the reconstruction of parallax rays. In order to display a 3D image of a real object which can be observed from surrounding multiple viewing points on our 3D display, it captures light ray data needed for reconstructing 3D images by using parallax rays reconstruction method from multiple images captured from multiple viewpoints around a real object. To reduce the number of component cameras of the circular camera system, we have also proposed an interpolation algorithm. This paper describes the implementation of an experimental 3D camera system which consists of multiple PC cameras. Each captured image was calibrated to the image captured at the correct camera position by image processing method. After that, we applied the interpolation algorithm, and light ray data of the target object were obtained.

Volumetric display using a roof mirror grid array
D. MIYAZAKI, N. HIRANO, Y. MAEDA, K. OHNO, S. MAEKAWA
Stereoscopic Displays and Applications XXI, Proc. Soc. Photo-Opt. Instrum. Eng., Vol. 7524, pp. 75240N (2010).
A volumetric display system using a roof mirror grid array (RMGA) is proposed. The RMGA consists of a two-dimensional array of dihedral corner reflectors and forms a real image at a plane-symmetric position. A two-dimensional image formed with a RMGA is moved at thigh speed by a mirror scanner. Cross-sectional images of a three-dimensional object are displayed in accordance with the position of the image plane. A volumetric image can be observed as a stack of the cross-sectional images by high-speed scanning. Image formation by a RMGA is free from aberrations. Moreover, a compact optical system can be constructed because a RMGA doesn't have a focal length. An experimental volumetric display system using a galvanometer mirror and a digital micromirror device was constructed. The formation of a three-dimensional image consisting of 1024 × 768 × 400 voxels is confirmed by the experimental system.

Volumetric Display System Using a Digital MicromirrorDevice Based on Inclined-Plane Scanning
D. MIYAZAKI, T. HONDA, K. OHNO, T. MUKAI
J. Display Technol., Vol.6, No.10, pp. 548-552 (2010)

Experimental results of a volumetric display system based on three-dimensional (3-D) scanning using an inclined image are reported. An optical real image of an inclined two-dimensional (2-D) display device is moved laterally by an optical mirror scanner. Inclined cross-sectional images of a 3-D object are projected in accordance with the position of the image plane. A 3-D real image is formed as a stack of 2-D cross-sectional images as a result of high-speed scanning. This 3-D image can satisfy all the criteria for stereoscopic vision. An experimental system using a galvanometer mirror and a digital micromirror device was constructed, and generated three- dimensional images consisting of 1024 × 768 × 200 voxels. Multi-level image can be formed by a spatial dithering technique, even though the binary display device was used.

Reconstruction of Three-Dimensional Image from Compound-Eye Imaging with Defocus Using Ray Tracing

Daisuke MIYAZAKI1, Katsuaki ITO, Yoshizumi NAKAO, Takashi TOYODA and Yasuo MASAKI

Int. J. of Innovative Computing Information and Control, Vol.5, No.11, pp. 4225-4235 (2009)

A three-dimensional (3-D) image reconstruction method from a compound-eye image degraded by low-resolution sampling and defocusing is proposed. The 3-D profile of a target object is acquired from parallax images captured by a compound-eye imaging system. The compound-eye imaging is modeled by ray tracing to relate the pixels on the 3-D surface of the object to the pixels of an image sensor. The point-spread function of an optical system is estimated by calculating many optical rays passing through the whole area of the pupil of the optical system. This enables us to take into consideration the influence of occlusion upon the point-spread function. A high-resolution 3-D image can be reconstructed by minimizing the difference between the captured image and the image calculated by ray tracing of the modeled composed-eye imaging. The validity of the proposed method is verified by computer simulations and preliminary experiments.

Applied Physics

Effects of Distributed Bragg Reflectors on Temporal Stability of CuCl Microcavities
K. MIYAZAKI, D. KIM, T. KAWASE, M. KAMEDA and M. NAKAYAMA
Jpn. J. Appl. Phys., Vol. 49, 042802 (4pages) (2010)
We have investigated the characteristics of exciton polaritons in a CuCl microcavity with distributed Bragg reflectors (DBRs). Two sets of multilayers, $PbBr_2/PbF_2$ and HfO_2/SiO_2, were adopted as the DBRs in order to study the temporal stability of the CuCl microcavity. The thickness of the CuCl active layer was fixed to an effective $3\lambda/2$ length. Angle-resolved reflectance spectra clearly demonstrate the formation of the cavity polaritons. From the phenomenological analysis with a 3x3 Hamiltonian for the cavity-polariton modes originating from the Z_3 exciton, $Z_{1,2}$ exciton, and cavity photon, the Rabi splitting energies are evaluated to be 97 and 162 meV for the Z_3 and $Z_{1,2}$ excitons, respectively, in the fresh CuCl microcavity with the $PbBr_2/PbF_2$ DBR. However, the Rabi splitting energies remarkably decrease within 6 days from the sample preparation, which is due to the degradation of the DBR resulting from alloying of $PbBr_2$ and PbF_2. On the other hand, in the CuCl microcavity with the HfO_2/SiO_2 DBR, the Rabi splitting energies of 105 and 168 meV for the Z_3 and $Z_{1,2}$ excitons, respectively, hardly change during 360 days from the sample preparation. This indicates that the stability of the oxide materials of HfO_2 and SiO_2 prevents the degradation of the DBR and CuCl active layer. Thus, a stable CuCl microcavity can be prepared by adopting the multilayer of HfO_2/SiO_2 as the DBR, which is a merit in applications.
DOI: 10.1143/JJAP.49.042802

Observation and Quantification of the Direction Reversal of the Surface Band Bending in $GaAs_{1-x}N_x$ Using Terahertz Electromagnetic Wave and Photoreflectance Measurements
H. TAKEUCHI, J. YANAGISAWA, J. HASHIMOTO and M. NAKAYAMA
Phys. Status Solidi C, Vol. 7, pp. 1844-1846 (2010)
We have investigated the polarity of terahertz (THz) electromagnetic waves from a $GaAs_{1-x}N_x$ epitaxial layer with x=0.43 % to clarify the effects of nitrogen incorporation on the direction of the surface band bending. The THz-wave polarity of the $GaAs_{1-x}N_x$ sample is reversed compared with that of an i-GaAs/n-GaAs sample that has an upward surface band bending; namely, the $GaAs_{1-x}N_x$ sample has a downward band bending. The polarity reversal is attributed to the phenomenon that the conduction band bottom is lowered by the band anticrossing due to the nitrogen incorporation, which changes the direction of the surface band bending. We also measured the photoreflectance (PR) spectrum of the $GaAs_{1-x}N_x$ sample to quantify the surface electric field produced by the surface band bending. The PR spectrum exhibits the Franz-Keldysh oscillations (FKOs) from the $GaAs_{1-x}N_x$ layer. From the FKOs, the surface electric field is estimated to be 24 kV/cm.
DOI: 10.1002/pssc.200983419

Photoluminescence from Exciton-Exciton Scattering in a $GaAs_{1-x}N_x$ Thin Film
J. HASHIMOTO, Y. MAEDA, and M. NAKAYAMA
Appl. Phys. Lett., Vol. 96, 081910 (3 pages) (2010)
We have investigated photoluminescence (PL) properties under high-density-excitation conditions at 10 K in a $GaAs_{1-x}N_x$ thin film (x=0.008) with a narrow band-gap energy of 1.34 eV. A PL band was observed with a threshold-like nature, and its intensity was found to exhibit quadratic dependence on the excitation power. At the threshold excitation power, the PL-peak energy is lower than the energy of the fundamental exciton by the magnitude of the exciton binding energy that is ~4 meV. The results described above indicate that the PL band originates from exciton-exciton scattering, the so-called P emission, which is typically observed in wide-gap semiconductors with large exciton binding energies. Furthermore, we have confirmed the existence of optical gain in the energy region of the P band using a variable-stripe-length method.
DOI: 10.1063/1.3309695

Direction Reversal of the Surface Band Bending in GaAs-based Dilute Nitride Epitaxial Layers Investigated by Polarity of Terahertz Electromagnetic Waves

H. TAKEUCHI, J. YANAGISAWA, and M. NAKAYAMA
Physics Procedia, Vol. 3, pp. 1109-1113 (2010)
We have investigated the polarity of terahertz (THz) electromagnetic waves from GaAs-based dilute nitride ($GaAs_{1-x}N_x$ and $In_yGa_{1-y}As_{1-x}N_x$) epitaxial layers to clarify the effects of nitrogen incorporation on the direction of the surface band bending. The THz-wave polarities of the dilute nitride samples are reversed compared with those of an i-GaAs/n-GaAs sample that has an upward surface band bending; namely, the dilute nitride samples have a downward band bending. The polarity reversal is attributed to the phenomenon that the conduction band bottom is lowered by the band anticrossing due to the nitrogen incorporation, which changes the direction of the band bending.
DOI: 10.1016/j.phpro.2010.01.147

Frequency Shift of Terahertz Electromagnetic Waves Originating from Sub-Picosecond-Range Carrier Transport in Undoped GaAs/n-Type GaAs Epitaxial Layer Structures
H. TAKEUCHI, J. YANAGISAWA, S. TSURUTA, H. YAMADA, M. HATA, and M. NAKAYAMA
Jpn. J. Appl. Phys., Vol. 49, 082001 (5pages) (2010)
We have investigated the terahertz electromagnetic waves from undoped GaAs/n-type GaAs (i-GaAs/n-GaAs) structures with various i-GaAs-layer thicknesses, focusing on the relation between the sub-picosecond-range carrier-transport processes and terahertz-wave frequency. It is observed that the intense monocycle oscillation induced by the surge current of photogenerated carriers is followed by the signal of the coherent GaAs longitudinal optical (LO) phonon. The Fourier power spectra of the terahertz waveforms reveal that an increase in the built-in electric field of the i-GaAs layer, which is controlled by the i-GaAs layer thickness, causes a high frequency shift of the band due to the surge current. Consequently, we conclude that the photogenerated carriers are accelerated by the built-in electric field in the sub-picosecond range without being affected by the intervalley scattering. This demonstrates that the frequency tunable terahertz emitters are realized. Furthermore, we find that terahertz band of the coherent LO phonon is relatively intense, compared with those from bulk crystals. This phenomenon is discussed from the viewpoint of the effects of the built-in electric field on the terahertz radiation mechanism.
DOI: 10.1143/JJAP.49.082001

Comparative study of laser-induced metastability-exchange optical pumping of ^{3}He atoms through the 2^3S_1-3^3P_J transition at 389 nm with the 2^3S_1-2^3P_J transition at 1083 nm
SHINGO MAEDA, YUTAKA TABATA, HIROKI YAMADA and HIROSHI KUMAGAI
Optical Engineering , 49, 091014 (2010)
We developed a metastability-exchange optical pumping technique for metastable triplet helium (^{3}He) atoms utilizing the 2^3S_1-3^3P_J transition at 389 nm with radiation generated by a frequency-doubled cw Ti:Sapphire laser and compared the results with our results obtained utilizing the 2^3S_1-2^3P_J transition at 1083 nm with a diode laser. We optically measured the nuclear polarization of ^{3}He in the hollow cathode discharge cell by monitoring the absorption of a weak longitudinal probe laser at 1083 nm. This provided, for the first time, nuclear polarization utilizing the $^2S_1$-^3P_J transition at 389 nm.

Novel TiO_2/ZnO multilayer mirrors at "water-window" wavelengths fabricated by atomic layer epitaxy
HIROSHI KKUMAGAI, YUJI TANAKA, MASAKI MURATA, YUSUKE MASUDA and TSUTOMU SHINAGAWA
Journal of Physics: Condensed Matter (2010) in press.
We propose that novel oxide superlattice structures of crystalline TiO_2 /ZnO on sapphire substrates can be used for multilayer mirrors with high reflectivity at 2.734 nm. In the experimental study, both rutile TiO_2 (200) and wurtzite ZnO (001) thin films were grown epitaxially on the same sapphire (001) substrate by atomic layer epitaxy (ALE) at 450 °C. We also demonstrated that the novel oxide superlattice structure of 10-bilayer TiO_2 /ZnO on a
sapphire su
bstrate gave a high reflectivity of 29.4% at 2.74 nm.

Self-limiting nature in atomic-layer epitaxy of rutile thin films from $TiCl_4$ and H_2O on sapphire (001) substrates

HIROSHI KUMAGAI, YUSUKE MASUDA and TSUTOMU SHINAGAWA

Journal of Crystal Growth (2010) in press.

The atomic layer epitaxy of rutile thin films on sapphire (001) substrates was studied in the controlled growth of titanium oxide films by sequential surface chemical reactions using a novel vapor combination of tetrachlorotitanium ($TiCl_4$) and water (H_2O). Optical constants and thicknesses of these rutile films were investigated in terms of vapor pressure using a variable-angle spectroscopic ellipsometer. As a result, the self-limiting nature in the atomic-layer epitaxy of rutile thin films was demonstrated clearly under various conditions of dosing reactant vapors, where growth rates were almost constant at approximately 0.077 nm/cycle (0.77 nm/min) and refraction indices were also constant at 2.59.

Self-limiting nature in atomic layer epitaxy of wurtzite thin films from sequentially pressurized $Zn(CH_2CH_3)_2$ and H_2O vapor pulses on sapphire (001) substrates

HIROSHI KUMAGAI, YUSUKE MASUDA and TSUTOMU SHINAGAWA

Thin Solid Films (2010) in press.

We studied the atomic layer epitaxy of wurtzite thin films on sapphire (001) substrates was studied in the controlled growth of zinc oxide films by sequential surface chemical reactions using a novel vapor combination of diethylzinc ($Zn(CH_2CH_3)_2$) and water (H_2O). The optical constant and thickness of these wurtzite films were investigated in terms of the $Zn(CH_2CH_3)_2$ and H_2O vapor pressures using a variable-angle spectroscopic ellipsometer. As a result, the self-limiting nature of the atomic layer epitaxy of wurtzite thin films was demonstrated successfully under various conditions of the dosing reactant vapors
, whereby the growth rate was almost constant at approximately 0.26 nm/cycle (2.6 nm/min) and the index of refraction was also constant at 1.94.

Recent Progress on Fabrication Technology of Short-Wavelength Soft X-Ray Multilayers and Their Application to Microscopy

HIROSHI KUMAGAI and MIHIRO YANAGIHARA

Rev. Laser Engineering (2010) (in Japanese) in press.

A new approach to the fabrication of multilayer mirrors on an atomic scale at soft x-ray wavelengths is desired to overcome serious problems regarding scattering loss at the rough surface and interface of the multilayer. In this review, resent progress regarding novel approaches utilizing atomic layer deposition and atomic layer epitaxy to the fabrication of multilayer structures for soft x-ray wavelengths is detailed. These novel approaches are expected to solve the above-mentioned problems and then take the place of conventional sputtering methods because of their control performance of the surface on an atomic scale through their self-limiting functions. Moreover, recent progress on the soft x-ray microscope with normal-incidence multilayer reflectors is also detailed in this review.

Design of novel titanium oxide / zinc oxide multilayer mirror for attosecond soft x rays

KOMEI NAGAI and HIROSHI KUMAGAI

IOP Conference Series:Materials Science and Engineering (2010) in press.

A novel attosecond multilayer mirror was designed at “water-window” wavelengths with a combination of TiO_2 and ZnO, because both rutile TiO_2 and wurtzite ZnO can be grown epitaxially on a c-plane sapphire substrate despite the different crystal structures of the molecule hexagonal units of rutile TiO_2, wurtzite ZnO and sapphire. . The theoretical calculation of the TiO_2/ZnO multilayer mirror indicated that the high reflectivity over 50% was attainable at 2.73 nm and at an incident angle of 18.9° from the normal incidence. Moreover, it also indicated that the simple 3-block structure could control the reflectivity and the phase of a 480-attosecond pulse.

70% frequency-doubling efficiency of 0.8-W mode-locked picosecond Ti:sapphire laser with external cavity

TATSUYA OHIRA, SHINGO MAEDA, YUMA TAKIDA and HIROSHI KUMAGAI
Proceedings of Photonics West 2011: LASE2011, (CD-ROM) (2011) in press.
Recently, high-performance light sources in the UV and VUV region is getting more and more essential in application fields such as photochemistry, spectroscopy, lithography, and material science. Therefore, many researches regarding on the frequency doubling of near-infrared coherent lights have been done to obtain high-efficiency and high-power coherent UV lights. However, the pump light of the high average power is necessary for such high-efficiency wavelength conversions. We have researched high-efficient, convenient and simple generation of UV continuous and quasi-continuous waves by optimizing an external cavity and then using a BiB_3O_6 (BiBO) as a nonlinear crystal of relatively high nonlinear optical coefficient. We report here the generation of a high-efficient 389-nm coherent light based on the second harmonic generation of a mode-locked picosecond-pulsed Ti:sapphire laser with the BiBO as a nonlinear crystal. As a result, more than 500 mW of output at 389 nm was obtained with the maximum input of 800 mW and a maximum efficiency of 63%. Furthermore, considering the reflection loss at the output mirror of the 389-nm light, we could obtain 70% conversion efficiency. This value is one of the best results of the second harmonic generation of less than 1W of average pump power.

Parametric generation of terahertz wave pumped by picosecond Ti:sapphire laser with MgO-doped $LiNbO_3$ installed in external enhancement cavity
YUMA TAKIDA, SHINGO MAEDA, TATSUYA OHIRA, HIROSHI KUMAGAI and SHIGEKI NASHIMA
Proceedings of Photonics West 2011: LASE2011, (CD-ROM) (2011) in press.
Terahertz waves have been expected to be applied in comprehensive application spheres. As for the generation of terahertz wave, there is a way to utilize optical parametric process or optical rectification, which is the second-order nonlinear optical effect. Using the method of optical parametric process, a Q-switched Nd:YAG laser often have been utilized as a pumping source. In many cases using the method of optical rectification, femtosecond pulses from a Ti:sapphire laser have been utilized as a pumping source. However, a picosecond-pulsed light source which provides pulses with the pulse duration between nanosecond and femtosecond, to our knowledge, have never been reported as a pumping source for generation of terahertz wave. We can obtain much higher repetition-rate terahertz wave than that by a Q-switched Nd:YAG laser. In addition, the value of enhancement factor using picosecond pulses is able to become larger than that using femtosecond pulses. Thus, we focus on the generation of terahertz wave by optical parametric process in nonlinear optical crystal pumped by a 81.7-MHz picosecond Ti:sapphire laser. Therefore, we built an external enhancement cavity with MgO-doped $LiNbO_3$ (MgO:LN) and enhanced the pump light in the cavity. Considering that the idler light generated in MgO:LN with the different angle of 1 degree to the pumping light, we designed the cavity in order to circulating the idler light as well as the pumping light simultaneously. Circulating idler light in the cavity, the circulated idler light might contribute the terahertz parametric generation induced by the next pumping pulse. As a result, when idler light circulating the cavity, we demonstrated a clear enhancement of the idler intensity.

Low-threshold, quasi-cw terahertz parametric amplificaton in an external ring cavity with an $MgO:LiNbO_3$ crystal
SHINGO MAEDA, TATSUYA OHIRA, YUMA TAKIDA, HIROSHI KUMAGAI and SHIGEKI NASHIMA
Proceedings of Photonics West 2011: LASE2011, (CD-ROM), (2011) in press.
Terahertz waves have been attracted recently because of their wide ranging applications in various fields. Since the appearance of a high power near-infrared light source, coherent terahertz waves have been generated successfully using PC antennas, Q-switch Nd: YAG laser or femtosecond ultrashort pulsed laser. Actually, however, there is no tunable and high-repetition terahertz wave source with narrow linewidth. Thus, we have been focusing on a picosecond-pulsed laser, because it has narrower linewidth than that of a femtosecond-pulsed laser and moreover higher-reputation than that of a Q-switch Nd: YAG laser. In addition, the picosecond-pulsed peak power can be enhanced in a high-finesse compact external cavity to overcome the threshold of terahertz parametric generation and amplification, because the pulse is relatively small spatially, and the spectrum is relatively narrow. Therefore, we developed a terahertz parametric amplifier with an MgO-doped $LiNbO_3$(MgO: LN) nonlinear crystal in an external ring cavity with the enhancement of pump power. Moreover, the generated idler light

was recycled by 2 additional flat mirrors so as to provide a contribution to parametric amplification. As a result, we obtained terahertz wave radiation at high-repetition of 80MHz. We additionally examined seed injection, which seed was provided a continuous-wave diode laser along the generated idler.

Study on periodic twinning of quartz crystal under bending stress
TAKAYA SHIMONO, HIROYA MATSUKAWA, NOBUYUKI HIRANO, HIROSHI KUMAGAI, NAOKI FUKUDA, TOSHIO TAKIYA, NORIHIRO INOUE and KOICHIRO NAKAYAMA
Proceedings of Photonics West 2011: LASE2011, (CD-ROM) (2011) in press.
Periodic inversion of spontaneous polarization in a ferroelectric substance realized quasi phase matching (QPM) and then revolutionized nonlinear optics. In these years, quartz crystal has been attracted attention as a nonlinear optical material without spontaneous polarization. Moreover, making of an inverted structure by impressing perpendicular stress has been researched because a quartz crystal turns to be twinned under sufficient stress. Thus, we paid attention that twinning of quartz crystal was able to be rather achieved effectively by impressing bending stress, and then studied on making a periodic inverted structure of spontaneous polarization to generate deep ultraviolet lights by QPM quartz crystal. We fabricated experimentally the inverted structure locally by impressing the stress to choose the specific location and direction for the AT-cut quartz substrate that was heated just below the phase transition temperature. Then, we observed the twin boundaries by X-ray topograph. To control inverted area, we introduced local stress by processing the surface of quartz crystal with reactive ion etching. Moreover, the stress distribution was calculated when the bending stress was impressed to the quartz crystal with the rectangle structure, and then the condition for the polarization inversion was also calculated.

A study on fabrication of $BaMgF_4$ thin film toward frequency-conversion device in UV/VUV region
HIROYA MATSUKAWA, TAKAYA SHIMONO, NOBUYUKI HIRANO and HIROSHI KUMAGAI
Proceedings of Photonics West 2011: LASE2011, (CD-ROM), (2011) in press.
$BaMgF_4$ is a novel ferroelectric fluoride which is transparent in the wavelength region from 125 nm to 1300 nm. Recently, the trial production of the frequency conversion device with the $BaMgF_4$ single crystal was reported for the ultraviolet (UV) and vacuum ultraviolet (VUV) wavelength regions, but there has been few report on it. The $BaMgF_4$ is very attractive ferroelectric crystal because it can be used as a quasi phase matching (QPM) device such as $LiNbO_3$ or $LiTaO_3$. Nonlinear crystals have very large nonlinear coefficients generally, but these coefficients limited wavelengths to use due to the birefringent phase matching. The QPM technique can provide the phase matching in the whole transparent wavelength region, in contrast to the conventional birefringent phase matching, which limited to the wavelengths from 573 nm to 5634 nm. Thus the QPM technique is attractive to fabricate frequency-conversion device in UV/VUV region. In this study, we have purpose to fabricate $BaMgF_4$ hetero-epitaxial thin films toward frequency-conversion devices. The optical-grade $BaMgF_4$ single crystal has been fabricated by Bridgman method. Rather, we focus on fabrication of $BaMgF_4$ thin films by the precise and careful method of ion beam sputtering.

Atomic layer epitaxy of TiO_2/ZnO multilayer optics using ZnO buffer layer for "water-window" x-rays
MASAKI MURATA, YUJI TANAKA, YASUTAKA SANJO, HIROSHI KUMAGAI and TSUTOMU SHINAGAWA
Proceedings of Photonics West 2011: LASE2011, (CD-ROM) (2011) in press.
A novel TiO_2/ZnO multilayer deposited by atomic layer epitaxy (ALE) technique has been fabricated to achieve a high-reflectance mirror and an attosecond mirror in soft x-rays "water-window" (λ=2.332-4.368 nm) wavelengths region. The technique is able to meet the needs for atomic layer control and epitaxial growth using sequential surface reactions and self-limiting nature. In preliminary experimental studies, both rutile TiO_2 (200) and wurtzite ZnO (0001) thin films were grown epitaxially on the same sapphire (0001) substrates at 450°C and moreover a high reflectivity of 29.8% was demonstrated with the TiO_2/ZnO multilayer structure at around 2.73 nm and a grazing angle of 2θ=10°. The authors conducted the ALE experiment of TiO_2/ZnO multilayer using a ZnO buffer layer. In the result, the multilayer using a buffer layer was able to be grown epitaxially on not only sapphire (0001) but also Si (100). In addition, reflectivity of the multilayer remained to be 24.6% even on Si

(100) in contrast with that (about 27.5%) on sapphire (0001). Thus, the ZnO buffer layer has the key material to fabricate the TiO_2/ZnO multilayer on various substrates.

Atomic layer deposition of amorphous TiO_2/ZnO multilayers for soft x-ray coherent optics
YASUTAKA SANJO, YUJI TANAKA, MASAKI MURATA, HIROSHI KUMAGAI and TSUTOMU SHINAGAWA
Proceedings of Photonics West 2011: LASE2011, (CD-ROM) (2011) in press.
The development of high-reflection mirrors with amorphous metal-oxide multilayers in the "water-window" (λ=2.332-4.368nm) wavelengths is desirable for various water-window applications, because the combination of two different metal-oxides may make big difference in refractive index between two different layers at the wavelengths and moreover decrease roughness on the surface and interface. One of the authors have already studied and fabricated amorphous Al_2O_3/TiO_2 multilayers for the "water-window" wavelengths by controlled growth with atomic layer deposition (ALD), and then acquired reflectance of 33.4 % at 2.73nm and at the incidence angle of 18.2° from the normal incidence. In order to fabricate amorphous multilayers with higher reflectance, we propose amorphous TiO_2/ZnO multilayers , because utilizing combination of TiO_2/ZnO is able to make refractive index difference for TiO_2 larger than that of Al_2O_3/TiO_2 at "water-window" wavelengths. In this study, amorphous TiO_2/ZnO multilayers are fabricated by ALD and then reflectance characteristics are investigated using monochromatized synchrotron radiation (SR) located Ultraviolet Synchrotron Radiation Facility (UVSOR), Institute for Molecular Science, Okazaki, Japan.

Efficient sum-frequency generation of continuous-wave tunable ultraviolet coherent light in BiBO-installed external cavity with dual wavelength enhancement
HIROSHI MORIOKA, KENTA MUKOYAMA, HIROSHI KUMAGAI, NORIHORO INOUE, NAOKI FUKUDA and TOSHIYA TAKIYA
Proceedings of Photonics West 2011: LASE2011, (CD-ROM) (2011) in press.
Recently, a continuous-wave (CW), high-power, tunable, ultraviolet (UV) light source is required strongly in material engineering, photochemistry, spectroscopy, micro fabrication and so on. There has been no UV light source to emit directly CW, high-power, tunable, UV lights. Therefore, we developed a CW, high-power, tunable, UV light source through efficient sum-frequency generation (SFG). As you know, most of CW laser doesn't have high peak-power enough to cause nonlinear optical phenomenon, so we built up two-stage frequency-conversion system with two external cavities for enhancement of the low peak-power. In the first stage, we used 10W of 1064nm fiber laser and MgO:PPLT crystal for the second harmonic (SH) generation. And we used a bow-tie external cavity incorporating four mirrors, and then controlled the cavity length by using Hänsch-Cöuillaud method. The MgO:PPLT crystal provided no walk-off effect, and so that the generated SH light presented good beam quality. And it has a large nonlinear coefficient. In the second stage, two lights which were the SH light from the first stage and the other light from the single-frequency CW Ti:Sapphire laser, should resonate simultaneously for efficient sum-frequency generation. In the second stage, we controlled cavity length at first. After controlling cavity length, we controlled laser frequency by using Hänsch-Cöuillaud method. In this study, we selected BiBO as a nonlinear crystal in the second stage, because its nonlinear coefficient is larger than BBO and moreover it is hard to deliquescent.

High intensity laser-driven particle and electromagnetic wave sources
Akito SAGISAKA, Hiroyuki DAIDO, Alexander S. PIROZHKOV, Michiaki MORI, Akifumi YOGO, Koichi OGURA, Satoshi ORIMO, Mamiko NISHIUCHI, Jinglong MA, Hiromitsu KIRIYAMA, Shuhei KANAZAWA, Shuji KONDO, Yoshiki NAKAI, Takuya SHIMOMURA, Manabu TANOUE, Atsushi AKUTSU, Hajime OKADA, Tomohiro MOTOMURA, Tetsuya KAWACHI, Sergei V. BULANOV, Timur Zh. ESIRKEPOV, Shigeki NASHIMA, Makoto HOSODA, Hideo NAGATOMO, Yuji OISHI, Koshichi NEMOTO, Il Woo CHOI, Seong Ku LEE, and Jongmin LEE
Second International Symposium on Laser-Driven Relativistic Plasmas Applied to Science, Industry and Medi-

cine, Jan. 2009, Kyoto, Japan.
We have proposed that high-intensity laser and thin-foil interactions produce intense highenergy particles, hard x-ray, high-order harmonics, and terahertz (THz) radiation. A proton beam driven by a high-intensity laser has received attention as a compact ion source for medical applications. In this paper, we describe the high intensity laser-driven particle beam mainly the multi-MeV proton beam simultaneously with x-ray and/or THz radiation and their possible applications.
We have performed the high intensity laser-matter interaction experiments using a thin-foil target irradiated by Ti:sapphire lasers of JAEA with a peak irradiance of ~10^{20} W/cm^2. A tape target driver provides a fresh surface of a thin-foil. We have developed several on-line real time monitors such as a time-of-flight proton spectrometer which is placed behind the target and along the target normal as well as interferometer for electron density profile measurement of preformed plasma, x-ray pinhole camera, THz detector, UV spectrometer for harmonics measurement. We have tested simultaneous generation of protons and intense THz radiation from a thin tape target as a feasibility study of pump-probe experiment with intense multiple beams.

Proton generation and terahertz radiation from a thin-foil target with a high-intensity laser
Akito SAGISAKA, Alexander S. PIROZHKOV, Michiaki MORI, Akifumi YOGO, Koichi OGURA, Satoshi ORIMO, Mamiko NISHIUCHI, Jinglong MA, Hiromitsu KIRIYAMA, Shuhei KANAZAWA, Shuji KONDO, Yoshiki NAKAI, Takuya SHIMOMURA, Manabu TANOUE, Atsushi AKUTSU, Hajime OKADA, Tomohiro MOTOMURA, Hiroyuki DAIDO, Kiminori KONDO, Sergei V. BULANOV, Timur Zh. ESIRKEPOV, Shigeki NASHIMA, Makoto HOSODA, Hideo NAGATOMO, Yuji OISHI, Koshichi NEMOTO, Il Woo CHOI, Seong Ku LEE, and Jongmin LEE
The Review of Laser engineering, The Laser Society of Japan, (in press)
We simultaneously observed both proton signals and terahertz (THz) radiation in laser-plasma interaction using a thin-foil target. Next, to get higher energy protons, the size of the preformed plasma is reduced by changing the laser contrast level. In the high-contrast laser pulse case, the maximum energy of the protons generated at the rear side of the target along the target normal direction increases to ~3.4 MeV.

Radially-polarized terahertz radiation from relativistic laser plasma of metal foil target
S. NASHIMA, M. HOSODA, S. ORIMO, K. OGURA, M. MORI, A. SAGISAKA, and H. DAIDO
35rd International Conference on Infrared, Millimeter, and Terahertz Waves, Sep. 2010, Roma, Italy.
We investigated the radiation distribution and polarization characteristics of terahertz (THz) waves from the relativistic laser plasma of a Ti foil target that was vertical to the incident plane. We found that the polarization of THz waves that radiated vertically was not linear and the polarizing axis was rotated, while the terahertz waves that radiated horizontally did so with complete p-polarization.

Ubiquity of chaotic magnetic-field lines generated by three-dimensionally crossed wires in modern electric circuits
M. HOSODA, T. MIYAGUCHI, K. IMAGAWA, and K. NAKAMURA
Phys. Rev. E, 80, #067202-1-4 (2009)
We investigate simple three-dimensionally crossed wires carrying electric currents which generate chaotic magnetic field lines (CMFLs). As such wire systems, cross-ring and perturbed parallel-ring wires are studied, since topologically-equivalent configurations to these systems can often be found in contemporary electric and integrated circuits. For realistic fundamental wire configurations, the conditions for wire dimensions (size) and current values to generate CMFLs are numerically explored under the presence of the weak but inevitable geomagnetic field. As a result, it is concluded that CMFLs can exist everywhere, i.e., they are ubiquitous in the modern technological world.

Coulomb-interaction-induced quantum irregularity in two electrons within a hard-walled circular billiard,
Shin-ichi SAWADA, Akira TERAI and Katsuhiro NAKAMURA

Chaos, solitons and fractals 40, pp. 862-873 (2009)
We investigate quantum mechanics of Coulomb-interacting two electrons within a hard-walled circular billiard. Despite the integrability of a system of non-interacting electrons confined within the highly symmetric billiard, the Coulomb interaction can make the system non-integrable and chaotic. The energy spectra show the interaction-induced level statistics which is in an overall agreement with the Wigner (GOE) level spacing distribution and spectral rigidity.
The Brody parameter as a function of the effective Coulomb interaction is evaluated, which quantifies a continuous transition from the Poisson to Wigner level spacing distributions. The case of the zero total angular momentum needs an extra classification of eigenfunctions to remove the degeneracy, which is required by the time-reversal symmetry of the system. The interaction-induced breaking of the spatial symmetry which leads to quantum irregularity can be visualized by using the two-particle correlation function and the single-particle density for eigenstates.

Phonon softening in triangular lattice,
Kenta MIYOSHI and Akira TERAI
Physica, B 405, pp. S188-S191 (2010)
We have numerically studied the phonon softening in a triangular lattice system with Su-Schrieffer-Heeger's (SSH) type interaction and with a three-quarter-filled electronic band. When the temperature is lowered, the simultaneous oftening of multiple phonon modes is observed at a critical temperature. These softened modes have momenta parallel to the vectors connecting neighboring vertices of the hexagonal structure of the Fermi surface, being irrelevant to nesting vectors. Therefore, this phenomenon that occurs when the temperature is lowered is not a conventional Peierls transition. It is found that the Fermi surface composed of straight lines is a necessary condition for the simultaneous phonon softening. Multi-mode states are realized below the critical temperature. However, all of the softened modes are not necessarily condensed at the lowest free-energy state.

Role of infinite invariant measure in deterministic subdiffusion
Takuma AKIMOTO and Tomoshige MIYAGUCHI,
Physical Review, E 82, 030102(R) (4 pages) (2010)
Statistical properties of the transport coefficient for deterministic sub-diffusion are investigated from the viewpoint of infinite ergodic theory. We find that the averaged diffusion coefficient is characterized by the infinite invariant measure of the reduced map. We also show that when the time difference is much smaller than the total observation time, the time-averaged mean square displacement depends linearly on the time difference. Furthermore, the diffusion coefficient becomes a random variable and its limit distribution is characterized by the universal law called the Mittag-Leffler distribution. DOI: 10.1103/PhysRevE.82.030102

Ubiquity of chaotic magnetic-field lines generated by three-dimensionally crossed wires in modern electric circuits,
M. HOSODA, T. MIYAGUCHI, K. IMAGAWA, and K. NAKAMURA
Physical Review, E 80, 067202 (2009)
We investigate simple three-dimensionally crossed wires carrying electric currents which generate chaotic magnetic field lines (CMFLs). As such wire systems, cross-ring and perturbed parallel-ring wires are studied, since topologically equivalent configurations to these systems can often be found in contemporary electric and integrated circuits. For realistic fundamental wire configurations, the conditions for wire dimensions (size) and current values to generate CMFLs are numerically explored under the presence of the weak but inevitable geo-magnetic field. As a result, it is concluded that CMFLs can exist everywhere; i.e., they are ubiquitous in the modern technological world.
DOI: 10.1103/PhysRevE.80.067202

Information and Communication Engineering

Measurement of 3d Distance Between Artificial Cup and Head from AP & Lateral Roentgens with Unknown Angle After THR

Shigeyoshi NAKAJIMA, Mitsuhiko IKEBUCHI and Takashi TORIU

Intr. J. of Innovating Computing, Information and Congrol, Vol.5, No.3, pp.743-750(2009)

The purpose of our work is precise measurement of 3D distance between a cup as an artificial acetabular and a head as an artificial femoral head in a patient body from AP and lateral Roentgen images without known angle between AP (anterior posterior) and lateral after THR(Total hip replacement). Recently Martell measured the 2D distance between a cup and a head of an artificial hip joint. And also RSA (roentgen stereophotogrammetric analysis) is famous as a 3D measurement method of things in a living body of a subject. But Martell's method needs a special Roentgen equipment and RSA needs extra surgical invasions. Our method needs only an ordinary Roentgen equipment and doesn't need to know the angle between AP and lateral. Also the invasion of our method is low. But our method is applied only to the cases of cups which rotations are identified with something like notches. We show the result of a computer simulation with CG images we made and also show the result of an experiment in vitro with real roentgen images of artificial cup and head moved by a micro-manipulator.

Measurement of Absolute Size of Moving Object Using An Omnidirectional Sensor Camera and Laser Range Sensor

Yuuki FUKUI, Shigeyoshi NAKAJIMA, and Takashi TORIU

Innovating Computing, Information and Control Express Letters, Vol.4, No.6(B), pp.2451-2456(2010)

We propose a new method to measure an absolute size of an object in sight using an omnidirectional sensor camera and a laser range sensor. With a camera (omnidirectional or else), an angle of a view of an object or its planer dimension tells us its relative size, but not its absolute size. And a range sensor tells us the distance from the sensors, to an object, also but not its absolute size. The combination of an omnidirectional sensor camera and laser range sensor tells us an absolute size of object and it is good at surveillance for security.

Applied Chemistry and Bioengineering

Applied Chemistry

Effect of Deviation from Ni/Mn Stoichiometry in $Li[Ni_{1/2}Mn_{3/2}]O_4$ upon Rechargeable Capacity at 4.7 V in Nonaqueous Lithium Cells
Yusuke MAEDA, Kingo ARIYOSHI, Toru KAWAI, Tomohito SEKIYA, and Tsutomu OHZUKU,
J. Ceram. Soc. Jpn., 117, pp. 1216-1220 (2009)
Lithium nickel manganese oxides having 20% nickel excess and deficient with respect to the stoichiometric $Li[Ni_{1/2}Mn_{3/2}]O_4$ having a space group symmetry of $P4_332$ were prepared and examined in nonaqueous lithium cells. Rechargeable capacity observed for the 20% nickel excess sample in voltage above 4.5 V is larger than that for the 20% nickel deficient sample. The effect of deviation from Ni/Mn stoichiometry from the ideal composition of $Li[Ni_{1/2}Mn_{3/2}]O_4$ upon the rechargeable capacity at 4.7 V is described in terms of the solid solution, phase separation, and superstructural $Li[Ni_{1/2}Mn_{3/2}]O_4$. From the results, the composition preferable to the five-volt lithium insertion material of $Li[Ni_{1/2}Mn_{3/2}]O_4$ is discussed. The cycling stability of $Li[Ni_{1/2}Mn_{3/2}]O_4$ in the cell with the $Li[Li_{1/3}Ti_{5/3}]O_4$-negative electrode is also examined in voltages ranging from 1.5 to 3.6 V at 25 ^oC for 250 cycles and shown that the capacity fading of the cell is negligibly small below 4% even after 250 cycles.

An Approach to 12-V Lead-free Batteries: High Temperature 3600-cycle Examinations on a 2.5-V LTO/LAMO Battery
Tsutomu OHZUKU, Mitsuyasu IMAZAKI , Naoya TSUKAMOTO, and Kingo ARIYOSHI,
Chem. Lett., 38, p.1202 (2009)
A 2.5-V battery consisting of lithium titanium oxide (LTO) and lithium aluminum manganese oxide (LAMO) having spinel-framework structures was examined from 1 to 3 V at 55^oC. After several trials on capacity retention at high temperatures, we have succeeded to show that the rechargeable capacity is retained at greater than 80% even after 3600 cycles at 55^oC by applying cellulose nonwoven cloth as a separator, satisfying requirement for 12-V automobile applications.

Lithium Insertion Materials Having Spinel-Framework Structure for Advanced Batteries
Kingo ARIYOSHI, Yoshinali MAKIMURA and Tsutomu OHZUKU
Lithium Ion Rechargeable Batteries, pp. 11-38 (2009)

Secondary Batteries – Lithium Rechargeable Systems – Lithium-ion – Negative Electrode: Spinel-Type Titanium Oxides
Tsutomu OHZUKU and Kingo ARIYOSHI
Encyclopedia of Electrochemical Power Sources, Vol 5, pp. 209-213 (2009)

Secondary Batteries – Lithium Rechargeable Systems – Lithium-ion – Positive Electrode: Layered Mixed Metal Oxides
Tsutomu OHZUKU and Yoshinari MAKIMURA
Encyclopedia of Electrochemical Power Sources, Vol 5, pp. 249-257 (2009)

TiO_2-Negative Electrodes
Kingo ARIYOSHI
Handbook of Batteries, pp. 406-409 (2010) (in Japanese)

$Li_4Ti_5O_{12}$-Negative Electrodes
Kingo ARIYOSHI
Handbook of Batteries, pp. 410-615 (2010) (in Japanese)

High-Voltage Positive Electrodes
Kingo ARIYOSHI
Handbook of Batteries, pp. 472-479 (2010) (in Japanese)

Twelve-volt Lead-free Batteries Consisting of Insertion Materials

Kingo ARIYOSHI and Tsutomu OHZUKU
Function & Materials (Kinou Zairyo), 30(3), pp. 51-57 (2010) (in Japanese)

Synthesis and Properties of Sulfonated Aromatic Fluoro-Polymers
Kiyoshi ENDO, Takashi YAMADE
J. Appl. Polym. Sci., 118, pp. 1582–1588 (2010)
Polycondensation of perfluorobiphenyl with α,α-bis(4-hydroxyphenyl)ethylbenzene and/or 9,9-bis (4-hydroxyphenyl)fluorene was investigated. The polycondensation of perfluorobiphenyl with α,α-bis (4-hydroxyphenyl)ethylbenzene and/or 9,9-bis(4-hydroxyphenyl)fluorene proceeded at low-temperature to a give high-molecular weight and thermal stable polymers. The ^{19}F-NMR spectra of the polymers indicate that the polymers consists of predominantly 1,4-phenylene structure with respect to the perfluoro-aromatic compound. The sulfonation of the polymers obtained from the polycondensation occurred at the phenyl groups and fluorenyl side chain. A tough and smooth film was prepared by a casting method from DMF solution of the sulfonated polymer. The films showed hydrolytic and oxidative stabilities, and a high-proton conductivity.

Synthesis and Characterization of Catenane-Structure Polymers
Kiyoshi ENDO
Functional & Materials 30(No5), pp. 50-59 (2010) (Japanese)
The study paid attention to the special structure of the polymer synthesis and function in recent years. Research has been evolving its structure and functions derived from synthetic polymer having a molecular structure of one of the special structure of catenane. This article describes the development and current status of catenane molecule synthesis, polymer synthesis and function are described using a cyclic disulfide catenane structure

Simultaneous Control of Molecular Weight and 1,4-cis-Selectivity in the Polymerization of 1,3-butadiene with *N,N'*-Bis(3,5-di-*tert*-butylsalicylidene)-1,2-diphenylethylene-diaminato cobalt in combination with diethylaluminum chloride
Kiyoshi ENDO, Kenji NAKATANI
Lecture No. 146, Full Paper, 176th ACS Rubber Division Technical Meeting, Pittsburgh, KY, U.S.A., October 15, 2009
We investigated the simultaneous control of molecular weight and 1,4-*cis*-selectivity the polymerization of 1,3-butadiene (Bd) with *N,N'*-Bis(3,5-di-*tert*-butylsalicylidene)-1,2-diphenylethylene-diaminato cobalt (**1**) in combination with alkylaluminiums. Among the alkylaliminums examined as a cocatalyst, Et_2AlCl showed a high activity for the polymerization of Bd with **1**/Et_2AlCl catalyst to give high molecular weight polymers in high yields. The activity for the polymerization was high even when the polymerization of Bd was carried out at the lower Al/Ti mole ratio, which is contrast to that a large amount of MAO was required to show high activity for the polymerization of Bd. The **1**/Et_2AlCl catalyst was found to promote 1,4-*cis* specific polymerization (1,4-*cis* content > 98 %) with a living nature in the polymerization of Bd in CH_2Cl_2 at -30 °C. Copolymerization of Bd and isoprene (Ip) with the **1**/Et_2AlCl catalyst was also investigated. It was found that the complex **1** in combination with Et_2AlCl was an effective catalyst for the copolymerization of Bd and Ip. The monomer reactivity ratios were determined to be r_{Bd} = 0.70 and r_{Ip} = 0.87 ($r_{Bd} \times r_{Ip}$ = 0.61). The **1**/Et_2AlCl catalyst gave high molecular weight random copolymers ($M_n > 10 \times 10^5$) in good yields.

Ring-Opening Polymerization of Cyclic Disulfides
Kiyoshi ENDO
New and Revised Edition Handbook of Radical Polymerization, Part 3, Chapter 10*,* NTS, Tokyo, pp. 522-529 (2010) (in Japanese)

Poly(vinyl chloride) and Copolymers with Vinyl Chloride
Yoshikatsu TSUCHIYA, Kiyoshi ENDO
New and Revised Edition Handbook of Radical Polymerization, Part 4, Chapter 1, Section 2, NTS, Tokyo, pp. 621-628 (2010) (in Japanese)

Rubber and tribology technology to contribute to promoting environmental conservation
Kiyoshi ENDO

Monthly The Tribology, 55(1), p.50 (2010) (in Japanese)

Polymerization of Vinyl Monomers with Radical Initiator Immobilized on the Inside Wall of Mesoporous Silica
Kiyoshi ENDO, Kenji IKEDA, Mariko KIDA
The 11th Pacific Polymer Conference, Cairns, Australia, Session: New Developments in Polymer Synthesis, December 8, 2009

Synthesis and Application of Labile Cyclic Polymer
Masutaro Hirayama, Kiyoshi ENDO
The 11th Pacific Polymer Conference, Cairns, Australia, Poster Session, December 7, 2009

Control of Molecular Weight in Polymerization of Vinyl Chloride with Half-titanocene/ MAO Catalyst
Yoshikatsu Tsuchiya, Kiyoshi ENDO
The 11th Pacific Polymer Conference, Cairns, Australia, Poster Session, December 8, 2009

Polymerization Catalysts and Polymerization Kinetics
Kiyoshi ENDO
Seminar on Group for the State of Art in Polymerization Process, The Kinki Chemical Society, Japan, Tokyo, October 28, 2008, Preprints pp. 1-12

Introduction of Polymer Science-
Kiyoshi ENDO
Short Course of Polymer Science, The Kinki Chemical Society, Japan, Osaka, March 15, 2010, Preprints pp. 1–14

Special Structured Polymers and Function of the Polymers
Kiyoshi ENDO
Plenary Lecture at The Annual Meeting of The adhesion Society of Japan, Osaka, June 25, 2010

Nondestructive Elemental Depth Profiling of Japanese Lacquerware Tamamushi-Nuri by Confocal 3D-XRF Analysis in Comparison with Micro GE-XRF
Kazuhiko NAKANO and Kouichi TSUJI
X-Ray Spectrom., 38, pp. 446-450 (2009)
We have applied recently two XRF (micro x-ray fluorescence) methods [micro-Grazing Exit XRF (GE-XRF) and confocal 3D-XRF] to Japanese lacquerware 'Tamamushi-nuri.' A laboratory grazing-exit XRF (GE-XRF) instrument was developed in combination with a micro-XRF setup. A micro x-ray beam was produced by a single capillary and a pinhole aperture. Elemental x-ray images (2D images) obtained at different analyzing depths by micro GE-XRF have been reported. However, it was difficult to directly obtain depth-selective x-ray spectra and 2D images. A 3D XRF instrument using two independent polycapillary x-ray lenses and two x-ray sources (Cr and Mo targets) was also applied to the same sample. 2D XRF images of a Japanese lacquerware showed specific distributions of elements at the different depths, indicating that 'Tamamushi-nuri' lacquerware has a layered structure. The merits and disadvantages of both the micro GE-XRF and confocal micro XRF methods are discussed.

Effects of an X-ray Absorber in Grazing Exit Micro X-ray Fluorescence Analysis of Arsenic Attached to an Aqueous Leaf of Cammelia Hiemalis
Tohru AWANE, Kazuo NAKAMACHI and Kouichi TSUJI,
e-Journal of Surface Science and Nanotechnology, 7, pp. 841-846 (2009)
Grazing exit micro X-ray fluorescence analysis (GE-μ-XRF) using an X-ray absorber method was applied to an analysis of Pb attached to an aqueous leaf of *Cammelia hiemalis*. As a result of the analysis, we found that X-rays emitted from the surface region of the leaf could be detected selectively and then X-rays of Pb could be detected with low background using this analytical method. In this research, an effect of the X-ray absorber was indicated by comparing between X-ray spectra gained with and without use of that. However, since Pb was not attached to a leaf analyzed for this comparison, peak/background ratios of the X-rays of Pb using the X-ray absorber were not compared with those without use of the X-ray absorber. Moreover, X-ray

exit angles did not correspond with each other between with and without use of that. We, therefore, applied the GE-μ-XRF to an analysis of As attached to a leaf of *Cammelia hiemalis*, and then investigated the effect of the X-ray absorber at identical X-ray exit angles with and without use of that. As a result of that, we found peak/background ratios of X-ray peaks of As with use of the X-ray absorber drastically increased at grazing exit angles as compared to those without use of that.

A Micro X-ray Fluorescence Analysis Method Using Polycapillary X-ray Optics and Grazing Exit Geometry

Jun YANG, Kouichi TSUJI, Xiaoyan LIN, Dongyan HAN and Xunliang DING

Thin Solid Films, 517, pp. 3357-3361 (2009)

Grazing exit X-ray fluorescence (GE-XRF), which has unique advantages in surface and film analysis, is a development of XRF related to total reflection XRF. The combination of polycapillary X-ray optics with total reflection geometry in the detection path allows micro analysis in thin layer characterization. This technique was applied to analyze a series of titanium and iron layers which were deposited on GaAs single crystal by metal vapor vacuum arc ion sources. Thickness and density of the layers result from fitting the experimental data to model calculations, and the information of layer uniformity can be acquired by two-dimensional scan analysis. The GE-XRF method has application for complete layer characterization and process control during the layer deposition.

***Grazing* Exit Micro X-ray Fluorescence Analysis of Hazardous Metal Attached to a Plant Leaf Surface Using an X-ray Absorber Method**

Tohru AWANE, Shintaro FUKUOKA, Kazuo NAKAMACHI and Kouichi TSUJI

Anal. Chem., 81, pp. 3356-3364 (2009)

If human beings or animals repeatedly ingest plant leaves contaminated with minute quantities of hazardous metals (Pb, As, Hg, Cd, etc.), the metals will gradually accumulate in their bodies. When the quantities of the metals in the bodies reach toxic levels, they may cause serious symptoms of poisoning. Therefore, it is significant to detect and analyze the minute quantities of hazardous metals that attach to plant leaves in terms of epidemiology and disease prevention. We developed grazing exit micro X-ray fluorescence analysis (GE-micro-XRF), which was expected to analyze the localized surface of an aqueous plant leaf with a much faster and simpler sample treatment than with conventional analytical methods, to detect Pb attached to a surface of a leaf of Camellia hiemalis. A micro X-ray beam was produced by using a polycapillary X-ray lens. GE-v-XRF is a grazing exit X-ray analysis (GE-XA) method in which X-rays emitted from only the near-surface region of a specimen are selectively detected under a grazing exit angle condition (extremely low exit angle near 0 degrees). In any GE-XA method, X-rays emitted from inside the specimen must be absorbed inside the specimen and attenuated when X-rays pass through the specimen. However, we deduced that X-rays emitted from inside aqueous organic material such as a plant leaf are scarcely absorbed because X-ray absorption in any aqueous organic material is much smaller than that in most metallic and semiconductor materials, which was analyzed with GE-XA methods. Therefore, we have developed a novel GE-micro-XRF method in which a chip of a silicon wafer is placed between the analyzed leaf and an X-ray detector as an absorber of the X-rays emitted from inside the leaf. As a result of GE-XRF analysis of a leaf dipped in Pb standard solution using the X-ray absorber, we have for the first time selectively detected X-rays emitted from the near-surface region of an aqueous plant leaf. Therefore, we have detected X-rays emitted from Pb with much higher peak/background ratios (P/B ratios) as compared to those of conventional XRF analysis. In the analysis, we also found a difference in element distributions between the leaf surface and its interior. Therefore, we observed and analyzed a cross section of the leaf with a SEM-EDX to confirm the validity of this result. The result of the analysis of the cross section has been in excellent agreement with that of the XRF analysis.

Fundamental Characteristics of Polycapillary X-ray Optics Combined with Glass Conical Pinhole for Micro X-ray Fluorescence Spectrometry

Akinori MATSUDA, Kazuhiko NAKANO, Shintaro KOMATANI, Sumito OHZAWA, Hiroshi UCHIHARA and Kouichi TSUJI

X-Ray Spectrom., 38, pp. 258-262 (2009)

We have developed a new micro x-ray fluorescence spectrometry (μ-XRF) instrument using polycapillary

x-ray lens (PCXL) combined with glass conical pinhole (GCP). The x-rays focused by the PCXL were focused again by the GCP. The size of the obtained x-ray microbeam was estimated by a wire scanning method. In our instrument, the size of the x-ray microbeam end was 25 μm for Cr K at 0.5 mm from the GCP. The divergence angle of x-ray microbeam was 15 mrad. In order to evaluate the performance of our instrument, the gain (x-ray flux density) was estimated. The gain in our instrument was corrected by comparison of the intensity per unit area for a Cu pinhole aperture. The gain thus obtained was approximately 1400. This highly intense micro x-ray beam will be useful for micro-XRF analysis.

Preconcentration of Environmental Waters by Agar for XRF Analysis
Kazuhiko NAKANO, Kenta OKUBO and Kouichi TSUJI
Powder Diffraction, 24, pp. 135-139 (2009)
We have developed a convenient and effective XRF analysis procedure for trace amount of K, Ca, V, Mn, Fe, Ni, Cu, Zn, Cd, and Pb in environmental waters by using a preconcentration using the natural polymer (agar). The thin agar film was prepared by drying a homogeneous agar gel after mixing the aqueous sample solution with the agar powder. XRF analysis of the preconcentrated thin agar films containing trace metals showed a good repeatability because agar films were homogeneous enough. SB (signal to noise) ratios of the XRF intensity of the analytes were improved drastically. The linear calibration curves of K, Ca, V, Mn, Fe, Ni, Cu, Zn, Cd, and Pb showed a good linearity within the calibration ranges. The lower limits of detection (LLD) were 1.4 μg/mL for K, 0.26 μg/mL for Ca, 0.088 μg/mL for V, 0.029 μg/mL for Mn, 0.11 μg/mL for Fe, 0.016 μg/mL for Ni, 0.030 μg/mL for Cu, 0.017 μg/mL for Zn, 0.20 μg/mL for Cd, and 0.066 μg/mL for Pb, respectively. The proposed preconcentration method was applied to several environmental water samples.

Total Reflection X-ray Analysis of Metals in Blood Samples
Takuya NAKAMURA, Hiroshi MATSUI, Masaya KAWAMATA, Kazuhiko NAKANO,
Takako KATAYAMA, Masayuki HINO, Hideki WANIBUCHI, Kazushi ARANAMI, Takashi YAMADA and Kouichi TSUJI
Advances in X-Ray Chemical Analysis, Japan, 40, pp. 249-257 (2009) (in Japanese)
The sample preparation for TXRF (total reflection X-ray fluorescence) quantitative analysis of trace elements in human blood samples was investigated. In the TXRF analysis, a solution sample is dropped and dried on a flat substrate, and then the dried residue is measured. In this case, the dried residue should be flat not to disturb X-ray total reflection on the substrate. In addition, it is required to simply measure the whole blood sample by TXRF method, although a serum is analyzed in many cases. Thus, we studied the optimum conditions of the sample preparation of the whole blood by adding the pure water to apply Hemolysis phenomenon, where blood cells are destroyed due to different of the osmotic pressure, leading to flat residue. It was found that the best S/B ratio was obtained when the whole blood was diluted 8 times with pure water. Moreover, it was investigated the influence of the surface chemical condition of the glass substrate on the shape of the dried reside of the blood sample. When the surface of the glass substrate was hydrophilic, the shape of the dried residues was not uniform, as a result, the quantitative data of TXRF analysis gave a large deviation.
On the other hand, when the surface of the glass was hydrophobic, the shape of the residue was almost uniform, as a result, a good reproducibility was obtained. Another problem was an outer ring of the dried residue of the blood. This uneven ring absorbs the primary X-rays, caused to low determined quantitative data. Thus, we tried the heating way of the dropped blood sample at a high temperature of 200 degrees. In this case, the blood sample was dried immediately, and a flat homogeneous dried residue was obtained without the outer ring. Using the optimized conditions for sample preparation, human blood sample was quantitatively measured by TXRF and ICP-AES. A good agreement was obtained in TXRF and ICP-AES determinations; however, the measurement of Cl and Br will be an advantage of TXRF, because they were difficult to be measured by ICP-AES.
Finally, the blood (whole blood and serum) of the rat given with the medicine including As was measured by TXRF. As was dominantly observed in the TXRF spectrum for the whole blood sample; however, As was very small intensity in the TXRF spectrum for the serum. This indicates that As element distributes with blood cells. Therefore, it is important to measure the whole blood sample to evaluate the total value of As, and the TXRF will be useful method by applying the sample preparation studied in this paper.

Monitoring of Trace Metal Elements in Elution from Surface of Plastic Toys
Masaya KAWAMATA, Kazuhiko NAKANO and Kouichi TSUJI

Perspective and Topics of 70th Discussion Meeting on Analytical Chemistry, 8 (2009) (in Japanese).

Tuning of the Spectroscopic Properties of Composite Nanoparticles by the Insertion of Spacer Layer: Effect of Exciton-Plasmon Coupling
Akihito YOSHIDA, Yoshiro YONEZAWA, and Noritsugu KOMETANI
Langmuir, 25, pp. 6683–6689 (2009)
Composite nanoparticles (NPs) having a double-shell structure; Au core, spacer layer (inner shell) and J-aggregate (JA) layer (outer shell), (Au/spacer/JA), have been synthesized. The spacer layer composed of *N*,*N*,*N*-trimethyl(11-mercaptoundecyl)ammonium chloride played an important role to promote the J-aggregation of anionic cyanine dyes on the surface, as evidenced by the successful formation of the JA layers with four kinds of anionic cyanine dyes. It was found that the presence of spacer layer causes the significant change in the line shape of the absorption spectrum particularly near the J-band; the appearance of a *peak*-type absorption for the composite NPs with the double-shell structure while a *dip*-type absorption for the ones without the spacer layer. The change from the *peak*-type absorption to the *dip*-type absorption in the Au/spacer/JA NPs occurs when the size of Au core is varied from 5 to 15 nm. These observations would indicate that the strength of exciton-plasmon coupling between the Au core and the JA layer is enhanced with the increase in the core size or the decrease in the separation between the Au core and the JA shell. The photoluminescence arising from the JA can be detected for the composite NPs with the double-shell structure, showing that the quenching by the Au core is effectively suppressed by the spacer layer.

Synthesis and Spectroscopic Studies of Composite Gold Nanorods with a Double-Shell Structure Composed of Spacer and Cyanine Dye J-Aggregate Layers
Akihito YOSHIDA, Naoko UCHIDA, and Noritsugu KOMETANI
Langmuir, 25, pp. 11802-11807 (2009)
The composite gold nanorods (Au NRs) having a double-shell structure composed of Au NR (core), spacer layer (inner shell) and J-aggregate (JA) layer (outer shell), have been synthesized to examine the spectroscopic properties of the hybrid system in which the localized surface plasmon is coupled with the molecular exciton of JA. The spacer layer consisting of *N*, *N*, *N*-trimethyl(11-mercaptoundecyl)ammonium chloride plays a significant role in the formation of JA shell for several kinds of cyanine dyes. The absorption spectra of composite NRs are characterized by a distinct dip near the J-band when the plasmon energy of Au core is close to the exciton energy of JA shell, whereas a normal J-band peak appears when two energies are widely different from each other. The gradual change from the dip type to peak type absorption was observed when the plasmon energy was modulated by varying the aspect ratio of Au NR. Furthermore, composite NRs with thicker spacer layers have been fabricated by inserting the multilayer shell of polyelectrolytes between TMA and JA layers. They exhibited an alteration of the spectral line shape from the dip type to peak type with increase in the thickness of spacer layer. These observations have been interpreted in terms of the strength of the exciton–plasmon coupling, which is sensitive to the configuration of composite NRs as well as the relative difference between plasmon and exciton energies.

Effect of the Interaction between Molecular Exciton and Localized Surface Plasmon on the Spectroscopic Properties of Silver Nanoparticles Coated with Cyanine Dye J-Aggregates
Akihito YOSHIDA and Noritsugu KOMETANI,
J. Phys. Chem. C, 114, pp. 2867–2872 (2010)
Silver nanoparticles (Ag NPs) covered with a double shell consisting of spacer layer and cyanine dye J-aggregate (JA) layer were synthesized to examine the hybrid effects of the molecular exciton and the surface plasmon on the spectroscopic properties. The absorption spectral features of the composite NPs are classified into two types; a peak type or dip type in which the J-band of JA appears as a normal peak or an anomalous dip, respectively. The peak type is observed when the plasmon energy of Ag NP core is far from the exciton energy of JA shell, while the dip type is observed when both energies are close to each other, indicating that the exciton–plasmon interaction is weak for the peak type and strong for the dip type, respectively. Both types of absorption spectra could be reproduced by the theoretical calculation based on the quasi-static approximation, which provides a qualitative explanation for the absorption spectral features of composite NPs. From the observations of photoluminescence lifetimes and relative quantum yields of composite NPs, it was suggested that the radiative rate of composite NPs were also influenced by the exciton–plasmon coupling.

High-Pressure Study of Solvation Properties of Room Temperature Ionic Liquids
Yoshinori MINAMIKAWA, and Noritsugu KOMETANI,
J. Phys.: Conf. Seri., 215, p.012067 (2010)
The solvation properties of some room-temperature ionic liquids consisting of imidazolium cations and various anions were examined by means of the high-pressure spectroscopy with solvatochromic probes. We measured the pressure dependence of Kamlet-Taft solvatochromic parameters (π^* and β) and microviscosity (η). It was found that π^* and β were not so sensitive to the types of imidazolium cations and polyatomic anions, but the type of monoatomic anions. The pressure dependence of microviscosity was found to obey the empirical power-law equation.

Photocatalytic Effect of TiO_2 on the Hydrothermal Gasification of Glucose
Akihiro NAKATANI, and Noritsugu KOMETANI,
J. Phys.: Conf. Seri., 215, p.012091 (2010)
The hybrid process of the hydrothermal gasification method and the TiO_2 photocatalysis has been developed and tested for the gasification of glucose. TiO_2 powder and those loaded with Pt or Ni were used as photocatalyst. 0.05 M glucose aqueous solutions suspending the photoctalysts were reacted by the flow-type reactor system in the dark or under near-UV illumination with pressure and temperature controlled to be 30 MPa and 350−450 °C, respectively. It was found that the evolutions of hydrogen and methane from glucose could be promoted by the photocatalytic action of TiO_2 under hydrothermal conditions, which was further enhanced by supporting Pt and Ni on TiO_2.

Degradation of chlorobenzene by the hybrid process of supercritical water oxidation and TiO_2 photocatalysis
Ai SHIMOKAWA, Noritsugu KOMETANI, and Yoshiro YONEZAWA
Sep. Sci. Tech., 45, pp. 1538-1545 (2010)
Novel hybrid process of hydrothermal or supercritical water oxidation and TiO_2 photocatalysis was developed to examine the degradation of chlorobenzene as a model of the oxidative decomposition of organic pollutants. Aqueous solutions of chlorobenzene containing H_2O_2 as the oxidizing agent and/or colloidal TiO_2 nanoparticles as catalyst, were fed into the reactor with the temperature and the pressure controlled to be T=25−400°C and P=30 MPa, respectively. Chlorobenzene was considerably decomposed in the presence of H_2O_2 under hydrothermal conditions for $T \geqq 300$°C. It appeared that photocatalytic decomposition of chlorobenzene takes place at all temperatures by colloidal TiO_2 nanoparticles under irradiation with near-UV light. We have realized synergic decomposition of chlorobenzene by the coexistence of H_2O_2 and TiO_2 in which maximum conversion is more than 80% under irradiation at T=200°C.

Photocatalytic Enhancement of Hydrogen Evolution from Ethanol by TiO_2 in High-temperature High-pressure Water
Noritsugu KOMETANI, Kazumi SUGIMOTO, Yohei OKUNO, and Yoshiro YONEZAWA
15th International Conference on the Properties of Water and Steam, Berlin, Germany, Sep.7-11, 2008, Preprint p.137.

High pressure study on solvation properties of room temperature ionic liquids
Noritsugu KOMETANI, and Yoshinori MINAMIKAWA
Jasco report, Vol.52, No.1, pp.25-29 (2010) (in Japanese)

Fabrication of Functional Materials using the Hydrothermal Process
Noritsugu KOMETANI,
Kinozairyo, Vol. 30, No.4, pp.67-71 (2010) (in Japanese)

Synthesis of metal nanoparticles by means of hydrothermal process 1
Noritsugu KOMETANI,
Kakougijutsu, Vol. 45, No. 8, pp. 469-478 (2010) (in Japanese)

Synthesis of metal nanoparticles by means of hydrothermal process 2
Noritsugu KOMETANI,

Kakougijutsu, Vol. 45, No. 9, pp.563-568 (2010) (in Japanese)

Synthesis and spectroscopic properties of silver:dye composite nanoparticles with a double-shell structure
Akihito YOSHIDA, and Noritsugu KOMETANI,
Trends in Nanotechnology (TNT2009), Barcelona, Spain, Sep. 7-11, 2009

Preparation of size-controlled silver nanoparticles by the hydrothermal method
Noritsugu KOMETANI, and Takeshi TERANISHI,
Trends in Nanotechnology (TNT2009), Barcelona, Spain, Sep. 7-11, 2009

Self-Assembly and Cellular Uptake of Degradable and Water-Soluble Polyperoxides
Tamami FUJIOKA, Shuji TAKETANI, Takeshi NAGASAKI and Akikazu MATSUMOTO
Bioconjugate Chem., 20(10), pp. 1879–1887 (2009)
Water-soluble polyperoxides (PPs) as a new type of degradable and polymeric materials were synthesized by the radical alternating copolymerization of sorbic derivatives containing a tetra(ethylene oxide) unit in the ester group using molecular oxygen. The obtained PPs showed a lower critical solution temperature (LCST)-type phase separation, and the transition temperature decreased according to the content of the hydrophobic ester group in the PPs. The PPs formed nano-aggregates with a diameter of 250–370 nm in water under the LCST. These PP aggregates were revealed to include 1-anilinonaphthalene-8-sulfonic acid as the fluorescence probe and epirubicin as the anti-cancer drug in their hydrophobic compartment. We evaluated the cytotoxicity and cellular uptake of the PPs in order to test their ability as a carrier used for the delivery of anti-cancer drugs. The cell viability in the presence of the PPs was comparable to those for the other biodegradable polymers and epirubicin was uptaken into the A549 efficiently with the PPs via an endocytosis mechanism.

Thermally Stable and Fluorescent Maleimide/Isobutene Alternating Copolymers Containing Pyrenyl and Alkynylpyrenyl Moieties in the Side Chain
Shotaro YUKAWA, Akitoshi OMAYU and Akikazu MATSUMOTO
Macromol. Chem. Phys., 210(21), pp. 1776–1784 (2009)
We synthesized the alternating copolymers of maleimides containing pyrenyl and alkynylpyrenyl moieties with isobutene as a new class of heat-resistant and fluorescent polymers. *N*-(1-Pyrenyl)maleimide and *N*-(4-(1-pyrenyl- ethynyl)phenyl)maleimide were copolymerized with isobutene in the presence and absence of *N*-methylmaleimide. The obtained maleimide-isobutene copolymers showed an excellent thermal stability and the high glass transition temperatures, and were soluble in the common organic solvents. The fluorescence characteristics in 1,2-dichloro- ethane solutions revealed that the copolymers including the alkynylpyrenyl fluorophore emitted strong fluorescences with a high quantum efficiency (F = 0.83) even in the presence of air and upon heating. Solid-state fluorescence was also investigated using the transparent polymer films and aggregation of the alkynylpyrenyl moieties in the solid state was discussed.

Soluble and Thermally Stable Polysulfones Prepared by the Regiospecific and Alternating Radical Copolymerization of 2,4-Hexadiene with Sulfur Dioxide
Tomoaki KITAMURA, Naruki TANAKA, Asako MIHASHI and Akikazu MATSUMOTO
Macromolecules, 43(4), pp. 1800–1806 (2010)
We synthesized the alternating copolymers of 1,3-diene monomers with sulfur dioxide (SO_2) as a new class of thermally stable polymers by the radical copolymerization process and the subsequent hydrogenation. The copolymerizations of 2,4-hexadiene (HD), 1,3-butadiene (BD), and isoprene (IP) with SO_2 were carried out at –78 to 0 ºC in toluene in the presence of *tert*-butyl hydroperoxide, which acts as one component in the redox initiating system in combination with SO_2. The resulting poly(diene-*alt*-SO_2)s were found to consist of highly controlled repeating units, i.e., an alternating and 1,4-regiospecific repeating structure. Poly(HD-*alt*-SO_2) was soluble in several organic solvents, such as chloroform, nitromethane, tetrahydrofuran, acetone, and dimethyl sulfoxide. In contrast, poly(IP-*alt*-SO_2) was soluble only in dimethyl sulfoxide, while poly(BD-*alt*-SO_2) was insoluble in all the solvents. The poly(diene-*alt*-SO_2)s readily degraded upon heating due to the expected fast depolymerization. We have demonstrated that the thermal stability of the poly(diene-*alt*-SO_2)s is modified by the hydrogenation of the double bond in the polymer main chain. The

hydrogenation of poly(HD-*alt*-SO_2) resulted in a drastic increase in the 5% weight-loss temperature from 135 to 317 °C.

Cohesive Force Change Induced by Polyperoxide Degradation for Application to Dismantlable Adhesion

Eriko SATO, Hiroshi TAMURA and Akikazu MATSUMOTO

ACS Appl. Mater. Inter., 2(9), pp. 2594-2601 (2010)

Polyperoxides containing peroxy bonds as the main-chain repeating units are a new class of degradable polymers due to significant changes in their molecular weight and physical properties during a degradation process. In this study, the application of linear and network polyperoxides to dismantlable adhesion was investigated. When the linear polyperoxide obtained from methyl sorbate and oxygen (PP-MS) was used as a pressure-sensitive adhesive (PSA), its shear holding power and 180° peel strength immediately decreased upon heating at 70 °C or under UV irradiation. Low-molecular-weight products, which were generated by the degradation of PP-MS, behaved as a plasticizer to effectively reduce the cohesive force. The adhesive properties of two types of polyperoxides-based network polymers, the cross-linking point and main-chain degradable network polymers, were evaluated. A cross-linking point degradable network polymer was produced by the oxygen cross-linking of dienyl-functional- ized poly(ethylene glycol). A main-chain degradable network polymer was formed by the diisocyanate cross- linking of a hydroxy-functionalized polyperoxide. Both network polymers showed a higher adhesive strength than PP-MS due to their three-dimensional network structure. Noteworthy, the adhesive strength of the main-chain degradable network polymer was varied from the level of PSA to structural adhesives by increasing the added amount of the diisocyanate cross-linker. After heating at 110 °C, the cohesive and adhesive strengths significantly decreased. The linear and network polyperoxides are shown to be promising materials for dismantlable adhesion.

Crystal Phase Transition and Solid-State Photoisomerization of Benzyl (*Z,Z*)-Muconate Polymorphs Studied by Direct Observation of Crystal Structure Change

Natsuko NISHIZAWA, Daisuke FURUKAWA, Seiya KOBATAKE and Akikazu MATSUMOTO

Cryst. Growth Des., 10(7), pp. 3203–3210 (2010)

We investigated the polymorph structures of benzyl (*Z,Z*)-muconate crystals (ZZ-Bn-a, b, and g) and their EZ photoisomerization behavior in order to clarify the EZ isomerization mechanism of diene compounds in the solid state. First, the thermodynamics and crystal phase transition of the polymorphs were investigated by differential scanning calorimetry and X-ray diffraction. A single-crystal-to-single-crystal transition was observed during the change in the polymorph structures from the ZZ-Bn-b to the a form. We also observed in-situ the migration of the boundary between the different polymorph domains during the phase transition of the ZZ-Bn-g to the a form by optical microscopy. We then investigated the change in the crystal structure of ZZ-Bn during the EZ photo- isomerization in the solid state. The photoisomerization of ZZ-Bn to the corresponding EE isomer (EE-Bn) proceeded according to a bicycle-pedal model via a single-crystal-to-single-crystal topochemical reaction mecha- nism, which was directly confirmed by an X-ray single-crystal structure analysis. During the photoirradiation of the polymorph crystals of ZZ-Bn-a and b, a structural strain was accumulated in the crystal lattice, and finally caused a phase transition accompanied by a change in the space group from $P2_1/c$ to $P2_1$, resulting in a stable crystal structure identical to that of the recrystallized EE-Bn. On the other hand, the ZZ-Bn-g crystals became amorphous during the photoirradiation because of the greater molecular motions in the crystals. Thus, we have demonstrated the validity of the in-situ single-crystal structure analysis for investigating the EZ photoisomeriza- tion of diene compounds in the solid state.

Effect of Phase Separationon on Thermal Aging Behavior of Styrene-Butadiene Rubber Vulcanizates Using Liquid Polyisoprene as Plasticizer

Takeo NAKAZONO, Anri OZAKI and Akikazu MATSUMOTO

Chem. Lett., 39(3), pp. 268–269 (2010)

Styrene-butadiene rubber (SBR) vulcanizates were prepared using liquid polyisoprene and hydrogenated polyiso- prene as the plasticizers, and their structure and mechanical properties were investigated. The effect of the phase- separated structures of the SBR and the liquid polymers on the mechanical properties of the SBR vulcanizates was investigated. The constant physical properties were observed for the SBR vulcanizates during the thermal aging process when SBR and the plasticizer were miscible with each other in the

vulcanizates.

Thermosetting Maleimide/Isobutene Alternating Copolymer as a New Class of Transparent Materials
Kyota TAKEDA and Akikazu MATSUMOTO
Macromol. Chem. Phys., 211(7), pp. 782–790 (2010)
We synthesized an alternating copolymer of *N*-allylmaleimide (AMI) and isobutene (IB) [poly(AMI-*alt*-IB)] as a new class of thermosetting polymers by the free radical copolymerization process. The reactivity of the maleimide group of the AMI monomer was evaluated to be 10^3 times higher than that of the N-allyl group based on the results for the ternary copolymerization system composed of *N*-methylmaleimide (MMI), *N*-allylphthalimide (AP), and IB. The maleimide moiety exclusively participated in the propagation during the copolymerization of AMI with IB, resulting in the formation of the soluble poly(AMI-*alt*-IB). The copolymer included an alternating repeat- ing structure consisting of maleimide and IB units in the main chain and the unreacted allyl group in the side chain. The onset temperature of the decomposition for poly(AMI-*alt*-IB) was over 400 ºC in a nitrogen stream. The transparent cast film of poly(AMI-*alt*-IB) was readily cured upon heating without any catalyst.

Synthesis of Degradable Network Polymers Containing Peroxy Units in the Main Chain or the Cross-linking Point
Asako MIHASHI, Hiroshi TAMURA, Eriko SATO and Akikazu MATSUMOTO
Prog. Org. Coat., 67(2), pp. 85–91 (2010)
We have synthesized degradable network polymers containing readily labile peroxy bonds as the repeating units in the main chain or as the cross-linking point in the side chain. Poly(2-hydroxyethyl sorbate-*alt*-O_2) was obtained by the radical copolymerization of 2-hydroxyethyl sorbate with oxygen, and then cross-linked using tolylene 2,4-diisocyanate as the cross-linking agent to obtain a new type of degradable gel. We also investigated the cross-linking of conventional polymers by the reaction of the diene moieties introduced into the polymer side chain with oxygen. The hydroxy group in the side chain of poly(vinyl alcohol) (PVA) was reacted with 1-iso- cyanate-1,3-pentadiene in order to introduce a diene moiety into the side chain of the PVA. The dienylated PVA was reacted with oxygen in the presence of a radical initiator, leading to the formation of a gel containing a labile peroxy linkage at the cross-linking point. These gels containing peroxy units in the main chain or at the cross-linking points degraded upon heating.

Mechanical Properties and Thermal Aging Behavior of Styrene-Butadiene Rubbers Vulcanized Using Liquid Diene Polymers as the Plasticizers
Takeo NAKAZONO and Akikazu MATSUMOTO
J. Appl. Polym. Sci., 118(4), pp. 2314–2320 (2010)
The mechanical properties of styrene-butadiene rubber (SBR) vulcanizates prepared using various plasticizers including liquid polybutadiene and styrene-butadiene copolymers were investigated. The effect of the liquid polymers as the plasticizers on the mechanical properties of the polymers, such as the hardness, tensile storage modulus, tand, and the stress at 100% elongation values, were determined before and after the thermal aging. As a result, it was revealed that the use of these liquid polymers gave less amount of change in the measurement values for the mechanical properties during the aging. The cross-linking density and the amount of free polymers were also determined on the basis of the swelling and extraction data, respectively, using several organic solvents. These results support the fact that the added liquid polymers are fixed to the SBR networks. We revealed the superiority of the liquid styrene-butadiene copolymers as the plasticizer, which provides sufficient mechanical properties after vulcanization and the excellent maintenance of the properties during the thermal aging process.

Preparation of Organic–Ceramic–Metal Multihybrid Particles and their Organized Assembly: Preparation and Assembly of Multihybrid Particles
Jun MATSUI, Salina PARVIN, Eriko SATO and Tokuji MIYASHITA
Polym. J., 42(2), pp. 142–147 (2010)
This paper describes the synthesis and assembly of multihybrid particles having a gold core, silica as an initial shell and poly(methyl methacrylate) (PMMA) as a second shell (Au@SiO_2@PMMA). Multihybrid particles were synthesized in a stepwise manner. First, direct sol–gel coating of silica onto gold nanoparticles was carried out to prepare Au@SiO_2 particles. The Au@SiO_2 particles were modified with 3-(triethoxysilyl)propyl 2-bromo-2- methylpropanoate (BMPS), which is an initiator for atom transfer radical

polymerization (ATRP) of MMA. Finally, bulk ATRP of MMA was conducted using BMPS-coated $Au@SiO_2$ particles. $Au@SiO_2@PMMA$ particles formed a closely packed monolayer at the air–water interface. The monolayer can be deposited onto a solid substrate using the Langmuir–Blodgett technique. Atomic force microscopy and scanning electron microscopy images of the deposited film show a uniform and closely packed monolayer film in an area a few tens-of-micro- meters in size with no voids. Moreover, a clear Au core, silica shell and PMMA shell structure were observed in a transmission electron microscopy image of the transferred film. It is particularly interesting that the monolayer film shows no clear plasmon absorption of the gold core, as observed in the chloroform solution of the particle. Results show that a thick silica shell masked the monolayer film's plasmon absorption.

Facile Synthesis of Functional Polyperoxides by Radical Alternating Copolymerization of 1,3-Dienes with Oxygen
Eriko SATO and Akikazu MATSUMOTO
Chem. Rec., 9(5), pp. 247–257 (2009)
We have developed the facile synthesis of degradable polyperoxides by the radical alternating copolymerization of 1,3-diene monomers with molecular oxygen at an atmospheric pressure. In this review, the synthesis, the degradation behavior, and the applications of functional polyperoxides are summarized. The alkyl sorbates as the conjugated 1,3-dienes gave a regiospecific alternating copolymer by exclusive 5,4-addition during polymerization and the resulting polyperoxides decomposed by the homolysis of a peroxy linkage followed by the successive *b*-scissions. The preference of 5,4-addition was well rationalized by the theoretical calculations. The degradation of the polyperoxides occurred with various stimuli, such as heating, UV irradiation, a redox reaction with amines, and an enzyme reaction. The various functional polyperoxides were synthesized by following two methods, i.e., one is the direct copolymerization of functional 1,3-dienes, and the other is the functionalization of the precursor polyperoxides. Water soluble polyperoxides were also prepared, and the LCST behavior and the application to a drug carrier in the drug delivery system were investigated. In order to design various types of degradable polymers and gels we developed a method for the introduction of dienyl groups into the precursor polymers. The resulting dienyl-functionalized polymers were used for the degradable gels. The degradable branched copolymers showed a microphase-separated structure, which changed due to the degradation of the polyperoxides segments

Synthesis of Polyperoxides and Application to Functional Polymer Materials Design
Eriko SATO and Akikazu MATSUMOTO
J. Adhes. Soc. Jpn., 46(6), pp. 230–237 (2010) (in Japanese)

Introduction to the Serial Reports on "Human×Environment×Materials: Development of Human-Adaptive Materials"
Akikazu MATSUMOTO
Function & Materials (Kinou Zairyou), 30, No. 1, p. 62 (2010) (in Japanese)

Functional and High Performance Polymer Materials: From Degradable Polymers to Heat-Resistant Polymers
Akikazu MATSUMOTO
Function & Materials (Kinou Zairyou), 30, No. 1, pp. 63–71 (2010) (in Japanese)

Introduction to the Special Issue on "Recent Development of Dismantlable Adhesive Technology"
Akikazu MATSUMOTO
Function & Materials (Kinou Zairyou), 30, No. 2, p. 5 (2010) (in Japanese)

Recent Development of On-Demand Debonding Technology and Materials
Akikazu MATSUMOTO
Function & Materials (Kinou Zairyou), 30, No. 2, pp. 14–21 (2010) (in Japanese)

Living Radical Polymerization Using Iniferter Technique; Polymer Structure Control Using Click Chemistry; Synthesis of Block Copolymers by Living Radical Polymerization; Alternating Copolymeriza- tion; Radical Polymerization of a,b-Disubstituted Ethylenes; Solid-State Radical

Polymerization
Akikazu MATSUMOTO
Radical Polymerization Handbook, Revised Edition, NTS, pp. 168–175; pp. 226–234; pp. 246–259; pp. 320–333; pp. 456–465; pp. 542–551 (in Japanese)

Polymer Synthesis Using Solid-State Polymerization
Akikazu MATSUMOTO
Symposium on Frontiers of Polymer Syntheses, The Society of Polymer Science, Japan, Invited Lecture, Fukuoka, July 9, 2010 (in Japanese)

Design of Dismantlable Adhesive Materials Using Main-Chain and Side-Chain Degradable Polymers
Akikazu MATSUMOTO
The Regular Meeting of Workshop on Adhesion and Coatings, The Society of Polymer Science, Japan, Invited Lecture, Tokyo, September 10, 2010 (in Japanese)

Dismantlable Adhesion Using Degradable Polymers
Akikazu MATSUMOTO
The Regular Meeting of Chugoku-Shikoku Branch of The Society of Polymer Science, Japan, Invited Lecture, Tokushima, September 22, 2010 (in Japanese)

Dismantlable Adhesion Technology Using Degradable Polymers
Eriko SATO
The Regular Meeting of the Consortium of Dismantlable Adhesion, Japan Adhesive Industry Association, Invited Lecture, Osaka, June 23, 2010 (in Japanese)

Light-Controllable Surface Plasmon Resonance Absorption of Gold Nanoparticles Covered with Photochromic Diarylethene Polymers
Hiroyasu NISHI, Tsuyoshi ASAHI, and Seiya KOBATAKE
J. Phys. Chem. C, 113(40), pp. 17359–17366 (2009)
Various sizes of gold nanoparticles covered with photochromic diarylethene polymers (Au–poly(DE)s) were prepared by Brust's method, citrate reduction, or a seeding growth method. The diarylethene polymers on the particles exhibited reversible photochromism upon alternating irradiation with ultraviolet and visible light, both in solution and in the solid state. Au–poly(DE) of larger size, prepared by the seeding growth method, showed a significant shift in the local surface plasmon resonance (LSPR) band photoreversibly as a result of photochromic reaction of the diarylethene polymers around the gold nanoparticles. This change is due to a change in the refractive index of the photochromic chromophore and is remarkably enhanced in the solid state. However, the smaller sized Au–poly(DE) prepared by Brust's method hardly showed any such spectral shift. These results are qualitatively reproduced by a theoretical simulation, which indicates that the sensitivity of the LSPR band strongly depends on the particle size of the gold nanoparticle. The Au–poly(DE)s can be potentially used as new types of plasmonic materials with a light-controllable LSPR band.

Unusual Photochromic Behavior of C3-methoxy-substituted Bis(2-thienyl)perfluorocyclopentene
Kingo UCHIDA, Hibiki SUMINO, Yumiko SHIMOBAYASHI, Yousuke USHIOGI, Atsushi TAKATA, Yuko KOJIMA, Satoshi YOKOJIMA, Seiya KOBATAKE, and Shinichiro NAKAMURA
Bull. Chem. Soc. Jpn., 82(11), pp. 1441–1446 (2009)
A bis(2-thienyl)perfluorocyclopentene having methoxy groups at both reactive carbon atoms was synthesized and the quantum yields of cyclization and cycloreversion reactions were found to be 0.29 and 0.27, respectively. Usual bis(3-thienyl)perfluorocyclopentenes with methoxy groups at both reactive carbon atoms show much lower cycloreversion quantum yields. The unusual large yield was explained by theoretical methods. Additionally the compound did not show any coloration in crystalline state upon UV irradiation, even though the distance between both reactive carbon atoms is less than 4 Å. The reason was discussed by using the crystallographic data.

Multiphoton-gated Cycloreversion Reactions of Photochromic Diarylethene Derivatives with Low Reaction Yields upon One-photon Visible Excitation

Yukihide ISHIBASHI, Katsuki OKUNO, Chikashi OTA, Toshiyuki UMESATO, Tetsuro KATAYAMA, Masataka MURAKAMI, Seiya KOBATAKE, Masahiro IRIE, and Hiroshi MIYASAKA
Photochem. Photobio. Sci., 9(2), pp.172–180 (2010)
Cycloreversion processes of three photochromic diarylethene derivatives with extremely low one-photon reaction yields (5.0×10^{-5} to 1.5×10^{-2}) were investigated by means of femtosecond and picosecond laser photolysis methods. Femtosecond visible laser photolysis revealed that the excited state of the closed form in these three derivatives decayed into the ground state with 0.7–8 ps time constants and with low cycloreversion yields that were consistent with those obtained by steady-state light irradiation. On the other hand, the cycloreversion reaction was drastically enhanced by picosecond 532 nm laser excitation for all of the three derivatives. From excitation intensity effects of the reaction yield and dynamic behavior, it was found that the successive two-photon absorption process leading to higher excited states opened an efficient cycloreversion channel, with reaction yields of 0.3–0.5. These results are discussed from the viewpoint of the one-photon inerasable but two-photon erasable photochromic system.

Photoinduced Micropatterning by Polymorphic Crystallization of a Photochromic Diarylethene in a Polymer Film
Daichi KITAGAWA, Itsuka YAMASHITA, and Seiya KOBATAKE
Chem. Commun., 46(21), pp.3723–3725 (2010)
A photochromic diarylethene was found to crystallize rapidly from the amorphous state in poly(methyl methacrylate) by heating at 130 °C. The diarylethene amorphous film was successfully patterned to form microcrystals upon ultraviolet light irradiation through a photomask, showing a high resolution as good as ca. 4 micrometers under optimal conditions. The surface of the microcrystals had a larger contact angle with water than the amorphous film. Such a photopatterning process offers a useful tool for controlling surface wettability in applications.

Fabrication and Photochromism of High-density Diarylethene Monolayer Immobilized on a Quartz-glass Substrate
Hiroyasu NISHI and Seiya KOBATAKE
Chem. Lett., 39(6), pp.638–639 (2010)
Diarylethene monolayer was fabricated on a quartz-glass substrate using a silane coupling technique. The coupling agent was easily prepared from a diarylethene with a hydroxy group and 3-aminopropyltriethoxysilane. It was found that the chromophore was introduced in high density on the substrate and still exhibited reversible photochromism with relatively high conversion upon photoirradiation despite being constrained on the quartz-glass surface. The coverage of the coupling agent on the quartz-glass surface was estimated to be 1.5 molecules per square nanometer. The method to fabricate the photochromic monolayer can be useful for development of light-controllable thin film devices on the substrate.

Morphology Changes of Photochromic Single Crystals
Seiya KOBATAKE and Masahiro IRIE
In *Molecular Nano Dynamics Vol. 2*, Chapter 23, pp. 443–457 (2009)
This chapter has focused on the geometrical structure changes and described the photochromic reactions of diarylethene derivatives in the single-crystalline phase and their photomechanical phenomena. Molecular materials that reversibly change shape and/or size in response to external stimuli have attracted much attention as photomechanical actuators because the materials can allow remote operation without any direct contact. The photomechanical phenomena are potentially induced by the photoisomerization of constituent molecules. The two isomers differ from one another not only in the absorption spectra but also in various physical and chemical properties, such as refractive indices, dielectric constants, and oxidation-reduction potentials. The instant property changes by photoirradiation without processing lead to their use in various optoelectronic devices, such as optical memory, photoswitching, display materials, and nonlinear optics.

Multiphoton-Gated Reaction in Organic Photochromic Molecules under Pulsed Laser Excitation
Yukihide ISHIBASHI, Seiya KOBATAKE, Yasushi YOKOYAMA, Masahiro IRIE, and Hiroshi MIYASAKA
The Review of Laser Engineering, 38(2), pp.90–95 (2010) (in Japanese)
Organic photochromic molecules such as diarylethene and fulgide derivatives with small ring-opening photochromic reaction yields at the lowest electronic excited state showed drastic enhancement of the pulsed

excitation did not induce such as effective reaction. Excitation intensity effect of the reaction yield and dynamic behaviors revealed that the successive multiphoton absorption process leading to higher excited states with a large reaction yield led to the enhancement of the reaction. On the other hand, the one-photon UV absorption directly pumped to a higher excited state did not lead to the efficient reaction. The selectivity of the reaction depending on the mode of the excitation was discussed from the viewpoints of optical selection rule of the electronic reaction.

Design and Properties of Gold Nanoparticles Covered with Photo-functionalized Polymers
Seiya KOBATAKE
Function & Materials, 30(8), pp.59–66 (2010) (in Japanese)
Recently, metallic nanoparticles have attracted much attention for not only physicochemical field but also widespread fields from electronics to biotechnology. This is because the local surface Plasmon resonance which is one of the characters of the metallic nanoparticle can greatly depend on the environment of the particle neighborhood, and nanosized particles do the sensing of a variety of material adsorptions. This review has focused on the design, the synthesis, and the characterization of gold nanoparticles covered with photo-functionalized polymers.

Control of Properties in Photofunctional Organic Molecular Crystals
Seiya KOBATAKE
Innovative Materials and Processing Research Center Symposium 2009, Invited Lecture, Ryukoku University, Seta, Japan, March 8, 2010; Preprints (in Japanese)

Photoresponsive Property Changes of Photochromic Diarylethene Crystals
Seiya KOBATAKE
International Symposium on Functional Nanosystems: Molecular Electronics and Photonics, Invited Lecture, Nara, Japan, July 2, 2010; Preprints p. 13.

Photoresponsive Solid State Property Change of Photochromic Crystals
Seiya KOBATAKE
Japan-China Joint Symposium on Functional Supramolecular Architectures, Invited Lecture, Chanchun, China, July 24-28, 2010; Preprints pp. 33–34.

Bioengineering

Biotinylated Bionanocapsules for Displaying Diverse Ligands Toward Cell-Specific Delivery
Takuya SHISHIDO, Yuki AZUMI, Takeshi NAKANISHI, Mitsuo UMETSU, Tsutomu TANAKA, Chiaki OGINO, Hideki FUKUDA, and Akihiko KONDO
J. Biochem., 146, pp.867–874 (2009)
Bionanocapsule (BNC) is hollow nanoparticle composed of the L-protein of the hepatitis B virus surface antigen. BNC allows targeted delivery of either genes or drugs only to hepatocytes, but not to other cell types. In this study, we attempted to alter the specificity of BNC by insertion of biotin-acceptor peptide (BAP), which is efficiently biotinylated using biotin ligase BirA from *Escherichia coli*. Using streptavidin as a linker, biotinylated BNC could be display various biotinylated ligands that are otherwise difficult to fuse with BNC, such as antibodies, synthetic peptides and functional molecules. BAP-fused BNC was efficiently biotinylated and effectively displayed streptavidin. Furthermore, we demonstrated that biotinylated BNC was internalized into targeted cells via biotinylated Nanobody displayed on the BNC surface. Biotinylated BNC permit display of diverse ligands, and thus have potential as a versatile carrier for drug delivery to a variety of target cells.

Application of the Fc Fusion Format to Generate Tag-Free Bispecific Diabodies
Ryutaro ASANO, Keiko IKOMA, Hiroko KAWAGUCHI, Yuna ISHIYAMA, Takeshi NAKANISHI, Mitsuo UMETSU, Hiroki HAYASHI, Yu KATAYOSE, Michiaki UNNO, Toshio KUDO, and Izumi KUMAGAI
FEBS J., 277, pp.477–487 (2010)
We previously reported the use of a humanized bi-specific diabody that targets epidermal growth factor receptor and CD3 (hEx3-Db) for cancer immunotherapy. Bacterial expression can be used to express small recombinant antibodies on a large scale; however, their overexpression often results in the formation of insoluble aggregates, and in most cases artificial affinity peptide tags need to be fused to the antibodies for purification by affinity chromatography. Here, we propose a novel method for preparing refined, functional, tag-free bi-specific diabodies from IgG-like bi-specific antibodies (BsAbs) in a mammalian expression system. We created an IgG-like BsAb in which bi-specific diabodies were fused to the human Fc region via a designed human rhinovirus 3C (HRV3C) protease recognition site. The BsAb was purified by protein A affinity chromatography, and the refined tag-free hEx3-Db was efficiently produced from the Fc fusion format by protease digestion. The tag-free hEx3-Db from the Fc fusion format showed a greater inhibition of cancer growth than affinity-tagged hEx3-Db prepared directly from Chinese hamster ovary cells. We also applied our novel method to another small recombinant antibody fragment, hEx3 single-chain diabody (hEx3-scDb), and demonstrated the versatility and advantages of our proposed method compared with papain digestion of hEx3-scDb. This approach may be used for industrial-scale production of functional tag-free small therapeutic antibodies.

Direct and Selective Immobilization of Proteins by Means of an Inorganic Material-Binding Peptide: Discussion on Functionalization in the Elongation to Material-Binding Peptide
Nozomi YOKOO, Takanari TOGASHI, Mitsuo UMETSU, Kouhei TSUMOTO, Takamitsu HATTORI, Takeshi NAKANISHI, Satoshi OHARA, Seiichi TAKAMI, Takashi NAKA, Hiroya ABE, Izumi KUMAGAI, and Tadafumi ADSCHIRI
J. Phys. Chem. B, 114, pp.480–486 (2010)
Using an artificial peptide library, we have identified a peptide with affinity for ZnO materials that could be used to selectively accumulate ZnO particles on polypropylene-gold plates. In this study, we fused recombinant green fluorescent protein (GFP) with this ZnO-binding peptide (ZnOBP) and then selectively immobilized the fused protein on ZnO particles. We determined an appropriate condition for selective immobilization of recombinant GFP, and the ZnO-binding function of ZnOBP-fused GFP was examined by elongating the ZnOBP tag from a single amino acid to the intact sequence. The fusion of ZnOBP with GFP enabled specific adsorption of GFP on ZnO substrates in an appropriate solution, and thermodynamic studies showed a predominantly enthalpy-dependent electrostatic interaction between ZnOBP and the ZnO surface. The ZnOBP's binding affinity for the ZnO surface increased first in terms of material selectivity and then in terms of high affinity as the GFP-fused peptide was elongated from a single amino acid to intact ZnOBP. We concluded that the enthalpy-dependent interaction between ZnOBP and ZnO was influenced by the presence of not only charged amino acids but also their surrounding residues in the ZnOBP sequence.

Contribution of Asparagine Residues to the Stabilization of a Proteinaceous Antigen-Antibody Complex, HyHEL-10-Hen Egg White Lysozyme

Akiko YOKOTA, Kouhei TSUMOTO, Mitsunori SHIROISHI, Takeshi NAKANISHI, Hidemasa KONDO, and Izumi KUMAGAI

J. Biol. Chem., 285, pp.7686–7696 (2010)

Many germ line antibodies have asparagine residues at specific sites to achieve specific antigen recognition. To study the role of asparagine residues in the stabilization of antigen-antibody complexes, we examined the interaction between hen egg white lysozyme (HEL) and the corresponding HyHEL-10 variable domain fragment (Fv). We introduced Ala and Asp substitutions into the Fv side chains of L-Asn-31, L-Asn-32, and L-Asn-92, which interact directly with residues in HEL via hydrogen bonding in the wild-type Fv-HEL complex, and we investigated the interactions between these mutant antibodies and HEL. Isothermal titration calorimetric analysis showed that all the mutations decreased the negative enthalpy change and decreased the association constants of the interaction. Structural analyses showed that the effects of the mutations on the structure of the complex could be compensated for by conformational changes and/or by gains in other interactions. Consequently, the contribution of two hydrogen bonds was minor, and their abolition by mutation resulted in only a slight decrease in the affinity of the antibody for its antigen. By comparison, the other two hydrogen bonds buried at the interfacial area had large enthalpic advantage, despite entropic loss that was perhaps due to stiffening of the interface by the bonds, and were crucial to the strength of the interaction. Deletion of these strong hydrogen bonds could not be compensated for by other structural changes. Our results suggest that asparagine can provide the two functional groups for strong hydrogen bond formation, and their contribution to the antigen-antibody interaction can be attributed to their limited flexibility and accessibility at the complex interface.

High Affinity Anti-Inorganic Material Antibody Generation by Integrating Graft and Evolution Technologies: Potential of Antibodies as Biointerface Molecules

Takamitsu HATTORI, Mitsuo UMETSU, Takeshi NAKANISHI, Takanari TOGASHI, Nozomi YOKOO, Hiroya ABE, Satoshi OHARA, Tadafumi ADSCHIRI, and Izumi KUMAGAI

J. Biol. Chem., 285, pp.7784–7793 (2010)

Recent advances in molecular evolution technology enabled us to identify peptides and antibodies with affinity for inorganic materials. In the field of nanotechnology, the use of the functional peptides and antibodies should aid the construction of interface molecules designed to spontaneously link different nanomaterials; however, few material-binding antibodies, which have much higher affinity than short peptides, have been identified. Here, we generated high affinity antibodies from material-binding peptides by integrating peptide-grafting and phage-display techniques. A material-binding peptide sequence was first grafted into an appropriate loop of the complementarity determining region (CDR) of a camel-type single variable antibody fragment to create a low affinity material-binding antibody. Application of a combinatorial library approach to another CDR loop in the low affinity antibody then clearly and steadily promoted affinity for a specific material surface. Thermodynamic analysis demonstrated that the enthalpy synergistic effect from grafted and selected CDR loops drastically increased the affinity for material surface, indicating the potential of antibody scaffold for creating high affinity small interface units. We show the availability of the construction of antibodies by integrating graft and evolution technology for various inorganic materials and the potential of high affinity material-binding antibodies in biointerface applications.

Target Cell-Restricted Apoptosis Induction by 528scFv-TRAIL Fusion Protein Specific for Human EGFR and Expressed in *Escherichia coli*

Adel BADRAN, Ryutaro ASANO, Makoto NAKAYAMA, Yasuhiro WATANABE, Takeshi NAKANISHI, Mitsuo UMETSU, Hiroki HAYASHI, Yu KATAYOSE, Michiaki UNNO, and Izumi KUMAGAI

Int. J. Oncol., 36, pp.1229–1234 (2010)

We report the preparation and functional characterization of an *Escherichia coli*-expressed recombinant fusion protein, 528scFv-TRAIL, specific for the human epidermal growth factor receptor (EGFR) and empowered by the tumor necrosis factor-related apoptosis-inducing ligand (TRAIL). The 528scFv-TRAIL, expressed as insoluble inclusion bodies in *E. coli*, was solubilized and then refolded by using a modified stepwise dialysis method. Treatment with 528scFv-TRAIL resulted in the specific binding to the cell surface of EGFR-positive cells with concomitant deployment of the TRAIL moiety to DR-5 receptor in a manner comparable to a commercially available form of recombinant TRAIL (cTRAIL). 528scFv-TRAIL, prepared by either of three refolding processes described herein, showed potent cytotoxic activity against

EGFR-positive TFK-1 cell line and was superior to its parental 528scFv; a recombinant variable fragment with single specificity against human EGFR. Narrow variations in the cytotoxic potential of 528scFv-TRAIL were ascribed to manipulation of redox conditions during the refolding process. Together, our findings point to the potential value of 528scFv-TRAIL for treatment of EGFR-expressing cancers. Furthermore, preparation of 528scFv-TRAIL from insoluble aggregates in a prokaryotic cell based expression system by means of in vitro refolding introduces a feasible cost-benefit, time-efficient approach for industrial-scale production.

Integration of PEGylation and Refolding for Renaturation of Recombinant Proteins from Insoluble Aggregates Produced in Bacteria-Application to a Single-Chain Fv Fragment
Izumi KUMAGAI, Ryutaro ASANO, Takeshi NAKANISHI, Kentaro HASHIKAMI, Sho TANAKA, Adel BADRAN, Hideaki SANADA, and Mitsuo UMETSU
J. Biosci. Bioeng., 109, pp.447–452 (2010)
The conjugation of polyethylene glycol (PEGylation) with downsized compact antibodies is an effective method for overcoming the problem of rapid elimination of the compact antibodies from the body. We integrated site-specific PEGylation with the refolding of a single-chain Fv (scFv) of humanized monoclonal antibody 528 with affinity for the epidermal growth factor receptor, to prepare active PEGylated scFv from insoluble aggregates produced in an *Escherichia coli* expression system. The insertion of a cysteine residue at the C-terminus of scFv to serve as the conjugation site for PEG led to the formation of highly multimeric scFv during the refolding process; however, PEGylation after refolding drastically dispersed the multimer into monomeric active scFv fragments. Further, the PEGylation of partially refolded scFv during the refolding process improved the PEGylation efficiency and suppressed the formation of highly multimeric scFv; consequently, monomeric active scFv fragments were obtained directly from the insoluble aggregates in E. coli. We show that in vitro refolding of PEGylated scFv should be useful for improving downstream processing performance in the production of clinically useful small antibodies from insoluble fractions.

Protein-Protein Interactions and Selection: Generation of Molecule-Binding Proteins on the Basis of Tertiary Structural Information
Mitsuo UMETSU, Takeshi NAKANISHI, Ryutaro ASANO, Takamitsu HATTORI, and Izumi KUMAGAI
FEBS J., 277, pp.2006–2014 (2010).
Antibodies and their fragments are attractive binding proteins because their high binding strength is generated by several hypervariable loop regions, and because high-quality libraries can be prepared from the vast gene clusters expressed by mammalian lymphocytes. Recent explorations of new genome sequences and protein structures have revealed various small, nonantibody scaffold proteins. Accurate structural descriptions of protein-protein interactions based on X-ray and NMR analyses allow us to generate binding proteins by using grafting and library techniques. Here, we review approaches for generating binding proteins from small scaffold proteins on the basis of tertiary structural information. Identification of binding sites from visualized tertiary structures supports the transfer of function by peptide grafting. The local library approach is advantageous as a go-between technique for grafted foreign peptide sequences and small scaffold proteins. The identification of binding sites also supports the construction of efficient libraries with a low probability of denatured variants, and, in combination with the design for library diversity, opens the way to increasing library density and randomized sequence lengths without decreasing density. Detailed tertiary structural analyses of protein-protein complexes allow accurate description of epitope locations to enable the design of and screening for multispecific, high-affinity proteins recognizing multiple epitopes in target molecules.

The Effects of Disappearance of One Charge on Ultrafast Fluorescence Dynamics of FMN Binding Protein
Haik CHOSROWJAN, Seiji TANIGUCHI, Noboru MATAGA, Takeshi NAKANISHI, Yoshihiro HARUYAMA, Shuta SATO, Masaya KITAMURA, and Fumio TANAKA
J. Phys. Chem. B, 114, pp.6175–6182 (2010)
Crystal structures of E13T (Glu13 was replaced by Thr13) and E13Q (Glu13 was replaced by Gln13) FMN binding proteins (FMN-bp) from *Desulfovibrio vulgaris*, strain Miyazaki F, were determined by the X-ray diffraction method. Geometrical factors related to photoinduced electron transfer from Trp32, Tyr35, and Trp106 to the excited isoalloxazine (Iso*) were compared among the three forms of FMN-bp. The rate of ET is considered to be fastest from Trp32 to Iso* in FMN-bp and then from Tyr35 and Trp106. The distances

between Iso and Trp32 did not change appreciably (0.705-0.712 nm) among WT, E13T, and E13Q FMN-bps, though the distances between Iso and Tyr35 or Trp106 became a little shorter by ca. 0.01 nm in both mutated FMN-bps. The distances between the residue at 13 and the ET donors or acceptor in the mutated proteins, however, changed markedly, compared to WT. Hydrogen bonding pairs and distances between Iso and surrounding amino acids were not modified when Glu13 was replaced by Thr13 or Gln13. Effects of elimination of ionic charge at Glu13 on the ultrafast fluorescence dynamics in E13T and E13Q were investigated comparing to WT, by means of a fluorescence up-conversion method. Fluorescence lifetimes were τ_1 = 107 fs (α_1 = 0.86), τ_2 = 475 fs (α_2 = 0.12), and τ_3 = 30 ps (α_3 = 0.02) in E13T and τ_1 = 134 fs (α_1 = 0.85), τ_2 = 746 fs (α_2 = 0.12), and τ_3 = 30 ps (α_3 = 0.03) in E13Q, which are compared to the reported lifetimes in WT, τ_1 = 168 fs (α_1 = 0.95) and τ_2 = 1.4 ps (α_2 = 0.05). Average lifetimes ($\tau_{AV} = \sum_{i=1}^{2or3} \alpha_i \tau_i$) were 0.75 ps in E13T, 1.10 ps in E13Q, and 0.23 ps in WT, which implies that τ_{AV} was 3.3 times longer in E13T and 4.8 times longer in E13Q, compared to WT. The ultrafast fluorescence dynamics of WT did not change when solvent changed from H_2O to D_2O. Static ET rates (inverse of average lifetimes) were analyzed with static structures of the three systems of FMN-bp. Net electrostatic (ES) energies of Iso and Trp32, on which ET rates depend, were 0.0263 eV in WT, 0.322 eV in E13T, and 0.412 eV in E13Q. The calculated ET rates were in excellent agreement with the observed ones in all systems.

Highly Enhanced Cytotoxicity of a Dimeric Bispecific Diabody, the hEx3 Tetrabody
Ryutaro ASANO, Keiko IKOMA, Yukiko SONE, Hiroko KAWAGUCHI, Shintaro TAKI, Hiroki HAYASHI, Takeshi NAKANISHI, Mitsuo UMETSU, Yu KATAYOSE, Michiaki UNNO, Toshio KUDO, and Izumi KUMAGAI
J. Biol. Chem., 285, pp.20844–20849 (2010)
We previously reported the utility for cancer immunotherapy of a humanized bispecific diabody (hEx3) that targets epidermal growth factor receptor and CD3. Here, we used dynamic and static light scattering measurements to show that the multimer fraction observed in hEx3 in solution is a monodisperse tetramer. The multimerization into tetramers increased the inhibition of cancer cell growth by the hEx3 diabody. Furthermore, 1:2 stoichiometric binding for both antigens was observed in a thermodynamic analysis, indicating that the tetramer has bivalent binding activity for each target, and the structure may be in a circular configuration, as is the case for the single-chain Fv tetrabody. In addition to enhanced cytotoxicity, the functional affinity and stability of the hEx3 tetrabody were superior to those of the hEx3 diabody. The increase in molecular weight is also expected to improve the pharmacokinetics of the bispecific diabody, making the hEx3 tetrabody attractive as a therapeutic antibody fragment for cancer immunotherapy.

Enzymatic Sulphate-Esterification of Phenol Derivatives
M. AZUMA, T. NISHIMO, K. IGARASHI and H. OOSHIMA
Proc. of The 3rd SCEJ(Kansai branch)/SSCCI Joint international Conference on Chemical Engineering, 2009, Osaka Japan
Arylsulfotransferase (AST) and Arylsulfatase (Asl) are the enzymes that relate to the sulfation of phenol derivatives. By applying the enzyme reaction on the industrial process, the environ-mental burden on the production of sulfated compounds like a surfactant may be decreased. In this study, AST gene from Salmonella sp. and Asl gene from Comamonas sp. were expressed in E.*coli* JM109, and the characteristics of the obtained enzymes were investigated.

Drawning-out Crystallization of Organic Compounds Using A Continuous ML-Scale Crystallizer
K. IGARASHI, N. KUBO, Y. YAMANAKA and H. OOSHIMA
Proc. of The Fifth Joint China/Japan Chemical Engineering Symposium (CJCES), 2009, Xi'an, China
A mL-scale continuous crystallizer was newly developed to produce small and homogeneous crystals and used for drawing-out crystallization of organic compounds. The crystallizer was composed of a stainless-steel mixing vessel and a high-speed agitator. The working volume of the mixing vessel was 0.9 mL. The crystals obtained by the crystallizer were smaller and more uniform than that obtained by conventional beaker-scale semi-batch and continuous crystallizers. The results suggested that the short residence time was advantageous for the production of uniform and small crystals.

Solution-Structure Control in Cooling Crystallization for Production of Micro Crystals with a Narrow Size Distribution
Z. XING, A. MORIOKA, K. IGARASHI and H. OOSHIMA

Proc. of The Fifth Joint China/Japan Chemical Engineering Symposium (CJCES), 2009, Xi'an, China
The cooling batch crystallization of an organic compound, p-acetanisidide, was carried out using methanol as a solvent and no seed crystal. The crystallization needed the induction time varying from 10 to 200 min before nucleation and the size distribution of product crystals was broad from 10 to 270 μm in diameter of a circle of equal projection area. Therefore, a dissolution process was introduced to the cooling crystallization. Namely, the product crystals once precipitated in the crystallizer were completely dissolved by heating the slurry to a temperature 1.5°C-higher than the saturation temperature and then the solution was cooled down again. As a result, the induction time disappeared and small crystals with a mean diameter of 40 μm and a narrow size distribution were obtained.

Relationship between Crystal Polymorphism and Solution Structure of an Imidazopyridine Derivative Developed as a Drug Substance for Osteoporosis
M. HIRANO, K. IGARASHI, K. MACHIYA, R. TAMURA, H. TUE and H. OOSHIMA
Journal of Chemical Engineering of Japan, 42(3), pp.204-211 (2009)
An imidazopyridine derivative developed for osteoporosis treatment (a bone proton pump inhibitor, abbreviated BPPI) was crystallized in two kinds of alcohol. Two crystal polymorphs appeared: an unstable B01 form and a stable B02 form. The B01 form was obtained only from an ethanol solution and was never obtained from a methanol solution. The B02 form was obtained from a methanol solution. In order to understand these different behaviors in the appearance of polymorphs from alcohol, the intra- and inter-molecular interactions of BPPI molecules in solution were analyzed by NMR. As a result, the conformation of BPPI molecules and the structure of molecular aggregates in solution were found to resemble those of the polymorphic crystals that appeared in each alcohol. This result suggests that the control of the conformation of solute molecules is important at first to control the appearing polymorph.

Development of Molecular Machinery as Nonviral Vectors
Tomomi. JINTA and Takeshi. NAGASAKI
Bottom-Up Nanofablication, K. ARIGA, H. S. NALWA (Eds.), American Scientific Publishers, New York, Chapter 7 in Volume 6, pp.111-124 (2009)
The development of a safe and efficiency means of *in vivo* gene delivery has been required for successful gene therapy. In non-viral self-assembly vector systems, polyelectrolyte complexes of DNA with synthetic cationic polymers or lipids, should work as molecular machines in human body and show additional behaviors such as gene expression. These systems have been studied in recent years and progressed very much. However, significant problems limiting to the efficiency of gene expression by non-viral vectors still remain. One of major reasons of the low transfection activity is the presence of various barriers between the site of administration and gene expression of the target cells. These barriers are classified into two categories, the intravascular and intercellular barriers, and the barriers in the target cells. The factors which non-viral vectors are required to overcome the first barriers are (A) biophysical stability of the complexes composed of pDNA and carriers, (B) antigenicity, (C) toxicity of the vectors, (D) blood compatibility, and (E) non-specific uptake. However, even if these machinery having several functional factors works inside the target cells, they cannot lead high efficiency of the gene delivery by reason why a lot of the non-viral vectors often are degradable in blood circulation. The second barriers which the gene carriers must overcome contain (A) cellular uptake, (B) resistance to nuclease in the endosomes, (C) escape from the endosomal compartment prior to trafficking to lysosomes, (D) nuclear transport, and (E) release of pDNA in the nucleus for transcription. Especially for lipoplex, escape from the endosome is the important step and for polyplex release of pDNA in the nucleus is also significant. The non-viral vectors are required different biophysical and biological properties to high efficiency of gene delivery *in vivo* and *in vitro*. One of factors to overcome the intravascular and intracellular barriers is high stability of the DNA complexes. However, after cellular uptake, it's inconvenient. Then non-viral vectors need the following functionality: high stability of the complexes in the extracellular phase, disassembly of the vectors and pDNA release in the nucleus of the target cells. Therefore, non-viral vectors should work as molecular machinery. So far, many studies that integrate these inconsistent properties within a single vector are noticed. If biophysical and biological properties of the vectors can be changed by internal and external stimulation, the machinery which recognize changes in the environment and response actively to them by changing its properties and behaviors. This machinery will enable high efficiency of gene delivery. In this chapter, recent advances in active or controlled DNA release by using supramolecular nanomachinary possessing stimuli-responsive system, such as redox-, pH-, temperature, and photo-responsive delivery systems, are discussed.

Target-Selective Vesicle Fusion System with pH-Selectivity and Responsiveness
Ayumi KASHIWADA, Mana TSUBOI, Toshihisa MIZUNO, Takeshi NAGASAKI, and Kiyomi MATSUDA
Soft Matter, 5, pp.4719-4725 (2009)
The present paper reports on induction of target-selective liposomal vesicle fusion triggered by molecular recognition on a vesicle surface. Phosphatidylinositol (PI) having a sugar-like cyclic *cys*-diol structure was selected as a recognition target. Since diol sugars are abundant on cell surfaces, vesicle fusion systems based on the recognition of diol functionalities can be relevant for liposome-based drug delivery. Here, we design and synthesize a novel phenylboronic acid derivative with a tertiary amine group adjacent to the boron atom as a pilot molecule toward PI at a physiological condition. The pilot vesicle, or EggPC liposome containing this phenylboronic acid derivative causes selective membrane fusion toward a target liposomal vesicle containing sugar-like cyclic *cys*-diol structure at a physiological condition. From lipid mixing and inner-leaflet mixing assays, we demonstrate that the fusion event activated by inter-vesicular complex formation occurs rapidly. Furthermore, we also construct the target selective fusion system working only at the endosomal pH by the use of weakly acidic lipid, 1,2-dipalmitoyl-*sn*-glycero-3-succinate (DPGS) containing the pilot vesicle. The lipid mixing and inner-leaflet mixing assays make it clear that the vesicle fusion proceeds over pH range 5.0–5.5, whose range is upper than the pK_a of the boronic acid moiety on *cys*-diol complexation and lower than the pK_a of the carboxyl group of DPGS.

Cytochrome *c*-Binding "Proteo-Dendrimers" as New Types of Apoptosis Inhibitors Working in HeLa Cell Systems
Hideki AZUMA, Yuuka YOSHIDA, Dharam PAUL, Satoshi SHINODA, Hiroshi TSUKUBE, and Takeshi NAGASAKI
Org. Biomol. Chem., 7, pp.1700-1704 (2009)
The suppressive effects of synthetic dendrimers on mitochondrial apoptosis were first demonstrated in human epithelial carcinoma HeLa cells. The employed proteo-dendrimers included polyanionic hepta(glutamic acids), a fluorescent zinc porphyrinate core, hydrophilic polyether surface and nonpeptide hydrophobic dendrons, and electrostatically interacted with cytochrome *c* in aqueous solutions. The ceramide analogue, (2*S*,4*E*)-2-acetylamino-3-oxo-4-octadecen-1-ol (C2-ketoCer) induced mitochondrial apoptosis into HeLa cells and the cell viability was significantly recovered by pretreatment with some dendrimers. Among a series of proteo-dendrimers, the second-generation dendrimer 2a had the lowest cytotoxicity and the highest solubility. When the cells were treated with this dendrimer, a decrease in the protein levels of active caspase-3 and proteolytically cleaved PARP was remarkably observed. Since cytochrome *c* release from the mitochondria to the cytoplasm was unaffected in the presence of dendrimer 2a, the observed suppressive effects probably indicate that the proteo-dendrimer trapped cytochrome *c*, not only in the aqueous solutions but also in the living cells.

Self-Assembly and Cellular Uptake of Degradable and Water-Soluble Polyperoxides
Tamami FUJIOKA, Shuji TAKETANI, Takeshi NAGASAKI, and Akikazu MATSUMOTO
Bioconjugate Chem., 20, pp.1879-1887 (2009)
Water-soluble polyperoxides (PPs) as a new type of degradable and polymeric material were synthesized by the radical alternating copolymerization of sorbic derivatives containing a tetra(ethylene oxide) unit in the ester group using molecular oxygen. The obtained PPs showed a lower critical solution temperature (LCST)-type phase separation, and the transition temperature decreased according to the content of the hydrophobic ester group in the PPs. The PPs formed nanoaggregates with a diameter of 250-370 nm in water under the LCST. These PP aggregates were revealed to include 1-anilinonaphthalene-8-sulfonic acid as the fluorescence probe and epirubicin as the anticancer drug in their hydrophobic compartment. We evaluated the cytotoxicity and cellular uptake of the PPs in order to test their ability as a carrier used for the delivery of anticancer drugs. The cell viability in the presence of the PPs was comparable to those for the other biodegradable polymers, and epirubicin was taken up into the A549 efficiently with the PPs via an endocytosis mechanism.

Enhanced Internalization and Endosomal Escape of Dual-Functinalized Poly(ethylenimine)s Polyplex with Diphtheria toxin T and R Domains
Shinji KAKIMOTO, Toshizumi TANABE, Hideki AZUMA, and Takeshi NAGASAKI
Biomed. Pharmacother., 64, pp. 296-301 (2010)

A new multifunctional gene delivery system was constructed with diphtheria toxin's functional domains. Used functional domains are T domain for endosomal escape and R domain for efficient internalization into cell. In order to conjugate these domains into PEI polyplex, diphtheria toxin T and R domains-streptavidin fusion protein (DTRS) was prepared. The conjugation of the DTRS with biotinylated PEI polyplex (DTRS-polyplex) lead to the significant enhancement of transfection efficiency when compared with plain PEI/pDNA polyplex in CHO-K1 cell. It was demonstrated that DTRS-polyplex had high endosomal escape efficiency and internalization efficiency by several measurements, such as in vitro intracellular trafficking observation and the internalization inhibition with several inhibitors. These results suggest that this multifunctional non-viral vector may contribute to the future cancer gene therapy.

Membrane Disc and Sphere: Controllable Mesoscopic Structures for the Capture and Release of a Targeted Object
Tsutomu HAMADA, Ryoko SUGIMOTO, Mun'delanji C. Vestergaard, Takeshi NAGASAKI, and Masahiro TAKAGI
J. Am. Chem. Soc., 132, pp.10528-10532 (2010)
Design of molecules for self-assembled mesoscopic structures with specific functions is an important and interesting challenge that spans across disciplines such as nanosciences. A closed lipid membrane is a good example of a self-assembled mesostructure. In this study, we developed controllable membrane formation by making a subtle change at the molecular level. We utilized a synthetic photosensitive amphiphile (KAON12) to achieve the photobased molecular manipulation of the opening and closing of membranes through reversible transitions between sphere and disk structures. We found that the mechanism is based on the photoswitching of the membrane line tension, as deduced from the fluctuation of the membrane edge, through the action of KAON12. Furthermore, we demonstrated the controllable capture and release of colloidal particles into and from a membrane sphere. The observation of Brownian motion of the particle confirmed colloidal encapsulation. This successful photomanipulation of mesoscopic membrane structures in a noncontact and reversible manner should lead to a better understanding of the mechanism of membrane self-organization and may see wider application, such as in microreactors and drug-delivery systems.

Photochemical Control of Membrane Raft Organization
Tsutomu HAMADA, Ryoko SUGIMOTO, Takeshi NAGASAKI, and Masahiro TAKAGI
Soft Matter, in press.
Controllable membrane phase separation through the action of a synthetic photoresponsive amphiphile is reported. We studied multi-component giant vesicles formed from a ternary lipid mixture of saturated and unsaturated phospholipid and cholesterol together with the photoresponsive amphiphile. A change in the conformation of the photoresponsive amphiphile can switch membrane lateral segregation in a reversible manner. Cis-isomerization induces lateral phase separation in one-phase membranes or produces additional lateral domains in two-phase membranes. Membranes that are close to miscibility boundary show high photo-responsiveness. This is the first report on the reversible control of membrane lateral segregation triggered by a conformational change in a membrane-constituting molecule. These findings may lead to new methods for controlling membrane self-organization such as raft engineering.

Comparison of Glutathione Reductase Activity and the Intracellular Glutathione Reducing Effects of 13 Derivatives of 1'-Acetoxychavicol Acetate in Ehrlich Ascites Tumor Cells
Shenghui XU, Akiko KOJIMA-YUASA, Hideki AZUMA, David Opare KENNEDY, Yotaro KONISHI, and Isao MATSUI-YUASA
Chem. Biol. Interact., 185, pp.235-240 (2010)
In a previous study, we showed that (1'*S*)-acetoxychavicol acetate ((*S*)-ACA) caused a rapid decrease in glutathione (GSH) levels less than 15 min after exposure. (*S*)-ACA-induced cell death was reversed by the addition of N-acetylcysteine. In the current study, we investigated the inhibitory activities of 13 derivatives of (*S*)-ACA on tumor cell viability, intracellular GSH level and GR activity. Correlations were found among a decrease in cell viability, intracellular GSH levels and the activity of GR in Ehrlich ascites tumor cells treated with the various ACA analogues. A test of the 13 derivatives revealed that the structural factors regulating activity were as follows: (1) the para or 1'-position of acetoxyl group (or other acyl group) was essential, (2) the presence of a C2'-C3' double or triple bond was essential, and (3) the *S* configuration of the 1'-acetoxyl group was preferable.

Photoresponsive Polymeric Materials for Drug Delivery Systems : Double Targeting with Photoresponsive Polymers
Takeshi NAGASAKI
Drug Delivery System, 23, pp.637-643 (2008) (in Japanese)
Photoresponsive polymeric materials are promising not only for cell-targeting *in vivo*, but also for intracellular navigations such as the internalisation, the endosomal escape, and the nuclear import. Furthermore, the controlled release as well as the activation of drugs is caused by the photoresponsive delivery. Finally, such photoresponsive polymeric system can pave the way for double targeting of drugs resulting in temporal and spatial delivery. The photoresponsive synchronization of biocompatible materials and novel photo-irradiating apparatus might bring a various happiness to the refractory patients in near future.

The Significance and Attempt to Establish the Intracellular Targeting on Gene Delivery System
Shinji KAKIMOTO and Takeshi NAGASAKI
Polymers, 58, pp.133-136 (2009) (in Japanese)
The intracellular targeting of nucleic acid medicines is important to maximally obtain the beneficial effects. Each nucleic acid medicine can function by interaction with several intracellular molecules localized in certain organelle and region. Thereby, the nucleic acid has to efficiently deliver to the certain target sites. We described about the previous results and perspective on controlled intracellular trafficking of gene medicines.

Essential Delivery Technology for Development of Nucleic Acid Medicines
Shinji KAKIMOTO and Takeshi NAGASAKI
Development of Technologies and Seeds for Biological Medicine, S. Yamamoto (Eds.), CMC Books, Tokyo, Chapter 26, pp.252-263 (2009)

Novel Anti-Apoptotic Agents with New Mechanism
Takeshi NAGASAKI and Hideki Azuma
Chemistry (Kagaku), Vol. 64, No. 10, pp.70-71 (2009) (in Japanese)

Health-Care Application of b-1,3-Glucan, "Aqua b"
Toshio SUZUKI and Takeshi NAGASAKI
Function & Materials, Vol. 30, pp.54-62 (2010) (in Japanese)

Cell micropatterning on albumin-based substrate using an inkjet printing technique
Hironori YAMAZOE and Toshizumi TANABE
J. Biomed. Mater. Res., Part A, 91, pp.1202-1209 (2009)
Positioning of cells on a desired pattern on a substrate is an important technique for cell-based technologies, including the fundamental investigation of cell function, tissue engineering application, and the fabrication of cell-based biosensors and cell arrays. Recently, the inkjet printing technique was recognized as a promising approach to the creation of cellular pattern on substrates, and it has been achieved by the printing of living cells or cell adhesive protein. In this article, we created complex cellular patterns by using an albumin-based substrate and inkjet printing technique. Albumin was cross-linked using ethylene glycol diglycidyl ether. Subsequent casting of the cross-linked albumin solution onto glass plates prevented cells from adhering to their surfaces. Through screening various chemical reagents, we found that these cross-linked albumin surfaces dramatically changed into cell adhesive surfaces after immersion in cationic polymer solutions. Based on this finding, cell adhesive regions were prepared with a desired pattern by printing the polyethyleneimine (PEI) solution onto a cross-linked albumin substrate using modified commercial inkjet printer. Various cellular patterns including figure, letters, and gradient could be fabricated by seeding the mouse L929 fibroblast cells or mouse Neuro-2a neuroblastoma cells onto the PEI-patterned substrate. Compared with the printing of fragile living cells or proteins, printing of stable PEI circumvents clogging of printer head nozzles and enables reproducible printing. Therefore, the present method will allow the creation of complex cell patterns.

Drug carrying albumin film for blood-contacting biomaterials
Hironori YAMAZOE and Toshizumi TANABE
J. Biomater. Sci., 21, pp.647-657 (2010)

Surface-induced thrombosis is a major complication in the development of blood-contacting medical devices. Serum albumin has the ability to bind to a wide variety of compounds, including drugs, and neither cells nor proteins adsorb to an albumin-coated surface. These properties of albumin are useful for improving the blood compatibility of biomaterial surfaces. In the present study, we prepared a water-insoluble film by cross-linking pharmaceutical grade recombinant human serum albumin aiming to the clinical applications, and loaded the film with a synthetic antiplatelet drug, cilostazol. The resultant film possessed native albumin characteristics such as drug binding ability and resistance to cell adhesion. Mouse fibroblast L929 cells did not adhere on the albumin film, just as they did not adhere on native albumin-coated surfaces. Furthermore, when the albumin film carrying cilostazol was placed in PBS containing Tween-80, the release of cilostazol was sustained over 144 h. The results indicate that the surface coating with thus prepared albumin film can confer the biomaterials with antithrombogenic surface by virtue of its non-adhesiveness to cells and its release of cilostazol.

Enhanced internalization and endothermal escape of dual-functionalized poly(ethyleneimine)s polyplex with Diphtera Toxin T and R domains
.Shinji KAKIMOTO, Toshizumi TANABE, Hideki AZUMA, Takeshi NAGASAKI
Biomed. Pharmacother., 64, pp.296-301 (2010)
A new multifunctional gene delivery system was constructed with diphtheria toxin's functional domains. Used functional domains are T domain for endosomal escape and R domain for efficient internalization into cell. In order to conjugate these domains into PEI polyplex, diphtheria toxin T and R domains-streptavidin fusion protein (DTRS) was prepared. The conjugation of the DTRS with biotinylated PEI polyplex (DTRS-polyplex) lead to the significant enhancement of transfection efficiency when compared with plain PEI/pDNA polyplex in CHO-K1 cell. It was demonstrated that DTRS-polyplex had high endosomal escape efficiency and internalization efficiency by several measurements, such as in vitro intracellular trafficking observation and the internalization inhibition with several inhibitors. These results suggest that this multifunctional non-viral vector may contribute to the future cancer gene therapy.

Recombinant human albumin hydrogel as a novel drug delivery vehicle
Masaaki HIROSE, Akira TACHIBANA, Toshizumi TANABE
Mater. Sci. Eng. C, 30, pp. 664-669 (2010)
Serum albumin acts as a physiological carrier for various compounds including drugs. A hydrogel consisting of recombinant human serum albumin (rHSA) was prepared to take advantage of drug binding ability of albumin for a sustained drug release carrier. The hydrogel was prepared by mixing rHSA and dithiothreitol and casted to a polystyrene mold. Hydrogel formation was thought to occur through the intermolecular interaction of the hydrophobic groups by protein denaturation. The release of sodium benzoate and salicylic acid from the hydrogel completed in 2 h, while warfarin release continued for 24 h. The total amounts of the drugs released from 100 mg of 15 and 5% rHSA hydrogel were 2.3 and 1.4 μmol for warfarin, 1.4 and 1.1 μmol for salicylic acid and 0.9 and 0.9 μmol for sodium benzoate. These results reflected the order of the binding ability of drugs for intact albumin indicating that the drug binding ability of HSA still remained after the hydrogel formation. However, fibroblast cells attached and proliferated well on the hydrogel, indicating that denaturation of rHSA proceeded to the extent to allow the cell attachment. The present rHSA hydrogel might be suitable for a sustained release carrier of drugs having affinity for albumin.

Development of Cell Scaffold for Tissue Engineering
Toshizumi TANABE
Function & Materials, 30(6), pp. 49-57 (2010) (in Japanese)
Development of cell scaffolds is the essential technique for tissue engineering. Here, we describe the fabrication of wool keratin scaffolds. Keratin is cystein-rich protein and gives water-insoluble materials by air-oxidation during the molding process. Furthermore, abundant SH groups in keratin can be modified with various bio-active substances. It is possible that the cells inside the three-dimensional scaffolds are kept viable by introducing blood vessels into the cell scaffolds, which are modified with the proteins having vascularizing activity.

Glucose fuel battery powered by yeast - Analysis of the battery for high performance -
Masayuki AZUMA, Yuichi ITO, Kosuke TAKANO, Taro TACHIBANA, Shinji KOYAMA, Yogo TAKADA and Tomoyuki YAKISAKA

APBioChEC'09, Kobe (Japan), CD-ROM FM-P34, (2009)
A microbial fuel cell attracts attention as a system producing electric energy. Until now Wakisaka et al have researched on glucose fuel battery using baker's yeast. The fuel cell consists of anode and cathode parts separated by a cation specific membrane, and electrons are generated by glucose oxidation by yeast in the anode part. The electrons are transferred to the electrode (carbon cloth) from yeast cells by mediators. The constitution of the suitable battery has been examined using commercial baker's yeast.
Here *Saccharomyces cerevisiae* laboratory yeast (BY4741 strain) was used to construct the suitable yeast using genetic recombination technology for the battery in the future, and culture condition of yeast and the suitable battery condition (pH of the anode solution and yeast amount) were examined. As a result the output of the level same as the baker's yeast was obtained, and it was shown that a fall of the pH in the anode affected the output.
To clarify the detail of electron generation in yeast cell, the effect of respiratory inhibitors on the electron generation and time courses of glucose consumption and ethanol concentration in the battery were examined. Many electrons were produced at the time of ethanol production (early period of electron generation). Electrons were also produced in the time when ethanol production was not detected (last period of electron generation). These results suggest that electrons are produced in both processes of fermentation and respiratory of yeast.

Cell surface display of protein through Pir protein in Saccharomyces cerevisiae mutants which have decreased GPI proteins
Aki SAIJO, Hiroyuki MATSUOKA, Taro TACHIBANA, Masayuki AZUMA, Akihiko KONDO
The 3rd SCEJ/SSCCI Joint International Conference on Chemical Engineering, Osaka (Japan), p46 (2009)

Screening of gene involved in cell wall synthesis using *Saccharomyces* genome database and analysis of function of ECM3 protein
Hiroki ASAI, Taro TACHIBANA and Masayuki AZUMA
The 3rd SCEJ/SSCCI Joint International Conference on Chemical Engineering, Osaka (Japan), p47 (2009)

Cell wall proteins involved in yeast flocculation of brewer's yeast
Tomohiro ASAYAMA, Taro TACHIBANA, Masayuki AZUMA, Toshinori SHIMANOUCHI, Hiroshi UMAKOSHI and Ryoichi KUBOI
The 3rd SCEJ/SSCCI Joint International Conference on Chemical Engineering, Osaka (Japan), p48 (2009)

Construction of yeast which activates macrophage and its application
Yuki TAKADA, Taro TACHIBANA, Masayuki AZUMA, Yumiko SAKAI, Chinatsu ITO, Ken KANZAKI and Hajime WATANABE
The 3rd SCEJ/SSCCI Joint International Conference on Chemical Engineering, Osaka (Japan), p50 (2009)

Live imaging system for visualizing nuclear pore complex (NPC) formation during interphase in mammalian cells.
H. IINO, K. MAESHIMA, R. Nakatomi, S. KOSE, T. HASHIKAWA, T. TACHIBANA, N. IMAMOTO
Genes Cells. 15, pp.647-660. (2010)
Nuclear pore complexes (NPCs) are 'supramolecular complexes' on the nuclear envelope assembled from multiple copies of approximately 30 different proteins called nucleoporins (Nups) that provide aqueous channels for nucleocytoplasmic transport during interphase. Although the structural aspects of NPCs have been characterized in detail, NPC formation and its regulation, especially during interphase, are poorly understood. In this study, using the temperature-sensitive RCC1 mutant tsBN2, a baby hamster kidney 21 cell line, we found that a lack of RCC1 activity inhibited NPC formation during interphase, suggesting that RanGTP is required for NPC formation during interphase in mammalian cells. Utilizing the reversible RCC1 activity in tsBN2 cells, we established a live-cell system that allows for the inhibition or initiation of NPC formation by changes in temperature. Our system enables the examination of NPC formation during interphase in living cells. As a lack of RCC1 decreased some Nups containing unstructured phenylalanine-glycine repeats in the NPC structure, we propose that RCC1 is also involved in maintaining NPC integrity during interphase in mammalian cells.

The mobile FG nucleoporin Nup98 is a cofactor for Crm1-dependent protein export.

M. OKA, M. ASALLY, Y. YASUDA, Y. OGAWA, T. TACHIBANA and Y. YONEDA
Mol. Biol. Cell, 21, pp.1885-1896 (2010)
Nup98 is a mobile nucleoporin that forms distinct dots in the nucleus, and, although a role for Nup98 in nuclear transport has been suggested, its precise function remains unclear. Here, we show that Nup98 plays an important role in Crm1-mediated nuclear protein export. Nuclear, but not cytoplasmic, dots of EGFP-tagged Nup98 disappeared rapidly after cell treatment with leptomycin B, a specific inhibitor of the nuclear export receptor, Crm1. Mutational analysis demonstrated that Nup98 physically and functionally interacts with Crm1 in a RanGTP-dependent manner through its N-terminal phenylalanine-glycine (FG) repeat region. Moreover, the activity of the Nup98-Crm1 complex was modulated by RanBP3, a known cofactor for Crm1-mediated nuclear export. Finally, cytoplasmic microinjection of anti-Nup98 inhibited the Crm1-dependent nuclear export of proteins, concomitant with the accumulation of anti-Nup98 in the nucleus. These results clearly demonstrate that Nup98 functions as a novel shuttling cofactor for Crm1-mediated nuclear export in conjunction with RanBP3.

Cytokeratin 8/18 as a new marker of mouse liver preneoplastic lesions.
A. KAKEHASHI, A. KATO, M. INOUE, N. ISHII, E. OKAZAKI, M. WEI, T. TACHIBANA
and H. WANIBUCHI
Toxicol. Appl. Pharmacol. 242, pp.47-55 (2010)
To search for a reliable biomarker of preneoplastic lesions arising early in mouse hepatocarcinogenesis the proteomes of microdissected basophilic foci, hepatocellular adenomas (HCAs), carcinomas (HCCs) and normal-appearing liver of B6C3F1 mice initiated with diethylnitrosamine (DEN) were analysed on anionic (Q10) surface-enhanced laser desorption/ionization time-of-flight mass spectrometry (SELDI-TOF-MS) ProteinChip arrays. Significant overexpression of cytokeratin 8 (CK8; m/z 54, 565), cytokeratin 18 (CK18; m/z 47,538) proteins was found in basophilic foci as well as in HCAs and HCCs. Furthermore, immunohistochemistry demonstrated profound overexpression of CK8 and CK18 proteins (CK8/18) in all basophilic foci, mixed cell type foci, HCAs and HCCs in B6C3F1 and C57BL/6J mice initiated with DEN. A strong correlation between CK8/18-positive foci development and multiplicity of liver tumors in B6C3F1 and C57Bl/6J mice was further observed. Moreover, formation of CK8 and CK18 complexes due to CK8 phosphorylation at Ser73 and Ser431 was found to be strongly associated with neoplastic transformation of mice liver basophilic foci. Elevation of CK8/18 was strongly correlated with induction of cell proliferation in basophilic foci and tumors. In conclusion, our data imply that CK8/18 is a novel reliable marker of preneoplastic lesions arising during mouse hepatocarcinogenesis which might be used for prediction of tumor development and evaluation of environmental agents as well as drugs and food additives using mouse liver tests.

Molecular characterization and expression of the low-density lipoprotein receptor-related protein-10, a new member of the LDLR gene family.
Y-H. JEONG, K. ISHIKAWA, Y. SOMEYA, A. HOSODA, T. YOSHIMI, C.YOKOYAMA,
S. KIRYU-SEO, M-J. KANG, T. TACHIBANA, H. KIYAMA, T. FUKUMURA, D-H. KIM and S.SAEKI
Biochem. Biophys. Res. Commun., 391, pp.1110-1115 (2010)
We report the characterization of a new member of the low-density lipoprotein receptor (LDLR) gene family designated LRP10. Human LRP10 cDNA encodes a 1905 amino acid type I membrane protein consisting of five functional domains characteristic of the LDLR gene family. CHO-ldlA7 cells transfected with human LRP10 cDNA bound LDLR-associated protein, but not beta-VLDL and HDL. Human LRP10 transcripts were primarily found in the brain, muscle and heart. In situ hybridization of the rat brain showed that the transcripts were intensely present in the cerebral cortex, hippocampus, choroid plexus, ependyma and granular layer. In the developing rat brain, transcript levels gradually increased from postnatal day 1 to 20. Immunofluorescence analysis indicated that LRP10 was observed in the ventricular zone of the embryonic day 14.5 mouse cerebral cortex. The present studies suggest that LRP10 may play a significant role in the brain physiology other than lipoprotein metabolism.

Production of a Rat Monoclonal Antibody Specific for Dhx9/NDHII/RHA.
M. KOTANI, A. HARADA, J. ODAWARA, M. AZUMA, S. OKADA, Y. NISHIYAMA, M. NAKAMURA,
T. TACHIBANA and Y. OHKAWA
Hybridoma, 29, pp. 259-261 (2010)

Dhx9/NDHII/RHA is a member of the DEAH family of proteins, which possess a double-stranded RNA-binding domain (dsRBD) and a helicase domain. The DEAH protein family plays a critical role in RNA metabolism. DEAH family members function as ATP-dependent RNA helicases and regulation of transcription. In the present study, we report the establishment of a monoclonal antibody specific for Dhx9 using the rat medial iliac lymph node method. Immunoblot analysis using our antibody against Dhx9 detected full-length Dhx9. In addition, immunocytochemical staining using our antibody against Dhx9 revealed the nuclear localization of Dhx9. This monoclonal antibody against Dhx9 will allow for further detailed studies of Dhx9 expression.

Generation of a Rat Monoclonal Antibody Specific for MyoD.
A. HARADA, Y. OHKAWA, S. AO, J. ODAWARA, S. OKADA, M. AZUMA, Y. NISHIYAMA, M. NAKAMURA and T. TACHIBANA
Hybridoma, 29, pp.255-258 (2010)
Myogenic determination 1 (MyoD) is a myogenic regulatory factor (MRF) possessing a basic domain and a helix-loop-helix domain. MRFs play a critical role in myoblast fate and terminal differentiation. MyoD is a transcriptional factor that induces transcription by binding with gene regulatory factors expressed in skeletal muscle. As a master gene, MyoD also determines skeletal muscle differentiation. In this study, we established a monoclonal antibody specific for MyoD using the rat medial iliac lymph node method. Immunoblot analysis revealed that our monoclonal antibody against MyoD could identify full-length MyoD. Moreover, immunocytochemical staining revealed a change in the expression of MyoD at the skeletal muscle differentiation stage. This monoclonal antibody against MyoD allows for further studies to elucidate the mechanism by which MyoD influences skeletal muscle differentiation.

Rat monoclonal antibody specific for the chromatin remodeling factor CHD1.
S. YOSHIMURA, A. HARADA, J. ODAWARA, M. AZUMA, S. OKADA, M. NAKAMURA, Y. OHKAWA and T. TACHIBANA.
Hybridoma, 29, pp.237-240 (2010)
CHD1 is a subfamily member of the CHD family, which possesses a chromodomain, a helicase domain, and a DNA-binding domain. The CHD family regulates gene expression by contributing to ATP-dependent chromatin remodeling. CHD1 exists in the transcriptionally active region and alters the chromatin structure. Little is known about the function of endogenous CHD1, however, and studies have been hindered by the lack of an antibody specific for CHD1 in mammals. In the present study, we established a monoclonal antibody specifically against CHD1 using the rat medial iliac lymph node method. Immunoblot analysis using our monoclonal antibody showed specific binding to CHD1, allowing us to identify the deduced full-length CHD1. In addition, cell immunostaining clearly revealed the nuclear localization of CHD1. This monoclonal antibody will be useful for further analysis of CHD1 function in mammals.

Generation of a Rat Monoclonal Antibody Specific for CHD2.
A.HARADA, S.YOSHIMURA, J. ODAWARA, M. AZUMA, S. OKADA, M. NAKAMURA, T. TACHIBANA and Y. OHKAWA
Hybridoma, 29, pp.173-177 (2010)
CHD2 is a member of the CHD family that contains chromodomain, helicase domain as well as DNA-binding domain. The CHD family is involved in gene expression and transcription by ATP-dependent chromatin remodeling. Analysis of mutant mouse revealed that CHD2 is involved in development as well as hematopoiesis, which suggests the involvement of CHD2 in gene expression. However, CHD2 has not yet been analyzed biochemically as there is no specific antibody against it. Here, we report on the establishment of specific monoclonal antibody (MAb) against CHD2 utilizing a rat medial iliac lymph node method. Through cell immunostaining utilizing established MAb to CHD2, we confirmed that CHD2 was localized in euchromatin. Additionally, IP-Western revealed that the expression level of full-length CHD2 did not change during the differentiation stage. Additionally, a specific signal was confirmed around 95 kDa at the undifferentiated stage. This clearly indicated that CHD2 was involved in specific gene expression at this stage. Thus, this antibody can contribute to elucidating the function of CHD2 in cell expression.

Rat Monoclonal Antibody Specific for Septin 9.
T. TACHIBANA, E. OKAZAKI, T. YOSHIMI, M. AZUMA, A. KAKEHASHI and H. WANIBUCHI
Hybridoma, 29, pp.169-171 (2010)

The septin family of GTPase proteins has been shown to be important for cell division, cytoskeletal organization, and membrane-remodeling events. Septin 9 (SEPT9) is a member of the septin family (also designated MSF/eseptin/Sint1) and has been implicated in tumorigenesis. The present study reports on the preparation and properties of a monoclonal antibody (MAb) directed against SEPT9. The antibody was produced by hybridization of mouse myeloma cells with lymph node cells from an immunized rat. The MAb 7B5 specifically recognized SEPT9, as evidenced by immunoblotting using a variety of extracts from cultured cells. In immunostaining using MAb 7B5, a filamentous pattern near the plasma membrane was observed. The MAb 7B5 promises to be useful in immunoblotting and immunostaining experiments in various cells and tissues to determine the expression levels of SEPT9, as well as to further the analysis of the biological function of this protein.

A Rat Monoclonal Antibody against the Chromatin Remodeling Factor, CHD5.
S.YOSHIMURA, T. YOSHIMI, Y. OHKAWA, M. AZUMA and T. TACHIBANA
Hybridoma, 29, pp.63-66 (2010)
CHD5 (chromodomain/helicase/DNA-binding protein 5) is a member of the CHD subfamily of chromatin remodeling Swi/Snf proteins, and has been recently identified as a tumor suppressor in a diverse range of human cancers. We report here on the establishment of a hybridoma cell line for producing a monoclonal antibody against CHD5 by the rat medial iliac lymph node method. Immunoblotting analyses indicated that this antibody, MAb 5A10, specifically recognizes endogenous CHD5. In immunostaining using the antibody, a nuclear staining pattern was observed. The monoclonal antibody will be useful in immunoblotting and immunolocalization experiments in a variety of cells and tissues, as well as in further studies of the biological function and cellular dynamics of this protein.

Production and Characterization of Monoclonal Antibodies to Mouse Germ Cells.
C.YOKOYAMA, Y. KATOH-FUKUI, K. MOROHASHI, D. KONNO, M. AZUMA and T. TACHIBANA
Hybridoma, 29, pp.53-37 (2010)
In mammals, primordial germ cells (PGCs) are generated in the extra-embryonic epiblast, and thereafter migrate into the developing gonads. Following the development of the gonads to the testes or ovaries, germ cells mature into sperms or eggs. In the present study, we report production and characterization of monoclonal antibodies (MAb) that recognize PGCs. Extracts from E12.5 mouse embryonic gonads were immunized as an antigen, and hybridomas were generated using the rat medial iliac lymph node method. The hybridoma supernatants were screened by immunohistochemical analyses of E12.5 mouse embryonic sections. The antibody, referred to herein as MAb 5B5, provided strong signals on PGCs. Moreover, immunofluorescence analyses using a variety of the tissue sections of mouse embryos revealed that MAb 5B5 also recognizes the ventricular zone of the cerebral cortex and the neural canal in the spinal cord in which neural specific stem cells are present in abundance. Based on these findings, MAb 5B5 might recognize stem cell-associated antigens.

Production of a Rat Monoclonal Antibody against BRG1.
Y. OHKAWA, A. HARADA, M. NAKAMURA, S. YOSHIMURA and T. TACHIBANA
Hybridoma, 28, pp. 463-466 (2009)
Brm-related gene-1 (Brg1) is a catalytic subunit of the SWI/SNF chromatin remodeling enzyme complex that has ATPase activity. This complex facilitates chromatin remodeling for gene expression by utilizing energy for ATP hydrolysis. It is well known that the SWI/SNF chromatin remodeling enzyme complex is essential for cell differentiation, cell cycle regulation, and embryogenesis. Here we report the establishment of a hybridoma cell line for producing an antibody against Brg1 subunit by the rat medial iliac lymph node method. Immunoblot analysis showed that our antibody can specifically recognize Brg1. It was revealed by immunocytochemistry that Brg1 is located in euchromatin of C2C12 myoblast nuclei. These data suggested this antibody is useful for analyzing molecular function of Brg1 protein in cells.

Gene expression dissection of the circadian neuronal circuit of Drosophila identifies novel circadian genes.
E. NAGOSHI, K. SUGINO, E. KULA, E. OKAZAKI, T. TACHIBANA and S. ET AL., Nelson
Nature Neuroscience, 13, pp.60-68 (2009)
Behavioral circadian rhythms are controlled by a neuronal circuit consisting of diverse neuronal subgroups. To understand the molecular mechanisms underlying the roles of neuronal subgroups within the Drosophila

circadian circuit, we used cell-type specific gene-expression profiling and identified a large number of genes specifically expressed in all clock neurons or in two important subgroups. Moreover, we identified and characterized two circadian genes, which are expressed specifically in subsets of clock cells and affect different aspects of rhythms. The transcription factor Fer2 is expressed in ventral lateral neurons; it is required for the specification of lateral neurons and therefore their ability to drive locomotor rhythms. The Drosophila melanogaster homolog of the vertebrate circadian gene nocturnin is expressed in a subset of dorsal neurons and mediates the circadian light response. The approach should also enable the molecular dissection of many different Drosophila neuronal circuits.

Urban Engineering

Architecture and Building Engineering

Effect of Member Layout on Elastic Buckling Behavior for Square-and-Diagonal Double-Layer Lattice Domes

Chongbing YAN, Yoshiya TANIGUCHI, Susumu YOSHINAKA

Proc. of the International Association for Shell and Spatial Structures, IASS 2009 Valencia, Llibre CD, pp.1941-1950 (2009)

Double-layer lattice structures composed of the square pattern and the diagonal pattern in top and bottom layers have the member layouts of 4 types as the arrangement of the mesh patterns as shown in figure 1. To design these lattice structures, the relationship between the member layout and the edge of plan must be decided. The mesh patterns in top and bottom layers of “large-square-on-small-diagonal” and “small-diagonal-on-large-square” have been already studied. However, the “large-diagonal-on-small-square” and “small square-on-large-diagonal” of the double-layer lattice structures have not been sufficiently studied yet. Therefore, in this paper 4 types of the mesh patterns composed of the square pattern and the diagonal pattern are discussed. The effect of member layout on the buckling behavior and stress states is investigated for double layer lattice domes. The other numerical parameter is the loading conditions. In addition, the usefulness of the method to estimate the effective strength by the segment consisting of 3 × 3 structural units is discussed.

Experimental Study on Tensile Properties and Presumption Index of Madake (P. Reticulata C. Koch) for Crafts

Fuminori KIMURA, Yoshiya TANIGUCHI

Journal of Structural and Construction Engineering (Transactions of AIJ), Vol.75, No.650, pp.839-848 (2010)

We have developed the new earthquake resisting wall which made KAGOME-knits of the bamboo material. This study proposes the tensile properties of the bamboo material for crafts used as the material. Full-size tensile tests were conducted in order to examine the tensile character of 162 tensile specimen. And the correlation of thickness(t) of a node and a internode, and tensile properties was mainly examined. Main findings are given in the below. First, very strong linear relationships are observed between breaking strain and failure modes. And the difference of the thickness of right and left of a node had influenced the failure modes. Second, strong linear relationships are observed between tensile properties and t. Therefore, the stress grading based on t was examined as a next phase. As a result, it was found that it was effective. From these results in the above, the bamboo material, of which quality is controlled by the present method, is available as structural bamboo, since stiffness, strength, and maximum load are guaranteed.

Bending Elasticity Properties of Medium Size Logs of 80-Years-Old Sugi (Cryptomeria japonica) Grown in Wakayama Prefecture

Fuminori KIMURA, Yoshiya TANIGUCHI

Mokuzai Gakkaishi, (Journal of the Japan Wood Research Society), Vol.56, No.1, pp.17-24 (2010)

The purpose of this study is to promote the utilization as a structural lumber of the medium size log of 80-years-old sugi (Cryptomeria japonica D.Don). We measured the dynamic Young's modulus by longitudinal vibration(E_{fr}) of 35 logs of the medium size log of 80-years-old sugi grown in Wakayama Prefecture. Then, we measured the dynamic Young's modulus by longitudinal vibration(Ed), and the static Young's modulus in bending measured by the dead weight method(MOE) of 275 rectangular-cut lumber (standard size:45x90mm) sawed from them. And the correlation of E_{fr}, Ed, and MOE has been tested relying on statistical tools. Main results are as follows. First, the correlation between Ed and MOE is statistically significant. Second, the classification for every lot was effective, since MOE for every lot is differed according to the lot type with a statistically significant level, and the correlation between Ed and MOE is statistically significant for every lot. Third, a strong correlation between E_{fr} and MOE has been observed. Therefore, the machine stress grading based on E_{fr} was tested as a next phase. As a result, we found it was effective. This method is effective in the case where a variety of lots exist in one area for the classification, since the quality of logs has variation for every lot.

Vibration Control of Transient Response for Spatial Structures by Using Tuned Mass Dampers with Initial Displacement－Fundamental Investigation about Design Formulas with Initial Displacement－

Susumu YOSHINAKA and Yoshiya TANIGUCHI

Journal of Structural and Construction Engineering (Transactions of AIJ), AIJ, No. 653, pp. 1299-1308 (2010) (in Japanese)
In this paper, we propose tuned mass dampers with initial displacement to control transient response for spatial structures. The initial displacement of the TMD changes the phase of a beat envelope curve resulted from two vibration modes with closely spaced natural frequencies. We propose design formulas of tuned mass dampers with initial displacement and studied analytically the effect of vibration control on an impulse force and an impulsive earthquake force. As a consequence, we could recognize that the proposed system improve especially the control performance of the initial response. Lastly, to confirm the applicability of the proposed design formulas for controlling real structures, we studied analytically the effect of vibration control of the proposed method in this paper by using a single layer lattice shell model.

Possible impact on temperature by differences in urban district configurations
Noriko UMEMIYA, Yuta SAKURAI, Masafumi KAWAMOTO and Ryoji OKURA
Proceedings of the 11th International Building Performance and Simulation Association Conference, Building Simulation 2009, pp.1767-1772(2009)
We simulated differences in a town's configuration between Meiji era year 44 (1988) and 2007 and its effect on the thermal component used for setting the surface temperature.(1) We selected and modeled the Senba area in Osaka city in 1917 as the objective town. (2) We measured the surface temperature of the wooden and soil walls during daytime because, in those days, the building materials differed from those used now. (3) We input surface temperatures, air temperature, air speed, and wind direction in this model. We applied to boundary conditions for stress of the free-slip conditions in and near the analysis region. We applied boundary conditions of thermal movement using the specified surface temperature conditions on the wall, ground, and water. (4) We compared results obtained using the simulations with various inputs of surface temperatures and searched for a relation with the town's configuration and the component of air temperature.

Evaluation and optimization of air-conditioner energy saving control considering indoor thermal comfort
Fulin WANG (Tsinghua Univ.), Harunori YOSHIDA (Okayama Univ. of Science), Bo LI (Kyoto Univ.), Noriko UMEMIYA, Satoshi HASHIMOTO (Daikin Industries Ltd.), Takaaki MATSUDA (Daikin Industries Ltd.) and Hideo SHINBAYASHI (Daikin Industries Ltd.)
Proceedings of the 11th International Building Performance and Simulation Association Conference, Building Simulation 2009, pp.88-95 (2009)
For the purpose of reducing the room air-conditioners' energy consumption, an energy saving control method is proposed formerly. In this paper its energy saving effect is confirmed through experiments conducted in six office rooms in actual use. The experiment results show that the air-conditioners controlled by the present energy saving control logic and parameter settings can save electric power up to 3.0% compared to ordinary control. Further, if the energy saving control parameters of room temperature set points are fixed at 27oC for cooling operation in summer and at 23oC for heating operation in winter, in average 18.7% and 23.8% electric power can be saved. At the same time, in order to check whether the indoor air temperature of 27oC in summer and 23oC in winter will cause uncomfortable complaints or not, questionnaires on indoor thermal comfort and sensation are conducted. The results show that these indoor temperatures are acceptable for the occupants. Finally a room model and the air-conditioner control model are developed to simulate the performance of one-minute interval room air temperature, which is used to determine on/off status of air-conditioners for the purpose of calculating electric power consumptions. The models finally are used to find out the optimal control parameter settings. The results show that the operation at optimal control set points can save 28.9% energy compared to the ordinary operation.

Effects of humidity on the relation between temperature and thermal control use during summer-autumn
Noriko UMEMIYA, Koichi TANIGUCHI, Xiaoyong LIN and Ryoji OKURA
Proceedings of the 9th International Conference and Exhibition Healthy Buildings 2009, P2-15D, pp.1-4 (2009)
Indoor and outdoor temperature and humidity, air conditioner use, status of window opening, and occupation were measured for 10 concrete apartments constructed according to the same simple plan in Osaka during summer–autumn. Only one air conditioner was installed for 1–2 occupants for each apartment. Temperatures were classified by 1–2°C; relative humidity was classified by 5–10% and the humidity ratio by 1–2 g in each bin of temperature. The mean ratio of control use was calculated for each bin of humidity only when the apartment was occupied. The relations were analyzed for three seasons divided according to the daily mean ratio of air-conditioner use. Results show that humidity is sometimes dominant in the choice of thermal control use. Sometimes, both temperature and humidity are unrelated to the choice. For the same temperature, the ratio of air-conditioner use is high and the ratio of opening is low when humidity is high.

Moving observation of waterway cooling effects in Osaka

Noriko UMEMIYA, Masafumi KAWAMOTO, Yuta SAKURAI, Koichi TANIGUCHI, Yumi MURANISHI and Ryoji OKURA

Proceedings of the 7th International Conference on Urban Climate, B18-1, pp.1-3 (2009)

The distributions of thermal environments for three streets across the East Yokobori River in central Osaka were measured during daytime in summer using moving observations. The magnitude and extent of the cooling effect of the river on urban warming were investigated. Temperatures were lower at divisions with the river. With higher west winds, the cooling effects moved east. The air velocity was lowest at divisions with the river. Results showed that the cooling effects of high-rise buildings were not negligible. They were sometimes superior to those of the river.

Numerical Study on Effect of Member Length Error on Structural Properties of Single Layer Pin-Jointed Grid Dome Composed of Wooden Truss System

M. FUJIMOTO, S. KATAYAMA(Takenaka Corporation), T. KANAME(Taisei Corporation),
K. IMAI(Osaka University) and T. MACHINAGA(Takenaka Corporation)

Proceedings of IASS Symposium 2009, Valencia, Sept. 28- Oct. 2, pp. 444-455 (2009)

This study examines a single layer three-way pin-jointed grid dome constructed from of wooden truss system. We show the effect of the member length error on the initial imperfection and nodal buckling behavior by the numerical analysis results considering geometrical nonlinearity. In numerical calculation, the member length errors are assumed to be a normal distribution. The distribution and magnitude of the initial axial force and displacement are evaluated with respect to the mean and SD (standard deviation) of the member length errors. The range of the initial imperfection and the tolerance of manufactured member length are also predicted by the mean and SD of the numerical results. The properties of nodal buckling load and buckling mode are also discussed. The nodal buckling load is mainly affected by the SD of member length error and the effect of mean of member length error on the buckling is secondary. When SD of member length error changes from zero to 0.10 cm, the mean of the nodal buckling load decreases by about 50 % and the area of nodal buckling mode changes from the overall dome to the inner region.

Civil Engineering

Statistical Seismic Risk Analysis of the Highway Bridges
Xi OH and Hajime OHUCHI
Memoirs of the Faculty of Engineering, *Osaka City University*, Vol.50, pp.9-16 (2009)
Lifecycle seismic risk of existing highway bridge piers which were retrofitted after the Hanshin Earthquake, have been estimated by probability analysis. Hazard and fragility curves for the seismic risk analysis and also a category of damage rank and recovery cost are explained practically, those are essentially required for the estimation. The obtained results and also some issues to be solved for the near future are described consequently.

A Life Cycle Assessment of the Existing Highway Bridge
Soichi SANO, Hajime OHUCHI, Hiroaki KITOH and Hisao TSUNOKAKE
Memoirs of the Faculty of Engineering, *Osaka City University*, Vol.50, pp.17-28 (2009)
Life cycle assessment has been carried out for the existing highway bridge in urban area. Environmental impacts from material production, construction, operation, dismantlement, abandonment and recycling stages, are analyzed by cost evaluation technique. Focusing points are a comparison of the amounts of the influence between stages and a comparison of the influences between environmental aspect and also between environmental elements especially from construction related aspect.

Flexural and Shear Failure Tests of Reinforced Concrete Beams with Low Grade Recycled Aggregate
Takuya IKEGAWA, Hisashi SAITO, Hajime OHUCHI, Hiroaki KITOH and Hisao TSUNOKAKE
Memoirs of the Faculty of Engineering, *Osaka City University*, Vol.50, pp.29-36 (2009)
Under ecological and natural resource shortage aspects, structural behavior of the reinforced concrete beams using low grade recycled aggregate has been investigated through six static load test specimens with various moisture conditions and mix proportions of aggregate. Using the recycle aggregate instead of normal aggregate, no obvious degradation was observed in flexural strength, while 30% reduction in shear strength.

Numerical Study on Compressive Concrete as a Strain Softening Material
Wataru KURAMOTO*, Hiroaki KITOH** and Hajime OHUCHI
Memoirs of the Faculty of Engineering, *Osaka City University*, Vol.50, pp.37-44 (2009)
The prediction of post peak behavior of compressive concrete is significant especially for ductility based on seismic design of reinforced concrete members. The present paper describes numerical modeling of post peak behavior of compressive concrete as a strain softening material with constitutive law based on incremental elasto plastic theory formulated in a strain space. A series of numerical parametric studies have been conducted for the existing experimental results of compressive concrete including useful post peak behavior test.

A Horizontal Loading Test of Viaduct Structure Model Retrofitted by Arc Shaped Damper
Kohei OHGI*, Yuki NAKATA**, Hajime OHUCHI*** and Hisao TSUNOKAKE
Memoirs of the Faculty of Engineering, *Osaka City University*, Vol.50, pp.45-54 (2009)
When considering social function of railway viaduct as infrastructure, less damage is expected even against significant earthquake such as the future Tokai and the Tonankai Earthquake. Response control technique with damping device can be one of alternative solutions. In responding, authors have developed the arc shaped damper retrofit technique. In order to investigate applicability of the proposed damper to rail way viaduct structures, horizontal loading test for verification were conducted focusing on strengthening and response control effect. Following results were obtained: the existing structure model provided post yielding shear failure, while retrofitted structure model assured flexural yielding ductile behavior with high energy absorption.

Arc Shaped Damper Retrofit Technique for Exisiting Rail Way Viaduct Structures
Hajime OHUCHI, Yuki NAKATA, Kohei OHGI, Hisao TSUNOKAKE
ATC&SEI Conference on Improving the SeismicPerformance of Existing Buildings and Other Structures, pp. 979-987 (2009)
When considering social function of railway viaduct as infrastructure, less damage control is demanded even against significant earthquake. Response control technique with damping device is highly expected as alternative solution. In responding, authors have developed Arc Shaped Dampers. In order to investigate applicability of the proposed damper to moment frame type rail way viaduct structures, seismic retrofit design, nonlinear analysis and experimental loading tests have been conducted to verify present technique. Following results were obtained: the

existing structure is failed in post yielding shear, while retrofitted structure assures flexural yielding ductile behavior with higher damping effect.

Shear Strengthening of Piled Pier Beam by DFRCC Winding
Tetsuya OGASAWA, Chunri JIN, Hisao TSUNOKAKE and Hajime OHUCHI
Proceedings of the Japan Concrete Institute, *JCI*, Vol.32, pp.1381-1386, (CD-ROM) (in Japanese)

Flexural Loading Tests of RC-DFRCC Composite Members corroded with Chloride Ions
Hisao TSUNOKAKE, Tetsuya OGASAWARA, Hajime OHUCHI and Hiroaki KITOH
Proceedings of the Japan Concrete Institute, *JCI*, Vol.32, pp.1387-1392, (CD-ROM) (in Japanese)

Durability and Mechanical Characteristics of DFRCC Winded Recycled Aggregate RC Member under Cyclic
Hisashi SAITO, Takuya IKEGAWA, Hajime OHUCHI and Hisao TSUNOKAKE
Proceedings of the Japan Concrete Institute, *JCI*, Vol.32, pp.1457-1462, (CD-ROM) (in Japanese)

A Study on Life Cycle Assessment of the Existing Highway Bridge in Urban Area
Soichi SANO, Hajime OHUCHI, Hiroaki KITOH and Hisao TSUNOKAKE
Proceedings of the Japan Concrete Institute, *JCI*, Vol.32, pp.1793-1798, (CD-ROM) (in Japanese)

Basic Analysis of the Travel Behavior and Self-Consciousness of aged People for Safety Education System

Yusuke KOTAKE, Yasuo HINO and Nagahiro YOSHIDA
Osaka City University, Memoirs of the Faculty of Engineering, Vol. 50, pp. 63-70(2009)
Recently, the aging has rapidly progressed in Japan, as a result, the half of traffic deaths were the aged people, 2007. In addition, the number of accidents in walking amounts to the half and more. Therefore, it should be important to consider the effective education system based on the features of travel behavior and consciousness for road safety of aged people.
In this study, the some characteristic findings for travel behavior and consciousness of aged people were obtained by the questionnaire survey and the actual condition of lecture courses for road safety were reviewed in Hyogo Prefecture. As a result, for the present, it must be concluded that the lecture course should be useful to prevent the accidents involved the aged people, and for the near future it may be necessary to increase not only the chances of lectures but also the number of staffs.

Mobile Phone Based Town Guide System for Arbitrary Tour
Yuki OKUHATA, Takashi UCHIDA
Memoirs of the Faculty of engineering, Osaka City University, Vol.50, pp.71-78 (2009)
Recently, a lot of systems to provide some information regarding local sightseeing through sound or WEB pages have been introduced. However, these systems have some demerits such like burden of preparations and lack of the sense of reality. Sound and picture can deliver more information than text-base information and also give reality. In addition, most people now have mobile phones and they could use them to get more information easily. Supposing that the performance of mobile phones improve possibility to install new system, mobile phone-based sightseeing information system which can resolve demerits mentioned above. This study proposes a system easy to use.

Investigation of Bus Demand and Service in Future based on Lifecycle Model and Scenario Analysis
Noboru ISE, Yasuo HINO and Koichi KAWASAKI
Proceedings of the Eastern Asia Society for Transportation Studies, Vol.17, 13p (CD-ROM) (2009)
In this paper, the future prospect of bus service based on the transport demand estimated by using the lifecycle model in housing estates was referred. Especially, the necessity and possibility of bus demand increment were investigated through the discussion by the workshop procedure, as one of integrated approaches, involved residents, staff of bus and taxi companies, commercial parties and related parties in addition to local government officials. Furthermore, some scenarios were developed by agreements in these workshops, and based on these scenarios, the possibility of sustainable bus service was investigated, from viewpoint of the bus demand increment in consideration of change of life stage in future.
Limitation of Walking Facilities in Jakarta; A Visual Analysis on Actual Condition and User's Perception

Muhammad Zulkifli MOCHTAR, Yasuo HINO and Max PATTINAJA
Proceedings of the Eastern Asia Society for Transportation Studies, Vol.17, 12p (CD-ROM) (2009)
In Jakarta, the limitation of walking facilities has contributed to transport issues, because many roads have no walking space and pedestrians have been facing many obstructions such as street vendors and on street illegal parked vehicles. Then, the purpose of this study intend to explore the actual condition on walking activities, the change of walking space's function and people's perception on limitation of facilities. The result shows that the existing condition force people to walk in the road shoulder and it will be high risky for both pedestrians and drivers. Analysis of people's perception also shows that the availability of facilities is consistent with the satisfaction level. After all, this study may provide a snapshot to know not only the actual condition of people behavior and their perception, but also the better knowledge and understanding. Therefore, these results should be useful as an indication to investigate a better plan for next generation**.**

An Experimental Study on Development and Effects of Colour Pavement to Encourage Safety Driving
Yasuo HINO, Norihiro IKEDA, Akihiro IDO and Hedenobu MATSUDA
Japan Society of Traffic Engineers, Papers on Traffic Engineering, No. 29, pp. 29-32(2009) (in Japanese)
In the former study, some road safety measures for speed reduction and attentive driving were required to keep safety for pedestrians and cyclists by the social experiment based on the public involved approach. Then, in this study, the color pavement material to be not only visible and non skid on wet pavement in the night but also noise preventive was developed. In addition, the effective method for introducing the measure and the evaluation method of measure were investigated. As a result, it revealed that the new color pavement was effective for road safety through the physical function as brightness and value of slipping resistance and subjective evaluation based on driving experiments by residents. Furthermore, the process from development of materials to the introducing approach of measures was proposed.

An Experimental Study on Cyclist's Behavior and Needs for Road Space according to Different Conditions
Yasuo HINO, Tomoya SANO, Nagahiro YOSHIDA and Takashi UCHIDA
Japan Society of Traffic Engineers, Papers on Traffic Engineering, No. 29, pp.173-176(2009) (in Japanese)
In aging society, as the use of bicycles become more required and the needs will change, the improvements for them must be considered. In this study, the actual condition for using was surveyed according to different types of road spaces. As a result, the some subjects required for aged users were revealed. In addition, the specified needs according to various age groups by each different road type were evaluated by introducing the satisfied indicator.

Effect of Road Safety by Widening Shoulder and Removing Center Line from Viewpoint of Conflict Dangerousness
Yasuo HINO, Noboru ISE, Hiroyuki MAEDA and Yutaka HONDA
Japan Society of Traffic Engineers, Papers on Traffic Engineering, No. 29, pp.25-28(2009) (in Japanese)
In this study, the specified road improvements to ensure the space for pedestrians and cyclists were proposed for the semi-arterial road with 8.0m width. That is, the widening the road shoulder as the space for pedestrians and cyclists and the removal of center line due to it were executed. As a result, by introducing the dangerousness indicator based on vehicle's speed and space between vehicle and pedestrian, it was revealed that the dangerousness due to conflicts among each road participant was improved.

Pedestrian ITS to Activate Round Trip —Ordinary Location Coded Objects for TEMBEA—
Hirokazu MATSUMOTO and Takashi UCHIDA
Japan Society of Traffic Engineers, Papers on Traffic Engineering, No. 29, pp.133-136 (2009) (in Japanese)
Recently, information technology is developed and pedestrian ITS approach is taken. In terms of provision of information, it is required to accept individual diversity. But the types of walking, which have variety, are not defined in clear term. So the study intends to classify and define foot traffic according to pedestrian mind and show the application to ITS. And we consider the problem and solution in the existing system.
In this paper, we make a classification of foot traffic on the basis of degree of curiosity and with or without destination. And TEMBEA is defined as the concept. Specific example, which the authors got involved in, is shown as information provision system applied to TEMBEA. Then the remaining problem is exhibited. Furthermore, we propose one of mode of settlement using ordinary location coded objects, which enable localization. The application potency is investigated with the field work.
Risk Analysis for Bicycle Accidents on Arterial Road by using Generalized Linear Model
Syougo KAMEI, Nagahiro YOSHIDA, Yasuo HINO and Chiyuki SYUNDOU

Japan Society of Traffic Engineers, Papers on Traffic Engineering, No. 29, pp. 13-16 (2009) (in Japanese)

Analysis of Driver's Satisfaction of Basic Expressway Segments and Satisfaction Rating Model
Takashi SAKAI and Takashi UCHIDA
Proceedings of Infrastructure Planning, No.40, 4pp(CD-ROM)(2009) (in Japanese)
The objective of this study is to analyze the relationship between traffic conditions and driver's satisfaction with level of services (LOS) for basic expressway segments.
Driver's perception and satisfaction about the traffic conditions has large difference among individuals, however, the aggregate satisfaction tends to constant. Then, by using the covariance structure analysis, causal relationships between drivers' satisfaction and both traffic indices and perceptions of traffic condition. Finally, for each number of lanes, a satisfaction rating model with traffic indices as independent variables is proposed.

A Method for Measuring Driver's Mental Reactions by Using Near Infrared Sensor
Masataka IHARA and Takashi UCHIDA
Proceedings of Infrastructure Planning, No.40, 4pp(CD-ROM)(2009) (in Japanese)
There are a lot of measures for the prevention of the traffic accident now. However, whether these measures work effectively from respect of the psychological condition is not considered. Because a method for measuring driver's mental reactions has not been established. Then, the purpose of the study is to propose a method for measuring driver's mental reactions by using Near Infrared Sensor. The sensor gives physiology index that is an oxygen saturation of the hemoglobin. This paper shows the utility of the technique and stability of this method.

A Study on Information Provision via Traceability System for Civil Structures
Hirokazu MATSUMOTO and Takashi UCHIDA
Proceedings of Infrastructure Planning, No.40, 2pp(CD-ROM)(2009) (in Japanese)
The citizens begin to have the doubt for trust about the safety being kept by specialists. Further information disclosure in public institution came to be requested. So, we aims to achieve the civil structure traceability system that everyone can acquire information that relates to the civil structure at once on the scene, and to contribute to creating administrative governances and a committed relationship between citizens and administration.
In this paper, by a thorough examination of existing traceability systems, we show the viewpoint needed to compose and provide information about the engineering works structure traceability system and make a prototype system. The social meaning and the method of using the system with the publicity are also discussed.

A Study of Navigation System for Visually Handicapped to Support Town Walk -Media and Messages for Guidance-
Yoshiaki YOSHII and Takashi UCHIDA
Proceedings of Infrastructure Planning, No.40, 4pp(CD-ROM)(2009) (in Japanese)
Recently, navigation systems for pedestrian are widespread with advancing positional specific technology, e.g. GPS. However, the accuracy of a positional specific technology is after low, and even audio guide is difficult for visually handicapped people.
In the study, a navigation system for the visually handicapped was experienced by using the signal of sound and the verbal map in the condition similar to practical use. In this paper, the classification of facilities intended for suburbs, a margin for error of timing , and the priority level of the element of the verbal map are clarified from the experiment and hearing. Then, the proposal of the practical use of the navigation is discussed.

Risk Analysis for Bicycle Accidents along Trunk Roads in Consideration of Extent of Damage
Syougo KAMEI, Nagahiro YOSHIDA and Yasuo HINO
Proceedings of Infrastructure Planning, No.40, 4p(CD-ROM)(2009) (in Japanese)

Evaluation System for Bicycle Road Facilities on Carriageway
Shinya NAKAMURA, Nagahiro YOSHIDA and Yasuo HINO
Proceedings of Infrastructure Planning, No.40, 4p(CD-ROM)(2009) (in Japanese)

Analysis of Air Bubbles in the Surf Zone Breaking Waves by Imaging Technique
Y. MATSUO, N. MORI, T. SHIGEMATSU and S. KAKUNO
Annual Journal of Coastal Engineering, JSCE, Vol. 56, pp. 69-100 (2009) (in Japanese)
The characteristics of bubble entrainment process in the surf zone are discussed. The two-phase flow measurements using two-dimensional imaging technique for bubble measurements, so called Bubble Tracking

Velocimetry (BTV) was conducted in the laboratory wave tank. The horizontal and vertical distributions of void fraction and characteristic bubble size were measured and analyzed in detail. The relationship between the void fraction and wave energy dissipation are proposed for the surf zone breaking waves.

Seasonal Variations in Characteristics of Oxygen Consumption by the Bottom of Ports and Harbors
T. ENDO and T. SHIGEMATSU
Annual Journal of Coastal Engineering, JSCE, Vol. 56, pp. 1051-1055 (2009) (in Japanese)
For effective restoration of enclosed coastal zone under anoxic environment such as Osaka bay, it is necessary to understand characteristics of oxygen consumption by the bottom sediment of ports and harbors. In this study, field measurements of the oxygen consumption rate were carried out during the year in a harbor. Seasonal variations in characteristics of the oxygen consumption by sediment were presented and the formulation of oxygen consumption by bottom sediment was attempted.

A Fundamental Study on the Two Perspective 3D-PTV system for Measurement of Complicated Flow
S. NAKAJO, T. SHIGEMATSU and S. UMASE
Annual Journal of Coastal Engineering, JSCE, Vol. 56, pp. 1461-1465 (2009)
A new algorithm of a 3D particle tracking velocimetry, 3D-PLCV is developed. The significant feature is the use of images capturing path lines without any blind duration between sequential images. Hence, particle matching becomes very easy by connecting path lines in sequential images. Further, use of information of connected path line is useful to restrain generation of ghost tracers in stereo-matching. After description of details of the algorithm of the 3D-PTVdeveloped in this study is presented, validity of the 3D-PTV is shown using artificial images. Finally, measurement result of fluid flow in pore of porous media by the developed PTV is presented.

A study on an index for improvement of sea bottom environment in eutrophied port and harbor
Keisuke MIZUTA, Toru ENDO and Takaaki SHIGEMATSU
Annual Journal of Civil Engineering in the Ocean, JSCE, Vol.26, pp. 135-140 (2010) (in Japanese)
In order to get knowledge of sediment oxygen consumption in a eutrophied port through a whole year, field investigation on oxygen consumption flux by the sea bottom was carried out using a chamber and a dark bottle with fluorescence type oxygen sensors. Based on the measurement data, biological and physical-chemical oxygen consumption processes are modeled with water temperature and dissolved oxygen concentration near the sea bottom. It is shown that the oxygen penetration depth can be a useful index which represents a restoration degree of sea area under low or no dissolved oxygen concentration. It is also shown that the presented sediment oxygen consumption model can predict the change of the oxygen consumption by oxygen supply with reasonable accuracy

A Field Experimental Study on Environmental Impact by Surface Water Supply to the Bottom in a Port and Harbor
T. ENDO, K. MIZUTA, R. USUI, H. TANAKA and T. SHIGEMATSU
Annual Journal of Civil Engineering in the Ocean, JSCE, Vol.26, pp. 135-140 (2010) (in Japanese)
In ports and harbors, hypoxic or anoxic water has occurred frequently at the sea bottom. In this study, we carried out a field experiment for supplying surface water with oxygen to the bottom of sea by using surface water supplying device. We supplied surface water to the bottom of sea by using the surface water supplying device in the actual sea under hypoxic condition and we measured water quality profiles near the device. In this paper, we examined the improvement effect on sea bottom environment by surface water supplying. Furthermore, we discussed about the flow pattern of water which was supplied to the bottom of sea by conducing numerical calculations.

Experimental Study on Strengthening Method of Lower Flange Plate of I Shaped Steel Girder with Bolted Connection by High Modulus CFRP Strips

Nobuhito OCHI (Akashi National College of Technology), Masahide MATSUMURA and Nobuhiro HISABE (Mitsubishi Plastics, Inc.)

Journal of Structural Engineering, Vol.55A, JSCE, pp. 43- 51 (2009) (in Japanese)

The installation of CFRP strips of high modulus can be effective for strengthening a superannuated existing steel I girder with regard to improving its load carrying capacity. Here, shear plates of the bolted connections become obstacles in installing the CFRP strips onto the lower flange plate of I shaped steel girder. Then, experimentally investigated in this study is the strengthening effect of the methods to prevent the CFRP strips of high modulus from debonding in the vicinity of the bolted connection of lower flange plate of I shaped steel girder through a bending test. It is concluded that the proposed methods are effective to prevent debonding of the CFRP strips and further investigations are needed to develop more effective methods.

Bending and Shear Behavior of a Steel I-Shaped Girder with a Transversely Profiled Steel Web Plate

Kunitaro HASHIMOTO (Kyoto University), Takashi YAMAGUCHI, Kosuke OTSUKA (Kyoto University), Kunitomo SUGIURA (Kyoto University), Yasuo SUZUKI (Utsunomiya University) and Takuji KUMANO (JFE Engineering Corp.)

Journal of Structural Engineering, Vol.55A, JSCE, pp. 144- 153 (2009) (in Japanese)

Steel plates with varied thickness have a potential for rationalization of steel bridge design. For example, longitudinally profiled steel plates already have been adapted to flanges of an I-shaped girder / a box girder to reduce the weight of the bridge and the process of bridge construction. Recently, the analytical study on the mechanical behavior of steel girders with a transversely profiled web plate has been carried out, and it has been concluded that there exists the preferable cross sectional shape of steel plate from the viewpoint of the load carrying capacity and ductility. In this paper, the static loading tests for I-shaped girders with a profiled web plate in thickness are carried out. It is found that the web plate whose thickness is larger at the middle height of the girder has superiority for shear buckling strength; on the other hand, that the web plate whose thickness is larger at the close to flange plate has superiority for bending strength.

Seismic Performance Evaluation of a Viaduct Supported by Steel Bridge Piers with EPS

Masahide MATSUMURA, Satoshi UCHIDA (NEWJEC Inc.) and Toshiyuki KITADA

Journal of Structural Engineering, Vol.55A, JSCE, pp. 653- 661 (2009) (in Japanese)

Embedded Plastic Segment (EPS), which has been developped as a seismic retrofitting technique for existing steel bridge piers, can enhance the ductility with less increment in the ultimate strength of the column members. In this paper, the seismic performance of a viaduct of the total length 200m with 5 spans supported by the steel bridge piers with the EPS is analytically investigated. The effectiveness of the steel bridge piers with the EPS is revealed in comparison with a viaduct supported by concrete filled steel bridge piers. It is concluded that the EPS enables the reduction of the construction cost of piles and footing concrete and the enhancement of redundancy of the viaduct.

Measurements of Initial Imperfections of Longitudinally Profiled Steel Plates and their Applied Box Cross Section

Takuji KUMANO (JFE Engineering Corp.), Yasuo SUZUKI (Utsunomiya University), Takeshi KITAHARA (Kanto Gakuin University), Kunitomo SUGIURA (Kyoto University) and Takashi YAMAGUCHI

Journal of Structural Engineering, Vol.55A, JSCE, pp. 977- 984 (2009) (in Japanese)

Recently, various kinds of high-performance steel have been developed in order to reduce construction costs and improve structural performances. LP steel plate is applied to flange plates of steel girders with a view to reduction of process for fabrication and simplifying structures. On the other hands, it is generally known that initial imperfections of steel plates affect on the characteristics of strength and deformation of steel girders. Therefore, in this study, the fabrication error of plate thickness and the residual stress distribution subjected to metal rolling and welding are measured for the actual LP plate and box cross section in order to correct the basic imformation of initial imperfections of LP steel plates.

Analytical Study on Mechanical Behavior of the High Strength Bolted Friction Joints with F18T Grade Super High Strength Bolts Subjected to Compression

Takashi YAMAGUCHI, Toshiyuki KITADA, Takayuki IKEDA (NTT Data Corp.) and Natsuki YOSHIOKA

Journal of Structural Engineering, Vol.55A, JSCE, pp. 1005- 1013 (2009) (in Japanese)

Recent years, rationalization of the joint structures is required from the viewpoint of reduction of the total cost of

steel structures. As one of such effective solutions, adoption of super high strength bolts for friction type joints, which strength is more than 1,600 MPa is considered in order to be a compact joint section with a few bolts and lines. However, the mechanical behavior of such joints, especially the behavior under compressive load, is not clear. Therefore, in this study, the mechanical behavior of the friction type joints with super/normal high strength bolts subjected to compressive load is discussed based on the FE analytical results paying attention to the maximum spacing of the bolts and contact between joint surfaces.

Experimental Study on the Strengthening of Bolted Tensile Joints with a Deformable Filler Plate
Yasuo SUZUKI (Utsunomiya University), Takashi YAMAGUCHI, Akinori NAKAJIMA (Utsunomiya University) and Takahiro SHIMIZU (Utsunomiya University)
Journal of Structural Engineering, Vol.55A, JSCE, pp. 1014- 1023 (2009) (in Japanese)
In the split tee joints, the prying force occurs due to the deformation of the tee flange plates, and the prying force reduces the strength of the joint. Therefore, it is very important for this type of joints to suppress the prying force. In order to make it possible to reduce the prying force of split tee joints easily, we propose to apply the sealant named as deformable filler plate for the split tee joints consists of soft rubber and steel rings. In this study, the mechanical behavior of split tee joints with the deformable filler plate is investigated experimentally. Particularly the influence of the sealant and shapes of the tee flange plates on strength and deformation of these joints are mainly discussed.

Dynamic Response of Isolated Bridge System Considering Knocking-off of Side Block as Displacement Restrainer of Superstructure
Masahide MATSUMURA, Nobuhito OCHI (Akashi National College of Technology), Masahiko YOSHIDA (Kawaguchi Metal Industries Co., Ltd), Minoru SAKAIDA (Sakaida Bridge Engineering & Consulting) and Toshiyuki KITADA
German-Japanese Bridge Symposium, Munich, (7 pages, CD-ROM) (2009)
Displacement restrainer of the superstructure in the transverse direction of the isolated bridge, like side block, is usually installed to protect expansion joints from damage during earthquake. Here, a more rational response of the isolated bridge to mitigate damage to bridge pier and/or base structure and to enhance redundancy against a strong earthquake like the Level 2 Earthquake can be considered to be that the displacement of the superstructure against a small and a moderate earthquake like the Level 1 Earthquake is restraint and the displacement against the Level 2 Earthquake is released. For instance, steel side block, improved to have a knock-off function, will provide these responses. This study presents the outline of the side block with the knock-off function, which is the side block with a slit and developed by the authors to control the breaking load accurately, reveals the effectiveness of the knocking-off in the isolated bridge system through dynamic loading test using a small-size shaking table and verifies the influences of the breaking characteristics of the side block with the knock-off function through the dynamic response analysis of the system.

Experimental Study on Static Mechanical Properties of Glass Plate Materials for Use as Structural Members
Yugo NAGAMACHI, Toshiyuki KITADA, Takashi YAMAGUCHI and Masahide MATSUMURA
German-Japanese Bridge Symposium, Munich, (4 pages, CD-ROM) (2009)
Developments of the glass technology and fundamental researches for the structural use of the glass enable the applications of the glass plate to structures. The glass plate has been widely used in architectural structures both as structural and non-structural members and the use of the glass plate as structural members creates more attractive and functional structures. On the other hand, the use of the glass to structures in civil engineering field is not so popular, because the cost-effectiveness may be first priority in the structural design and planning. Here the use of the glass plate for structures in civil engineering field, for instance, for principal structural members of bridge can be considered to create more attractive and fascinating bridge and construction, which will bring a drastic change to images of the bridge. In the study, fundamental material properties of the glass plate are clarified through material tests. Then, a new type of glass plate beam with a joint is proposed through numerical calculations based on the material test results. Here, SGP foils is used for the joint in the beam.

Inspection and Damages of Bridge Expansion Joints in Urban High Way in Japan
Masahide MATSUMURA, Takashi YAMAGUCHI, Yoshihiko TAKADA (Hanshin Expressway Management Technology Center) and Toshiyuki KITADA
German-Japanese Bridge Symposium, Munich, (7 pages, CD-ROM) (2009)
Bridge expansion joints, installed at the edges of the girders and subjected to the impact loading of moving

vehicles, take important roles in providing smooth running of the vehicles. A proper type of the expansion joint, which can secure enough interspaces between the girders, should be selected to prevent their interaction against expansion movements with the changes in temperature and during the earthquake. Adoption of the finger joint is a general solution when larger interspaces between the girders are required. However, the finger joint is designed only against the static vertical design load corresponding to the truck live load according to the present design method in the Japanese Specification of Highway Bridges (JSHB), however some damages of the finger joint are reported. Presented in this paper are the outlines of inspection results and damages of the expansion joints, which is carried out by Hanshin Expressway Corp., and the discussion based on the test results of the two kinds of the field test passing the vehicles over the joints. It is concluded that the impact loading derived from the vehicle passing and enlarged by the faulting between the joints is not negligible in the design of the finger joint.

Slip Behavior of High Strength Bolted Friction Joints for Composite Girders Subjected to Bending
Natsuki YOSHIOKA, Takashi YAMAGUCHI, Masatsugu NAGAI (Nagaoka University of Technology) and Takeshi MIYASHITA (Nagaoka University of Technology)
German-Japanese Bridge Symposium, Munich, (8 pages, CD-ROM) (2009)
In recent years in Japan, various studies on rational design of steel bridges focusing on cost reduction, such as consideration of plastic behavior for ultimate state are performed. In Euro Code, AASHTO-LRFD, plastic moment is already adopted to the ultimate strength for the positive bending state of the composite girder. However, in Japan, there are a few researches about it and as a result, plastic moment is not allowed to the ultimate strength in the design specifications. Accordingly, in this study, in order to collect basic information for design of composite girder connection, FE analyses were executed referring to the experiment which has been carried out by authors. Finally, based on these analytical results, the evaluation method of ultimate bending strength of the composite girder with high strength bolted friction joints are proposed and desirable design concept of the friction type joints for composite girder bridges are summarized.

Analytical Study on Residual Load Carrying Capacity of Damaged Steel Bridge with Large Crack
Takashi YAMAGUCHI, In ho KIM (Miyaji Iron Works Co., Lid.), Toshiyuki KITADA and Kazuyuki MURAMOTO (Japan Bridge Engineering Center)
Steel Construction Engineering, *Vol.16, No.63*, JSSC, pp. 15- 25 (2009) (in Japanese)
In recent, much damage has been detected in superannuated bridges. Especially, the fatigue problems of aged steel bridges become serious in the maintenance of bridges. Recently, the serious and large crack of approximately 1.1m length was detected. In the web plate of interior main girder at the intersection of the main girder and the transverse girder, and at the location near the interior support in the center span of a three-span continuous girder bridge. If such a large crack occurs, the load carrying system of bridge should be changed and its capacity will be decreased. Accordingly, it is important to evaluate the residual load carrying capacity of damaged bridges with a large crack from the viewpoint of the management of the bridge system. The objective of this study is to investigate analytically change of the load carrying system of the various damaged three-span continuous girder bridges with four main girders.

Friction Test for High-Strength Bolted Joints with Long-Exposed weathering Steel
Minoru SAKAIDA (SAKAIDA Bridge Engineering & Consulting), Kunitomo SUGIURA (Kyoto University), Takashi YAMAGUCHI, Shigeyuki MURAKAMI (Gifu University) and Kunitaro HASHIMOTO (Kyoto University)
Steel Construction Engineering, *Vol.16, No.63*, JSSC, pp. 37- 48 (2009) (in Japanese)
Strength and slip factor of high strength bolted friction joints were obtained through loading tests. Specimens were assembled from weathering steel base members and blasted splicing members. Weathering steel plates were cut out from lower flange plate of a bridge that was exposed for 8 years in open inland field, and it has been generated protective rust on its surface. Base members were treated in some levels of rust removing. Applied treatments are blasting, disk sanding, powered wire brushing, manual wire brushing and cloth wiping. Protective rust decreases the slip factor, and thin crystalloid rust increases it, but thick rust over 100 μm decreases it.

Assessment on Fatigue Cracks in Orthotropic Steel Decks
Kunitomo SUGIURA (Kyoto University), Kunitaro HASHIMOTO (Kyoto University), Yoshinobu OSHIMA (Kyoto University) and Takashi YAMAGUCHI
Steel Construction, Vol.2, No.3, Ernst & Sohn, pp. 175- 180 (2009)
In this study, proposed is the new health evaluation system for fatigue cracks of orthotropic steel bridge decks by measuring strain changes of the asphalt pavement on steel plate decks. In order to consider applicability of this

system, carried out are parametric FE analyses in which the type of cracks, their position, and their length are varied. From these analytical results, it is found that strain changes of the asphalt pavement on steel plate decks by the length and the positions of cracks can be significant enough to be detected.

Experimental Study on Vibration Control of Pole Type Steel Structures on Bridges by Using Damping Members/Elements

Tomohiko ISHIBASHI (Nasu Denki-Tekko Co., Ltd.), Takashi YAMAGUCHI and Kazuyuki HENMI (Nasu Denki-Tekko Co., Ltd.)

Journal of Constructional Steel, Vol.17, JSSC, pp. 247- 254 (2009) (in Japanese)

Recently, it is pointed out that the bridge vibration due to traffic may cause fatigue damages to pole type steel structures like a lighting pole or a marker pole on bridges. As such damage tends to cause severe accidents, the vibration damage is to be eliminated as soon as possible. It is important to avoid resonance phenomenon and to increase damping effect of the steel poles with possible fatigue damages by economical techniques, because the number of pole type steel structures on bridges is large. Authors suggest two vibration controlling techniques for these steel poles, by using wire ropes and by using chloroprene rubber plates underneath the lower end plate of the steel pole. It is verified through a vibration experiment that both techniques are effective and the response displacement of the pole can be reduced substantially.

Fundamental Study on Characteristics of Extremely Low Cycle Fatigue Crack of Steel Members in Bridges

Shigeharu YAMANE (Mitsubishi Heavy Industries Bridge & Structures Engineering Co,. Ltd.), Toshiyuki KITADA, Takashi YAMAGUCHI and Masahide MATSUMURA

Journal of Constructional Steel, Vol.17, JSSC, pp. 289- 294 (2009) (in Japanese)

Extremely low cycle fatigue crack phenomenon is not yet clarified enough. In this paper, crack initiation mechanism in a range of the repetition number of several times to 20 is clarified by the extremely low cycle fatigue experiment focusing on strain at crack initiation point and fractography of the crack fracture. It is concluded that the crack is not brittle but ductile in the case of the extremely low cycle experiment using the specimens with welding part and notches at their central part.

A Fundamental Experiment on Mechanical Behavior of Panel Point of Steel Truss Bridges

Shinsuke YOSHIDA (Kyoto University), Takashi YAMAGUCHI, Kunitaro HASHIMOTO (Kyoto University) and Kunitomo SUGIURA (Kyoto University)

Journal of Constructional Steel, Vol.17, JSSC, pp. 391- 398 (2009) (in Japanese)

In this study, in order to clear the mechanical behavior of panel point of steel bridges using high strength bolted frictional connection, tensile loading experiment is carried out. In the experiment, two specimens modeled the panel points of steel truss bridges which the gusset plate and the diagonal member are connected by high strength bolts are prepared. One has the ordinal gusset plate whose thickness is 9 mm, and the other has thin (6 mm) gusset plate in which is considered the decrease of the thickness due to corrosion. From the result of this experiment, it is found the collapse behavior of panel points of steel truss bridges and it is suggested the optimum calculating method for yielding strength of the such panel point.

Study on Methods for Effectively Using Down-Sized Vibration Table to Evaluate Seismic Performance of Bridge Structures

Yasuyuki NAKANISHI (NEWJEC Inc.), Masahide MATSUMURA, Toshiyuki KITADA and Takashi YAMAGUCHI

Journal of Constructional Steel, Vol.17, JSSC, pp. 415- 420 (2009) (in Japanese)

Dynamic response analysis requires many idealizations regarding the unknown factors, such as dumping coefficient, dynamic characteristics of material, etc, but simulates the dynamic behavior the idealized of structure, although it's unknown whether the predicted behavior is exact. While shaking table test without idealizations shows dynamic response. Using a down-sized specimen, the dimensional reduction from a full scale is same question as to the realization of exact behavior, but the cost effectiveness will be much attractive. Then the shaking table test using down-sized specimens are carried out in this study to examine the advantages and disadvantages. Also the experimental results are compared with the numerical ones using the idealized analytical models. Effectiveness of using down-sized specimen in the small shaking table in evaluating seismic performance of steel structures is discussed comparing experimental and analytical results.

Repairing Design of Stiffeners on the Support of a Plate Girder for Highway Bridges

Kennichi SATO (New Structural Engineering, Ltd.), Yukiko MITSUGI (New Structural Engineering, Ltd.), Takashi

YAMAGUCHI, Kunitaro HASHIMOTO (Kyoto University) and Kunitomo SUGIURA (Kyoto University)
Journal of Constructional Steel, Vol.17, JSSC, pp. 673- 680 (2009) (in Japanese)
In this paper, the repairing design of stiffeners on the support of a plate girder for Highway Bridges is studied referring the literature and executing simple calculation. We treated the stiffener on the support, whose effective sectional area is decreased by corrosion at is the end of the bottom portion. From the viewpoint of the performance based design, we considered the role of the each member/element that consists of the girder on the support. The mechanics of resistance and the limit states of them are discussed. In the case that the thickness of the plate at the bottom end is decreased by the corrosion, the bearing limit state of the bottom-end is dominant.

Fatigue Failure Assessment Considering Actual-Working Load and Running Position of Orthotropic Steel Deck by using BWIM
Yoshihiko TAKADA (Hanshin Expressway Management Technology Center) and Takashi YAMAGUCHI
Memoirs of the Faculty of Engineering, Osaka City University, Vol.50, pp. 55- 61 (2009)
Recent considerable increase in traffic intensity and wheel loads causes fatigue cracks in orthotropic steel decks in Hanshin Expressway. From results of the periodic inspection, fatigue cracks are detected by 167 spans in 1347 spans in orthotropic steel decks as of April, 2009. Under traffic loading, in particular the effect of local wheel loads, longitudinal welds between deck plate and trough are subjected to local transverse bending moments and are susceptible to fatigue cracks. The stress in trough to deck plate welds is strongly influenced by actual-working load and run position .Then, in orthotropic steel decks in Kobe route of Hanshin Expressway, measurement of the load of actual-working traffic and generating stress is performed by Bridge-Weigh-In-Motion. This papert presents the outline of fatigue failure in orthotropic steel decks. Next, Fatigue failure assessment based on this measurement results are described.

Environmental Urban Engineering

Regulation of Outbreaks of Green Tide Occurring on the Artificial Salt Marsh along the Coast of Osaka Bay, Japan

Tomoki NISHIKAWA, Shota TAKEDA and Susumu YAMOCHI

Journal of Coastal Engineering, JSCE, pp.1221-1225 (2009) (in Japanese)

Field surveys and indoor experiments were conducted to reduce the outbreak of green tide by *Ulva pertusa* at Osaka Nanko bird sanctuary. Reduction of biomass of *Ulva* spp. was observed at stations where the exposure rate to air was from 30 to 40%. In addition, the exposure rate of 30 to 40% to air showed no negative impacts on the biomass of benthic microalgae, infauna and non-motile epibenthos. Laboratory experiments revealed that photosynthetic activity of *Ulva pertusa* decreased when exposed to air for 4 to 7 hours at 25-35℃. Salinity decrease from 30 to 25 or 20 psu in accompanied with exposure to air drastically inhibited the photosynthesis of this species. These results suggest the possibility of controlling a green tide of *Ulva pertusa* without serious physico-ecological damages to benthic microalgae, infauna and non-motile epibenthos by the combination of exposure to air with low salinity.

Occurrence of Ayu *Plecoglossus altivelis* at the Mouth of the Yamato River, Japan

Hiromitsu ONCHI and Susumu YAMOCHI

6th International Conference on Marine Pollution and Ecotoxicology, Hong Kong (China), 31 May-3 June, 2010, Abstract p.53

Field surveys were conducted on the seaward drifting of larval Ayu *plecoglossus altivelis* and their distributions at the mouth of the Yamato River, central Japan from 2007 to 2009. Total numbers of drifting Ayu were estimated to be about three million individuals in 2007, while no individuals of Ayu were observed in 2008. This is partly due to the change of grain size distributions of the riverbed around the spawning site. Thirty-four individuals of Ayu were caught at the most seaward reach of the river, while none of the juvenile Ayu was collected at the upper areas of the river mouth. Values of ORP were low (min. -156mV) in sediments of the upper site of the river mouth when compared with its seaward sites. These findings reveal that the deterioration of the bottom sediment partly inhibit the upstream migration of the Ayu at seaward areas of the mouth of the Yamato River.

Profile and removal of endocrine disrupting chemicals by using an ER/AR competitive ligand binding assay and chemical analyses

Ze-hua LIU, Mamoru ITO, Yoshinori KANJO and Atsushi YAMAMOTO(Osaka City Institute of Public Health and Environmental Sciences)

Journal of Environmental Sciences, Vol.21, No.7, pp.900–906 (2009)

An estrogen receptor (ER)/androgen receptor (AR) ligand competitive binding assay (ER/AR-binding assay) and chemical analyses were used to evaluate the endocrine disrupting chemicals (EDCs) behavior of two municipal wastewater treatment plants (WWTPs) (K and S). In the influents, estrone (E1), androsterone (A), androstenedione (AD), BPA (bisphenol A), NP (nonylphenol) and daidzein (DZ) were detected in high amounts with subsequent 24 h-average concentrations of 350, 1000, 29, 1300, 3900, and 5700 ng/L in K-WWTP and of 310, 620, 59, 1600, 2600, and 8400 ng/L in S-WWTP. The estrogenic (androgenic) activity as 17β-estradiol (E2) equivalents (EEQ) or testosterone (Te) equivalents (TEQ) was consequently 620 ng E2/L (570 ng Te/L) and 580 ng E2/L (800 ng Te/L) for the two WWTPs. The removal eficiencies of the above mentioned sole target chemicals were 51%–100% for K-WWTP and 55.6%–100% for S-WWTP. The removal eficiencies of EEQ were about 73% for both WWTPs, while the removal eficiencies of TEQ were 62.1% for K-WWTP and 98.4% for S-WWTP. In addition, chemical-derived EEQ were about 1.2%–52.4% of those by ER-binding assay for K-WWTP and the corresponding ratios were 1.3%–83.3% for S-WWTP, while chemical derived TEQ were less than 3% of values measured by the AR-binding assay for both WWTPs.

Urinary excretion rates of natural estrogens and androgens from humans, and their occurrence and fate in the environment: A review

Ze-hua LIU, Yoshinori KANJO and Satoshi MIZUTANI

Science of the Total Environment, Vol.407, No.18, pp.4975–4985 (2009)

Endocrine disrupting compounds (EDCs) are pollutants with estrogenic or androgenic activities at very low concentrations and are emerging as a major concern for water quality. For sewage of municipal wastewater treatment plants in cities, one of the most important sources of EDCs are natural estrogens and natural androgens (NEAs) excreted from humans. Therefore, estrogenic/androgenic potencies or relative binding affinity of the

NEAs were first outlined from different sources, and data of urinary excretion rates of NEAs were summarized. To evaluate their estrogenic activities, their excretion rates of estrogen equivalent (EEQ) or testosterone (T) equivalent (TEQ) were also calculated. Based on our summary, the total excretion rates of EEQ by estrone (E1), 17β-estradiol (E2), and estriol (E3) only accounted for 66–82% of the total excretion rate of EEQ among four different groups, and the other corresponding natural estrogens contributed 18–34%, which meant that some of the other natural estrogens may also exist in wastewater with high estrogenic activities. Based on the contribution ratio of individual androgens to the total excretion rate of TEQ, five out of 12 natural androgens, T, dihydrotestosterone (DHT), androsterone (AD), 5β-androstanediol (β-ADL), and androstenediol (ANL) were evaluated as the priority natural androgens, which may exist in wastewater with high androgenic activities. Published data on occurrence and fate of the NEAs including natural estrogen conjugates in the environment were also summarized here.

Distribution of polycyclic aromatic hydrocarbons and nitroarenes in road sediments and drainage and their discharge in a nearby river

Takaya KAWASAKI, Yuichi ITO, Katsuto KOBAYASHI, Satoshi MIZUTANI and Yoshinori KANJO

Environmental Engineering Research, Japan Society of Civil Engineering, Vol.46, pp.337-343 (2009)(in Japanese)

18 kinds of Polycyclic Aromatic Hydrocarbons (PAHs) and 4 kinds of nitroarenes (NPAHs) contents in road drainage and sediments on Abiko bridge, which spans the Yamato River in Osaka prefecture, were surveyed. The results show that the total content of 18 PAHs in road drainage and sediments ranged from 0.5 to 9.1μg/L and from 1.2 to 3.6μg/g, respectively. On the other hand, total NPAHs content were less than 0.7μg/L and 0.1μg/g, respectively. In Comparison with the PAHs content in road drainage, only 6.5% of PAHs in road sediments were discharged into Yamato River. Moreover, the PAHs compositions in road sediments were different from those in road drainage.

Analytical condition for natural conjugated estrogens with Gas Chromatography – Mass Spectrometry

Takeshi HASHIMOTO, Ze-hua LIU, Yoichi OKUMURA, Satoshi MIZUTANI and Yoshinori KANJO

Environmental Engineering Research, *Japan Society of Civil Engineering*, Vol.46, pp.329-336 (2009) (in Japanese)

Suitable deconjugation condition of acid hydrolysis method and enzyme hydrolysis method were examined for natural estrogen and their conjugates. The result shows that suitable condition for acid hydrolysis method was 80℃ for 270 minutes, and that for enzyme hydrolysis method was 37℃ for 24 hrs with 50μl of each enzyme and buffer (pH4.8). The result of additive recovery test with sewage samples confirmed that natural estrogens (E1,E2) and their conjugates(E1-3S,E2-3S,E3-3S and E1-3G) are analyzed simultaneously. In addition, average recovery ratio was by the enzyme hydrolysis higher than that by acid hydrolysis method.

Application of modified BCR sequential extraction procedure for evaluation of acid extraction performance

Mitsuo MOURI(Shimizu Corp.) and Yoshinori KANJO

JSCE Journal G, Japan Society of Civil Engineering, Vol.65, No.4, pp.246-259 (2009) (in Japanese)

Heavy metal-contaminated soils are separated into two parts by soil washing, clean sands and highly polluted sludge for further treatment or disposal. At times the so-called clean sands, products of physical soil washing process consisted of wet screen and hydrocyclone, do not meet the soil leaching standard, while satisfying the constituent test. Putting the clean sand through the acid extraction process may be an alternative to improve its leaching characteristics, assuming extraction of such mobile portions as water-soluble and acid soluble fractions that are determined by the modified BCR extraction procedure. The process of acid extraction is a complex physicochemical phenomenon of heavy metals of different morphology in the soil. Then, the validity of acid extraction process is only determined experimentally. This study has tested three types of acid, hydrochloric acid, sulfuric acid and acetic acid, for typical heavy metal contaminants, lead and fluorine. Two types of feed soil, highly contaminated and lightly contaminated soils, and their underflow of the process or clean sands were subject to acids of different concentrations under different liquid solid ratios. The acid extracted fractions were compared to five soil fractions, water-soluble, acid-soluble, reducible, oxidizable and residue, as determined by the modified BCR method extraction procedure. Generally, the fractions most amenable to metal removal by acid extraction are: water-soluble, acid-soluble (carbonates), and reducible (Fe-Mn oxides). As a result, the acid extraction process was valid for reducing lead leaching value to a certain extent, but not for fluorine. It was also

observed that the fractionation data by the modified BCR method did not always clearly explain the leaching characteristics of clean sands because a part of mobile portions still remained or some other mobile portions were newly formed through the acid extraction and/or the rinsing processes.

Deconjugation characteristics of natural estrogen conjugates by arylsulfatase/glucuronidase enzyme and its application for wastewater

Ze-hua LIU, Yoichi OKUMURA, Takeshi HASHIMOTO, Yoshinori KANJO, and Satoshi MIZUTANI

Proceedings of The First Forum on Studies of the Environmental & Public Health Issues in the Asian Mega-cities(EPAM2009), pp.15-24 (2009)

Natural estrogens and their conjugates excreted from human urine/feces are regarded as one of the main sources of the endocrine disrupting chemicals (EDCs) in municipal wastewater. It is necessary and important for monitoring all of them on evaluation of their removal by wastewater treatment plants (WWTPs). GC-MS is the most available instrument to researchers for its relative low cost. Therefore, it is important for the simultaneous analysis of natural estrogens and their conjugates by GC-MS. In this paper, a solid-phase extraction (SPE)-GC-MS analytical method for the simultaneous analysis of them was developed. In the method, natural estrogens and their conjugates in wastewater were separated using SPE, then the conjugates were enzyme hydrolyzed by β-glucuronidase or arylsulfatase. The enzyme hydrolysis was done in pH 4.8 buffer solution with addition of 50μL enzyme, which incubated in 37℃ for 24hrs. The method was successfully applied for wastewater samples.

Remediation of Groundwater Contained with Heavy Metals and Volatile Organochlorinated Compounds by Permeable Reactive Barrier

Yoshinori KANJO, Satoshi URAMOTO, Akihiko OSHIMA, Harue MASUDA and Satoshi MIZUTANI

Proceedings of The First Forum on Studies of the Environmental & Public Health Issues in the Asian Mega-cities(EPAM2009), pp.159-166 (2009)

In urban area, we have a lot of problems about groundwater pollution and high levels of groundwater. To solve these problems, we should develop an economical and simple treatment method which can be applied to the huge amount of polluted groundwater. In this paper, we focused on the suitable materials for PRB systems to apply for groundwater polluted with low levels of VOC and heavy metals, and performance of the PRB system. As the results of screen test and flow-through experiments, the suitable material for PRB was the mixture of iron dust and black soil, and the effluent of the column with this mixture was kept almost zero with neutral range of pH for more than 40 days.

How to Reduce Solid Waste and Wastewater in Small and Medium Enterprise

Osamu YAMAMOTO(Osaka City Institute of Public Health and Environmental Sciences), Zensuke INOUE(Environmental Management and Technology Center in Kansai), Isao FUKUNAGA(Former Osaka University of Human Sciences), Takashi NISHITANI(Osaka City Institute of Public Health and Environmental Sciences), Yoshinori KANJO, Satoshi MIZUTANI and Taizo IMOTO(Technology Research Institute of Osaka Prefecture)

Proceedings of The First Forum on Studies of the Environmental & Public Health Issues in the Asian Mega-cities(EPAM2009), pp.197-203 (2009)

Reduction of environmental impacts from the manufacturing activities has been an important issue. However, it is difficult for Small and Medium Enterprises (SMEs) to conduct such kind of activities because of the shortage of human, information and financial resources. The advisory activity for SMEs that purpose is to reduce and/or recycle solid waste and waste water, is introduced in this paper. The activity is conducted by the group of the Chambers of Commerce and Industry (CCIs) and researchers from the public research institutes and the universities in Osaka Prefecture. The researchers are organized as the Technical Advisory Committee for Recycle which is operated by the group. The Committee visits the company and discusses with the member of the company on the method to reduce and recycle. This paper also introduces the procedure to find the method from the experiences of the activity.

Estimation of the amounts of general solid wastes from daily life and business activities in Osaka City

Satoshi MIZUTANI, Yoshinori KANJO, Mamoru SAKAI(Osaka City Institute of Public Health and Environmental Sciences) and Osamu YAMAMOTO(Osaka City Institute of Public Health and Environmental Sciences)

Proceedings of The First Forum on Studies of the Environmental & Public Health Issues in the Asian Mega-cities(EPAM2009), pp.205-212 (2009)
The amounts of general wastes from daily life (household wastes) and wastes from business activities (business wastes) for 24 administrative districts in Osaka City are estimated. The amounts of household waste are estimated by multiplying the generation weight unit of household waste (g/capita/day) by population in each administrative district. The amounts of business wastes are estimated by multiplying the generation weight unit of business waste (g/working person/day) by the working population in categorized industry. The estimation methods and estimated values are appropriate. The ratio of business wastes in general wastes is from 34 to 95 % for each administrative district. "Waste generation density" of each administrative district vary from 5.3 to 70.9 t/km^2/day. More business wastes are generated from central area, and more household wastes are generated from the surrounding area. Central district generate a lot of general waste from business activities.

A review of phytoestrogens: Their occurrence and fate in the environment
Ze-hua LIU, Yoshinori KANJO and Satoshi MIZUTANI
Water Research, Vol.44, No.2, pp.567-577 (2009)
Phytoestrogens are plant compounds with estrogenic activities. Many edible plants, some of which are common in the human diet, are rich in phytoestrogens. Almost all phytoestrogens eaten daily by people were reported partly recovered in urine or feces, which can be regarded as one of the main sources of their occurrence in municipal wastewaters. As they may act as one part of the endocrine disrupting compounds (EDCs) in water systems, some phytoestrogens have been monitored and detected in wastewater and other various environments. It is very difficult to monitor numerous unknown EDCs in complex wastewater samples, and it is helpful if some estimation of target EDCs can be done before monitoring. With this in mind, this review will: (1) summarize estrogenic activities or estrogenic potencies of phytoestrogens by different bioassays; (2) summarize daily urinary excretion rates of phytoestrogens by humans, and compare their urinary excretion rates to that of estrone, which suggests that most phytoestrogens may occur in municipal wastewaters; (3) collect and summarize published data on the occurrence and fate of phytoestrogens in various environments.

Simultaneous analysis of natural free estrogens and their conjugates in wastewater by GC/MS
Ze-hua LIU, Takeshi HASHIMOTO, Yoichi OKUMURA, Yoshinori KANJO and Satoshi MIZUTANI
Clean-soil, air, water, Vol.38, No.2, pp.181-188 (2010)
A solid-phase extraction (SPE)-gas chromatography (GC)-mass spectrometry (MS) analytical method was developed for the simultaneous analysis of natural free estrogens and their conjugates in wastewater samples. Natural free estrogens and their conjugates in wastewater were successfully separated by the oasis hydrophilic-lipophilic balance solid phase extraction (Oasis HLB SPE) method, and the conjugates were initially enzyme hydrolyzed by b-glucuronidase or arylsulfatase from Helix pomatia prior to derivatization. N-methyl-N-(tert-butyldimethylsilyl)trifluoroacetamide (MTBSTFA) plus 1% tert-butyldimetheylchlorosilane (TBDMCS) was chosen as the derivatization reagent, and the most appropriate conditions of derivatization were determined to be at 958C for 90 min. The recovery ratios of nine target chemicals were determined by spiking them in 1 L of ultra-purified water or the influent of a wastewater treatment plant (WWTP). The recovery ratios of six out of nine for the analytes ranged from 73.3–114.9% with relative standard deviations (RSD) from 1.6–19.9%. The established method was successfully applied to environmental wastewater samples which were collected from one municipal wastewater treatment plant (WWTP) in Osaka, Japan, for the determination of natural free estrogens and their conjugates. In the influent sample, E1, E2, E1-3S, E3-3S, and E1-3G were detected at concentrations of 16.6, 9.6, 8.2, 21.9, and 3.2 ng/L, respectively. However, only E1 was detected at a high concentration of 44 ng/L in the effluent sample, suggesting that it is the dominant natural free estrogen in the effluent.

Recharge sources of the groundwater in the Osaka City and the surroundings estimated from geochemical characteristics
Kazuya MAKINO, Harue MASUDA, Muneki MITAMURA, Yoshinori KANJO, Ichiro TAYASU(Kyoto University) and Shinji NAKAYA(Shinshu University)
Journal of Japanese Association of Groundwater Hydrology, Vol.52, No.2, pp.153-167 (2010) (in Japanese)
Major and minor element chemistry, hydrogen and oxygen stable isotopes and VOCs were analyzed for the groundwaters taken from Osaka City and its surroundings, located at the alluvial plain and fluvial terrace (Uemachi terrace). Salinitization occurs in the groundwater <100m depths in the western alluvial plain from the Uemachi terrace, due to seawater invasion along river into the aquifer. The level of seawater contamination is

higher in the depth between 50 and 100 m depth than in the <50 m depth. The groundwaters taken from Uemachi terrace give diluted Ca-HCO3 type chemistry. While the fresh groundwater from the alluvial plain gives Na-HCO3 type chemistry. However, both would be recharged from the local rain and/or river water. Fresh groundwater >100 m depth close to the coast line of Osaka Basin gives Na-HCO3 type and low SiO2 (<10mg/L) chemistry and lightest stable isotope ratios among the studied groundwater, suggesting that the groundwater was originated from the precipitation at the mountain area north of Osaka City, or ultrafiltrated porewater from the less permeable layer in that depth. All the studied groundwaters except one do not contain VOCs, suggesting the recharging period after 1989.

Applied Mathematics

Designing of Double Cross Catenary Screen as Sunlight Catcher and Diffuser for Daylighting from High Side Window

Hirotaka. SUZUKI

Journal of Light & Visual Environment, The Illuminating Engineering Institute of Japan, Volume 34, Number 1, pp.35-41 (2010)

Daylighting is highly significant from the viewpoint of energy saving and healthy life. However, considering density of housing in residential area of large cities, it is very difficult to secure sufficient daylight and lead daylight to whole space in the house. High side lighting is one of the solutions for such situation. And when high side windows are designed with open ceiling, high side light can be propagated to lower level through open ceiling. On the other hand, high side light brings highlight area on walls or floors. The area may cause glare phenomenon or may lower brightness of surrounding area by contrast effect. And open ceiling may cause excessive impression of air volume for detached house. This paper reports designing of diffusing screen to solve these problems. The screen is designed to meet the condition of existing detached house in densely built residential area considering the way of sunlight, the shape of detached house and the use of the detached house. The designed screen was simulated by computer graphics images. Finally, designed screen was installed to the house. And authors made clear that the screen realize required objectives through measurement survey. The screen was also designed to work as lamp shade at night.

A Study Stones Arrangement in the Garden of RYOAN-JI Temple Making Use of Voronoi Diagram

Hirotaka SUZUKI, Yoshinori FUJIMOTO and Takeshi TSUJI

Proc. of the 14th International Conference on Geometry and Graphics, 8pages in Conference CD-ROM, Intl. Society for Geometry and Graphics (2010)

In the garden of Ryoan-ji temple, a world heritage in Japan, 15 stones are placed and they give visitors special impression. Almost all past research about the stones arrangement were analysis of intension of the garden designer or that of rules of arrangement. This paper discussed the relationship between physical stones arrangement and psychological impression. We form 5 stone groups from 15 stones and generate different arrangements based on the 5 groups. To abstracted physical characteristics of the stones arrangement, we adopted Voronoi diagram method. We abstracted variance of areas of Voronoi polygons (VA), variance of lengths of Delaunay graphs (VL) and variance of distance from the center point of stone group to the gravity center of Voronoi polygons (VD). And we abstracted the impression of each stones arrangement by subjects experiment with magnitude estimation method.

We conducted 2 experiments, preliminary experiment and regular experiment. In preliminary experiment, we showed stones arrangement by two different styles; orthographic drawings only (case-O), and both orthographic drawings and perspective drawings (case-OP). The sizes of the drawings are A4 (210mm X 297mm). From the result of the preliminary experience we got following points.

- Comparing case-O and case-OP, variance of impression score among subjects was higher in case-OP. It seems case-O is reliable for presentation method of stones arrangement.
- In case-O, existing stones arrangements got the highest impression score.

In regular experiment, we showed stones arrangement by two different styles; orthographic drawings only (case-O) and wide angle perspective drawings only (case-P). From regular experiment, we got following points.

- Comparing case-O and case-P, existing pattern got the highest impression score and pattern based on existing arrangement got higher score in case-P. It seems that if we secure wide angle, perspective drawing can tell similar impression to that of existing 3D world than orthographic drawing only.
- There were clear relationship between physical characteristics (VA, VL and VD) and impression scores.

Utilization of Rapid Prototyping System for Lamp Shades Design

Hirotaka SUZUKI1 and Naoki IIDA (College of Industrial Technology)

Proc. of the 14th International Conference on Geometry and Graphics, 7pages in Conference CD-ROM, Intl. Society for Geometry and Graphics (2010)

Manufacturing of objects with complicated curve surface had limitation in terms of both designing aspect and modeling aspect. 3-Dimensional modeler solved the limitation of designing stage. Now, rapid prototyping system is solving the limitation of modeling stage as the system can complete modeling of objects with highly complicated curve as long as data of the objects is described electronically.

The characteristic of curved surface is clearly reflected when the surface is for lamp shades because normal vector of the surface has close relationship with reflection and luminance of the point. This paper presents utilization of rapid prototyping system to lamp shade design.
We proposed 2 works named 'Refracting Mobius Loop' (hereafter RML) and 'Reflecting Paraboloid Shell' (hereafter RPS). RML is constructed by ruled surface generated from double helix on a sphere. As normal vector of each point change gradually on RML surface, luminance on RML should change gradually as well. RPS is constructed by set of paraboloid curved lines sharing focus point. If point light source is located at the focus point and the surface have specular reflection characteristic, the light reflected by RPS should be parallel.

We designed both RML and RPS by 3D renderer POV-Ray to evaluate from viewpoint of visual aspect. Then, set of commands for 3D modeler Rhinoceros was automatically generated from POV-Ray scene file to construct STL format data. Finally we got actual products developed by rapid prototyping system. We also applied specular reflection paint to RPS surface to secure mirror-like (specular reflection) surface.
After development of products, we conducted luminous performance test. We measured luminance distribution on RML and illuminance level of the point under RPS to examine luminous performance. In case of RML, luminance made by reflection and transmission of the surface change gradually as designed. In case of RPS, though flow of reflected light was not perfectly parallel because of designing, modeling and applying problems, illuminance level was increased by RPS reflection.

Evaluation of Diffuse Reflectance of Diffuse Reflectance of Water Screen and Open Experiment with Projected Animation

Kouji TAKECHI1 and Hirotaka SUZUKI

Proc. of the 14th International Conference on Geometry and Graphics, 8pages in Conference CD-ROM, Intl. Society for Geometry and Graphics (2010)

As a serious of activities conducted by the group of Urban Study, Osaka City University, authors had been proposed plans for environment improvement and activation of Higashiyokobori-gawa river district of Osaka, Japan. This area is located under an elevated highway, resulting in an uncomfortable environment in terms of light, view, air, water and sound environment though the district had been a key point of river transportation historically. The plans are composed by project proposal making use of water screen, VR system for evaluating project proposal. To realize project proposal at the district, we started evaluation of diffuse reflectance of water screen. And we also conducted open experiment with projected animation on the water screen.
First, we conducted preliminary survey for evaluating reflectance of the screen. At the preliminary survey, we projected white and black images to measure luminance and luminance contrast. As spray pressure and nozzle type changed, value of luminance and luminance contrast changed.
As measured reflectance level is quite low, we performed public experiment to make sure whether people can recognize images projected on water screen or not. We set up water screen in front of Osaka City University Media Center on 9th Dec. 2008 and projected animation of changing text and changing face. Though the light from library existed and disturbed people's visual recognition, almost all people joined the experiment could recognize the images on water screen. From open experiment, we found following points.

· As water screen is almost transparent, dynamic motion of animation give people strong sense of perspective.
· As water screen is not plane surface but 3D volume, projected images extended as 3D bright volume. There is possibility of new expression of image make good use of the characteristic.

Finally, we conducted lighting experiment to establish the way of determine reflectance of water screen.